

NASA CR 152011
MRC/SD-R-14

RADIATION DESIGN HANDBOOK FOR THE JUPITER PROBE

7 May 1977

Prepared for: NASA/AMES RESEARCH CENTER
Moffett Field, California 94035

Contract No. NAS2-9444

(NASA-CR-152011) RADIATION DESIGN HANDBOOK
FOR THE JUPITER PROBE (Mission Research
Corp., La Jolla, Calif.) 168 p

N77-83137

Unclas
00/15 46208

MISSION RESEARCH CORPORATION
1150 Silverado Street
P. O. Box 1209
La Jolla, California 92038
(714) 454-3046

REPRODUCED BY
NATIONAL TECHNICAL
INFORMATION SERVICE
U. S. DEPARTMENT OF COMMERCE
SPRINGFIELD, VA. 22161

N 77-83137

NASA CR 152011
MRC/SD-R-14

Copy No. _____

RADIATION DESIGN HANDBOOK FOR THE JUPITER PROBE,

V. A. J. van Lint
J. P. Raymond
A. R. Hart
M. L. Price

7 May 1977

Prepared for: NASA/Ames Research Center
Moffett Field, California 94035

Contract No.: NAS2-9444

MISSION RESEARCH CORPORATION
1150 Silverado Street
P. O. Box 1209
La Jolla, CA 92038
(714) 454-3046

CONTENTS

SECTION		PAGE
	Preface	1
1.0	INTRODUCTION	3
1.1	Probe Overview	3
1.1.1	Jupiter Probe Mission	3
1.1.2	Jovian Radiation Environment	7
1.2	Critical Radiation Effect	13
1.2.1	Long-Term Ionization Effects	13
1.2.2	Displacement Damage Effects	21
1.2.3	Transient Interference Effects	25
1.2.4	Radiation Survivability	27
1.3	Critical Design Considerations	28
1.3.1	Component and Circuit Design Applications	29
1.3.2	Shielding Design	32
2.0	COMPONENT RADIATION EFFECTS	35
2.1	Bipolar Transistors	35
2.1.1	Long-term Ionization Effects	35
2.1.2	Displacement Effects	48
2.1.3	Transient Interference Effects	51
2.2	Other Discrete Semiconductor Components	52
2.2.1	Junction Field Effect Transistors (JFETs)	52
2.2.2	Silicon Controlled Rectifiers (SCRs)	54
2.2.3	Diodes	54
2.2.4	Electro-Optical Devices	56

CONTENTS (Cont'd)

SECTION	PAGE	
2.3	Integrated Circuits	65
2.3.1	Bipolar Digital	68
2.3.2	Bipolar Analog	70
2.3.3	MOS	75
2.3.4	CCD's Image Sensors and Other Complex Types	81
2.3.5	Interference Effects	87
2.4	Optical Materials	88
2.5	Quartz Crystals and Filters	90
2.6	Miscellaneous Devices and Materials	91
2.6.1	Surface Accoustic Wave Devices	91
2.6.2	Magnetic Bubble Domain Memories	91
2.6.3	Cabling	91
2.6.4	Other Materials	93
3.0	DESIGN GUIDELINES FOR RADIATION EFFECTS	94
3.1	Design Considerations	96
3.1.1	Bipolar Transistors	96
3.1.1.1	Displacement Effects	96
3.1.1.2	Long-Term Ionization Effects	98
3.1.2	Other Discrete Semiconductor Components	98
3.1.2.1	Junction-FETs	98
3.1.2.2	SCRs	99
3.1.2.3	Diodes	99
3.1.2.4	Electro-Optical Devices	100
3.1.3	Integrated Circuits	100

CONTENTS (Con't)

SECTION	PAGE
3.1.3.1 Bipolar Digital	101
3.1.3.2 MOS	102
3.1.3.3 Bipolar Analog	103
3.1.3.4 CCD's and Image Sensors	104
3.1.4 Miscellaneous Materials and Devices	105
3.1.4.1 Optical Materials	105
3.1.4.2 Quartz Crystal Oscillators and Filters	106
3.1.4.3 Cabling	107
3.1.5 Interference	107
3.2 Component Selection and Procurement-Statistical Approach	108
3.2.1 Introduction	108
3.2.2 Statistical Considerations	114
3.2.3 Data Review	117
3.2.3.1 Bipolar Transistors and Similar Discrete Components	117
3.2.3.2 Bipolar Integrated Circuits and Complex Devices Not Covered In (3.2.3.3)	118
3.2.3.3 MOS and Bipolar Linear Integrated Circuits	119
3.2.3.4 Block Descriptions for Flow Charts I, II and III	119

CONTENTS (Con't)

SECTION	PAGE
3.2.4	Hardness Assurance Approaches For Procurement 136
3.2.4.1	Approaches "A", "B" and "C" 136
3.2.4.2	Radiation Procurement Classes- Definition 148
3.3	Experimental Characterization 149
3.3.1	Electrical Bias Conditions During Radiation Exposure 150
3.3.2	Electrical Parameter Measurement 151
3.3.3	Characterization of Complex Microcircuits 153
4.0	SUMMARY 155
	REFERENCES 156
	APPENDIX A - Statistical Analysis 161
	APPENDIX B - Example of Radiation Hardness Assurance Guideline Assessments 166

ILLUSTRATIONS

FIGURE		PAGE
1.1	Jupiter Probe Mission Profile	4
1.2	Jupiter Probe Mission Description	5
1.3	Probe Side View	6
1.4	Electron Integral Fluence vs Energy	9
1.5	Proton Integral Fluence vs Energy	10
1.6	Probe Entry Sequence and Radiation Flux	11
1.7	Probe Structural Shielding	14
1.8	Ionization Dose Conversion Factors For Protons And Electrons	17
1.9	3-MeV Equivalent Displacement Factor For Electrons	23
1.10	20 MeV Equivalent Displacement Factors For Protons Of Various Energy Levels	24
1.11	Total Dose vs Shielding	32
1.12	Effects Of Additional Shielding	34
2.1	Damage Curve Of Gain vs Ionization Dose	37
2.2	Typical Bipolar Transistors Ionization Effects On Gain- Several Manufacturers.	38
2.3	Typical Long-Term Ionization Effects In 2N2222 Transistors- Manufacturer/Date Code Variations	39
2.4	Long-Term Ionization Gain Degradation Rates - Several NPN Transistor Types	40

ILLUSTRATIONS (Con't)

FIGURE		PAGE
2.5	I_{CBO} vs Irradiation Time	41
2.6	Device Current Gain vs Dose - PNP Transistor With Bias	45
2.7	Device Current Gain vs Dose - PNP Transistor Without Bias	46
2.8	Transistor Voltage Dependence of Degradation	47
2.9	I_{CBO} As a Function of Dose For Various Bias Conditions	48
2.10	Quantum Efficiency vs Wavelength Of Incident Light of An Array	60
2.11	Dark Current vs Target Voltage Of An Array Irradiated By Electrons	61
2.12	Light Intensity Degradation for Irradiation of GaAs, LEDs	63
2.13	Effects of Electron Irradiation on Light Output of GaAs Light Sources	64
2.14	Variation of Solar Cell Short Circuit Density With Fluence	66
2.15	Range in ΔV_{OS} for Increasing Dose for Several Bipolar Analog ICs	70
2.16	Range in ΔI_{OS} for Increasing Dose For the Same ICs As In Figure 2.15	77
2.17	Range in ΔI_B For Same Conditions As In Figure 2.15	73
2.18	MOS Transistor Threshold Voltage Shifts	76
2.19	Statistical Variation of MOS Transistor Threshold Voltages	78
2.20	Variation of C/MOS CD4024 Total Dose Vulnerability With Bias	80
2.21	ϵ vs Total Dose for 500 x 1 CCD	82

ILLUSTRATIONS (Con't)

FIGURE		PAGE
2.22	Dark Current vs Total Dose for 500 x 1 CCD	83
2.23	ΔV_{FB} vs Total Dose for Same Device as in Figure 2.21	84
2.24	ΔV_{FB} vs Total Dose for 64 x 1 CCD	85
2.25	Effects of Low Rate Gamma Radiation on CCD Storage Time vs Total Dose	86
2.26	Composite Steady-State Frequency Shift Data vs Dose For Quartz Crystal Resonators	90
2.27	Frequency Offsets for 5 MHz Resonators Of Swept Synthetic Quartz vs Dose	92
3.1	Probability of Failure vs Neutron Fluence - DTL Flip-Flop	127
3.2	Probability of Failure vs Neutron Fluence - General Purpose Amplifier	128
3.3	Probability of Failure vs Neutron Fluence - 2N5038 Power Transistor	129
3.4	Flow Chart I: Radiation Hardness Assurance Guidelines For Bipolar and Discrete Components	133
3.5	Flow Chart II: Radiation Hardness Assurance For Bipolar Digital ICs	134
3.6	Flow Chart III: Radiation Hardness Assurance For MOS and Bipolar Linear ICs	135

ILLUSTRATIONS (Con't)

NUMBER		PAGE
3.7	Flow Chart IV: Approach "C" to Hardness Assurance	137
3.8	Flow Chart V: Approach "B" For Hardness Assurance	138
3.9	Flow Chart VI: Approach "A" For Hardness Assurance	139

TABLES

NUMBER		PAGE
1.1	Electron and Proton Integral Fluence vs Energy For Probe Entry at Best and Worst Trajectories	8
1.2	Dose/Fluence Calculated For 2 Locations Inside Probe	15
1.3	Radiation Sensitive Components	30
1.4	Example Calculation of Total Dose at An Arbitrary Location Within Probe	33
2.1	Noise Current Corner Frequency	43
2.2	Transistor Types in Parallel-Irradiation Group	44
2.3	Transistors In Serial Irradiation Group	44
2.4	Behavior of I_{GSS} of N-Channel JFETs	53
2.5	Summary of Proton Irradiations	57
2.6	Threshold Limits of Partical Fluence and Flux in Phototubes	62
2.7	Complex Microcircuit Radiation Hardness Examples	69
2.8	Proton Damage in Op Amps	74
2.9	11402 Dynamic MOS Shift Register Failure Level as a Function of Refresh Frequency	87
2.10	Absorption in Optical Materials	89
3.1	Values of Power of Standard Deviation for Required Probability of Failure	116
3.2	Standard Deviation Factors for 90% Confidence	116
3.3	20 MeV Proton Damage Constants	121
3.4	3 MeV Electron Damage Constants	121

PREFACE

The purpose of this Handbook is to provide basic guidance in the design of electronics equipment for the Jupiter Probe to ensure that it will survive exposure to the Jovian radiation belts.

To those unfamiliar with the design of hardened electronics both technical and non-technical hurdles must be overcome. Of the non-technical hurdles the first is the unfamiliarity with the radiation environment, units of measure, and the nature of the effects in components. The second non-technical hurdle is apprehension that a successful design can be realized. We believe that successful designs will be difficult but are possible for all Probe experiments.

The principal technical hurdle in hardened electronics design is the scarcity of radiation effects data on components of interest. Radiation effects in critical components are potentially a function of details of device geometry and processing steps during fabrication as well as electrical bias conditions during radiation exposure. Thus, even published data on the same component type may not accurately reflect those effects on the components procured for system use.

The information presented in this Handbook is intended to supplement the design process. Tutorial information has been minimized with references to many excellent sources discussed in Section 1 of the Handbook.

Section 2 of the Handbook presents a general discussion of component radiation effects and design considerations. Emphasis has been placed on

presenting the scope of effects rather than an extensive compilation of available data. Design considerations are suggested but it is expected that, with knowledge of the basic component effects, individual design considerations familiar to designers can be applied directly to realize hardened equipment.

The principal contribution of the Handbook is presented in Section 3: Hardness Assurance Guidelines. Step-by-step procedures are outlined to support the evolution of design by establishing a component data base sufficient to support and assure adequate survival. Input parameters are the defined radiation environment, survival probability and failure criteria on each component parameter. Analysis procedures are outlined to proceed based on the determined element of risk, each leading to a component specification for design and fabrication of hardened equipment.

In preparing this handbook we have attempted to foresee all the radiation effects problems in Probe electronics and to recommend safe, but useful, design rules for dealing with them. However, radiation tolerant electronics design is not yet a mature discipline, particularly in the face of rapidly evolving electronics device technologies. Therefore, it is recommended that after the design has been accomplished according to this handbook's rules, it be reviewed by experienced radiation-effects personnel to ensure that there is no failure mode that was not anticipated in writing the handbook, or that more recent radiation-response data on parts do not invalidate the assumptions on statistical extrapolation.

SECTION 1

1.0 INTRODUCTION

1.1 PROBE OVERVIEW

1.1.1 Jupiter Probe Mission

The overall Jupiter Probe mission is the combination of an orbiting spacecraft with an atmospheric probe to explore Jupiter, its atmosphere, the surrounding physical environment, and its extensive satellite system.¹ The scientific objectives of the probe are the measurement of near-planet charged particle concentrations and the determination of the composition and physical properties of the atmosphere, the radiative energy balance, and the location and structure of the clouds as the probe descends to a depth equivalent to a pressure level of at least 10 atmospheres.

The probe mission profile is shown in Figure 1.1. An illustration of the mission timeline is shown in Figure 1.2. It is expected that significant changes will occur in the probe configuration during the Phase B studies, but a first cut at placement of experiments within the probe would have the appearance of Figure 1.3.

The mission is described in detail in "Mission Description Document for Jupiter Orbiter Probe 1981/1982 Mission" - JPL #660-21.²

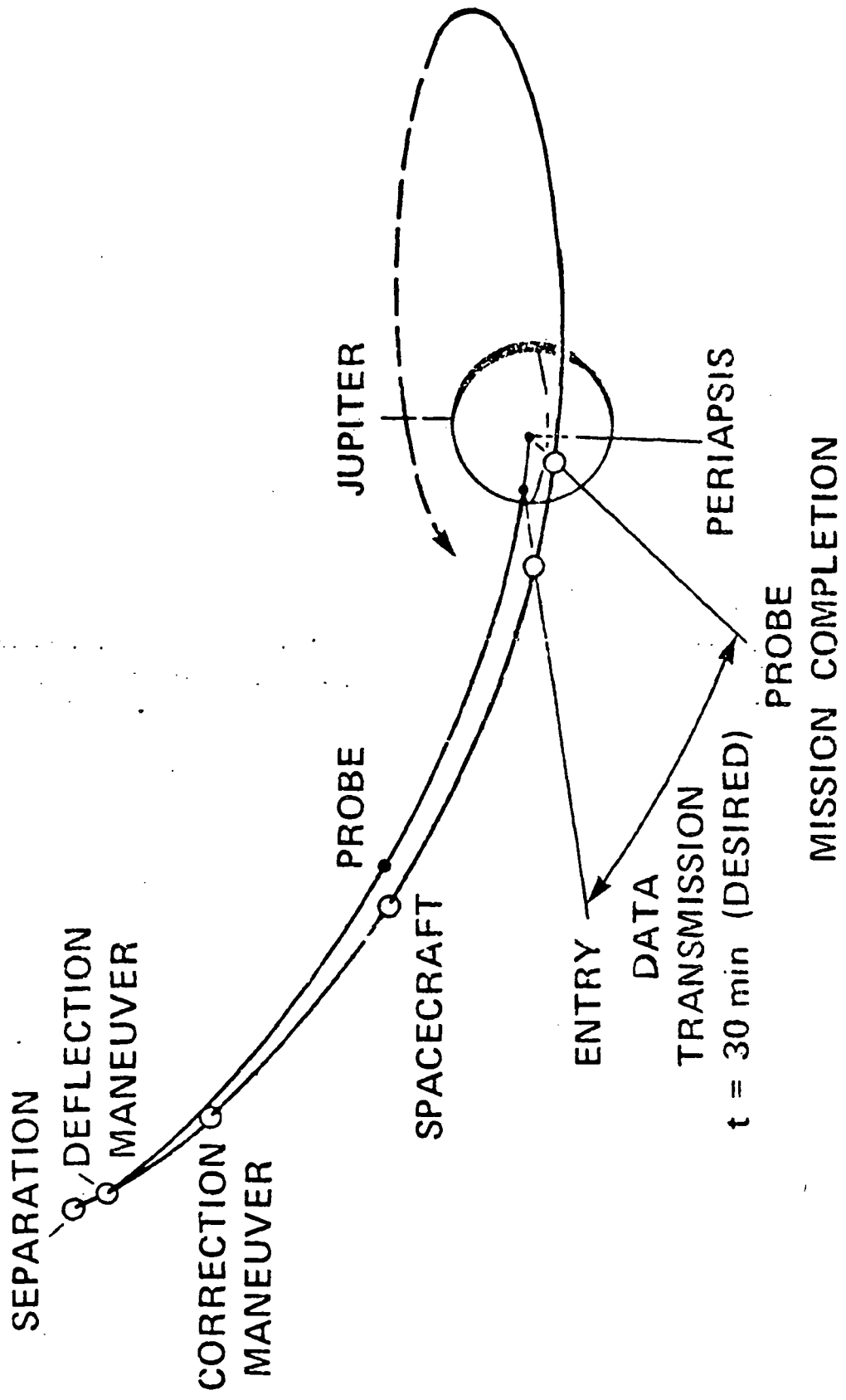


Figure 1.1: Representative Jupiter Probe Mission Profile¹

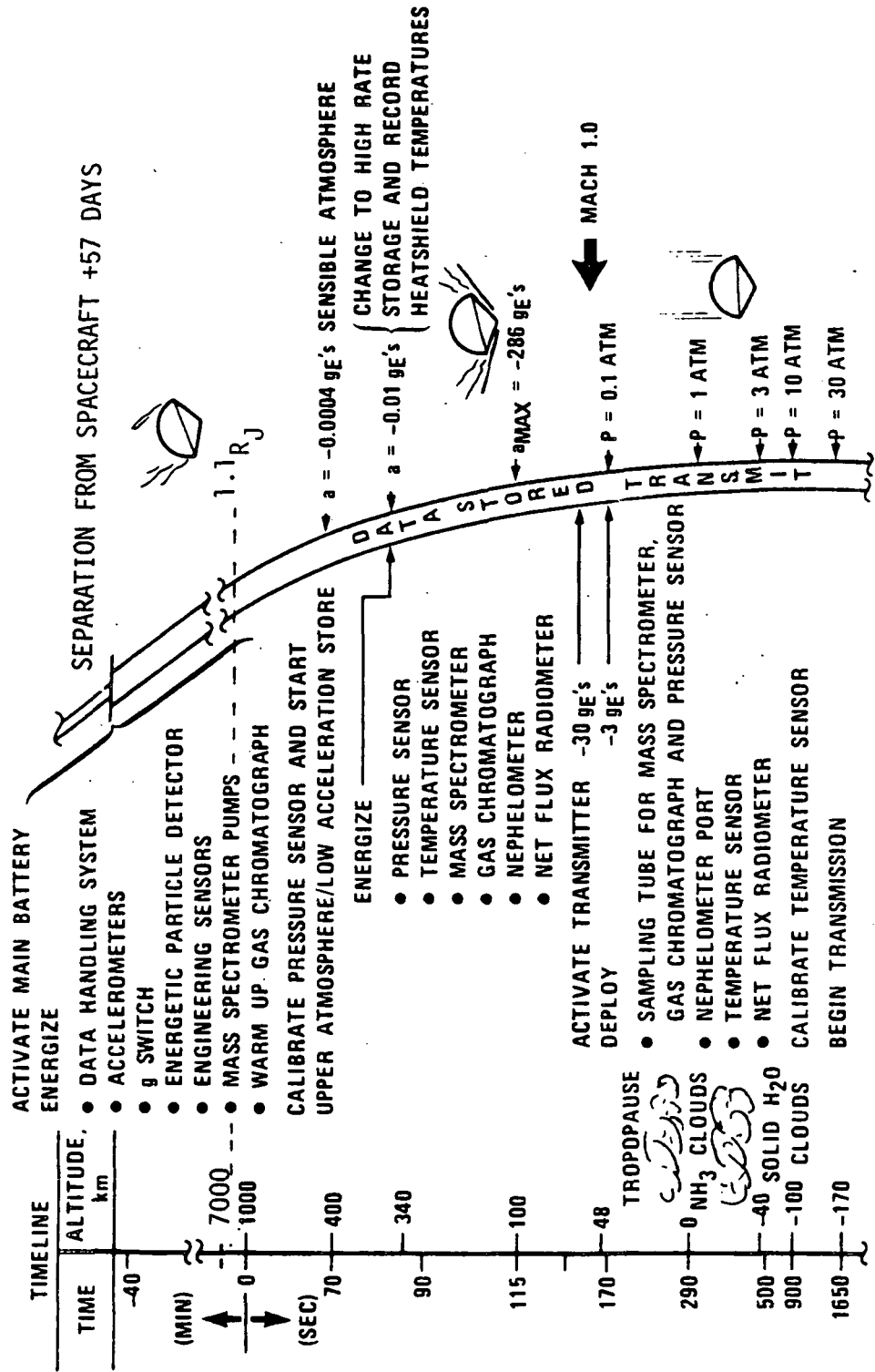


Figure 1.2: Representative Jupiter Probe Mission Description²

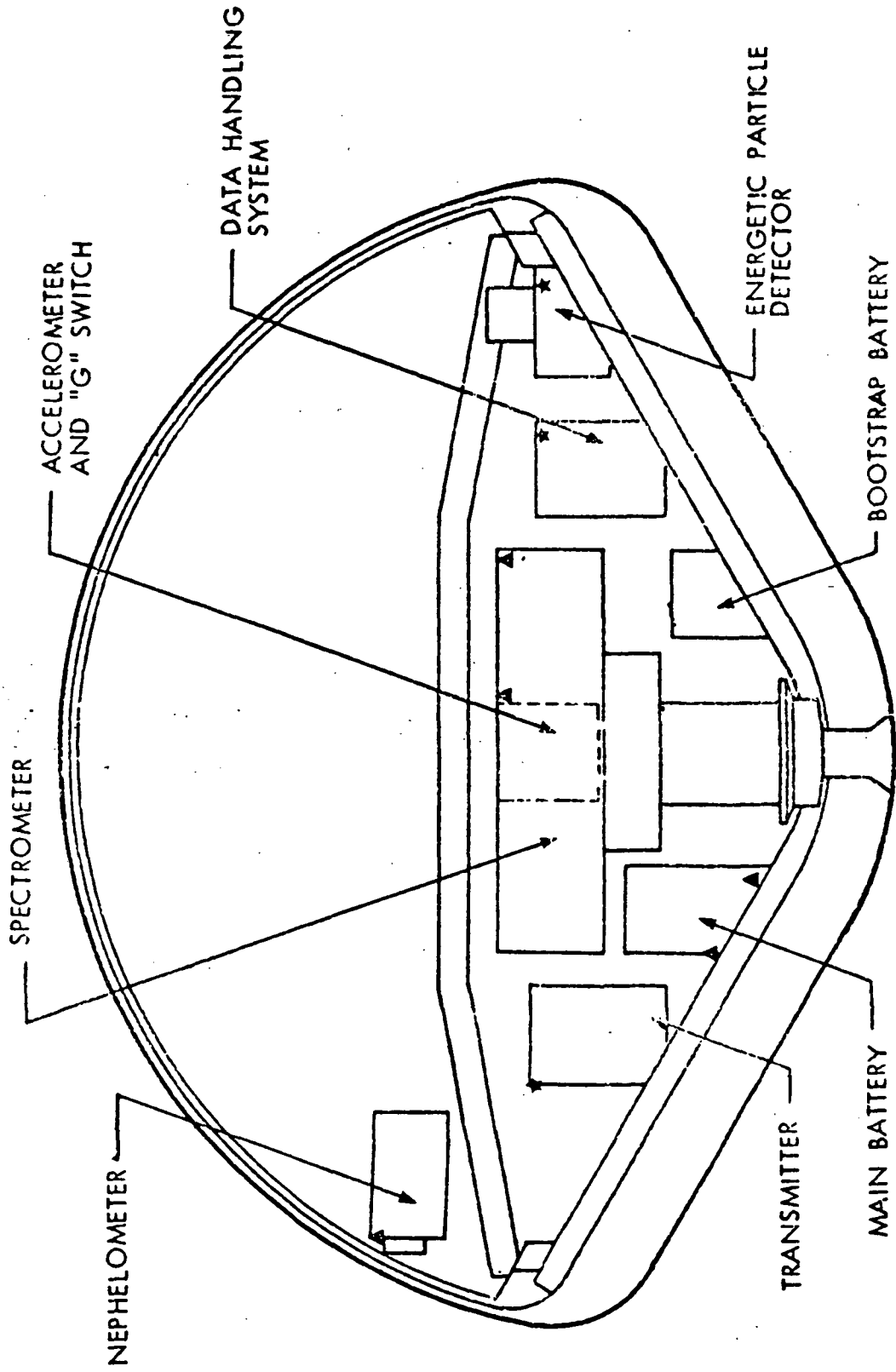


Figure 1.3: Probe Side View¹

1.1.2 Jovian Radiation Environment

Existence of intense Jovian radiation belts was confirmed by the Pioneer 10 (1973) and 11 (1974) spacecraft. Subsequent analysis and modeling of the belts indicated the potential for severe hazard to Jovian spacecraft. Consequently, in order to define the impact on the probe mission and design requirements, an analysis of the available radiation models and their implications for hazard to probe electronics was necessary.¹

Analysis of the Jovian trapped radiation environment to determine its impact on a Jupiter Probe mission has involved three distinct aspects: Jovian environment definition for the magnetic field and trapped particles, parametric analysis of the particle flux and fluence incident on the probe over the trajectory range of interest, and a parametric shielding analysis of the penetrating characteristics of the incident radiation. In this section the magnetospheric modeling, trajectory analysis, and radiation transport analysis results are presented and discussed. These radiation environment results then form the basis for the radiation hazard assessment of the Jupiter Probe.

Discussion of the radiation environment is presented in this Handbook to generally identify the radiation levels of interest. The basic model is defined from a nominal model of the Jovian radiation environment, and a worst-case assessment of the radiation environment has yet to be finalized. The uncertainties between the nominal model, as presented, and the worst-case could be as great as a factor of five increase in the total dose of the Probe ionizing radiation environment. Definition of the worst-case Jovian radiation environment will be made available by NASA Ames Research Center in separate documents.

TABLE 1.1: Electron and Proton Integral Fluence
Vs. Energy for Probe Entry at Best and Worst
Trajectories.

ENERGY (MeV)	INTEGRAL ELECTRON FLUENCE		INTEGRAL PROTON FLUENCE	
	e/cm ² > E		P/cm ² > E	
	Best	Worst	Best	Worst
<10 ⁻⁴	1.65 x 10 ¹⁴	1.55 x 10 ¹⁵	2.5 x 10 ¹³	5.3 x 10 ¹³
10 ⁻⁴	1.63 x 10 ¹³	5.7 x 10 ¹³	-	-
10 ⁻³	1.58 x 10 ¹³	5.6 x 10 ¹³	5.8 x 10 ¹²	5.9 x 10 ¹²
10 ⁻²		-	4.5 x 10 ¹²	4.5 x 10 ¹²
10 ⁻¹	5.2 x 10 ¹²	9.1 x 10 ¹²	4.0 x 10 ¹²	4.2 x 10 ¹²
1	1.2 x 10 ¹²	1.8 x 10 ¹²	6.2 x 10 ¹¹	9.8 x 10 ¹¹
3	5.7 x 10 ¹¹	1.0 x 10 ¹²	-	-
20	8.3 x 10 ¹⁰	1.7 x 10 ¹¹	1.6 x 10 ¹⁰	1.3 x 10 ¹¹
35	2.9 x 10 ¹⁰	6.1 x 10 ¹⁰	7.8 x 10 ⁹	7.4 x 10 ¹⁰
50	1.48 x 10 ¹⁰	3.0 x 10 ¹⁰	-	-
80	-	-	3.1 x 10 ⁸	4.2 x 10 ⁹
100	3.90 x 10 ⁹	7.6 x 10 ⁹	1.1 x 10 ⁸	1.55 x 10 ⁹

NOTE: Best: Latitude = -5.5° South
Longitude = 57°

Worst: Latitude = + 2.3° North
Longitude = 313°

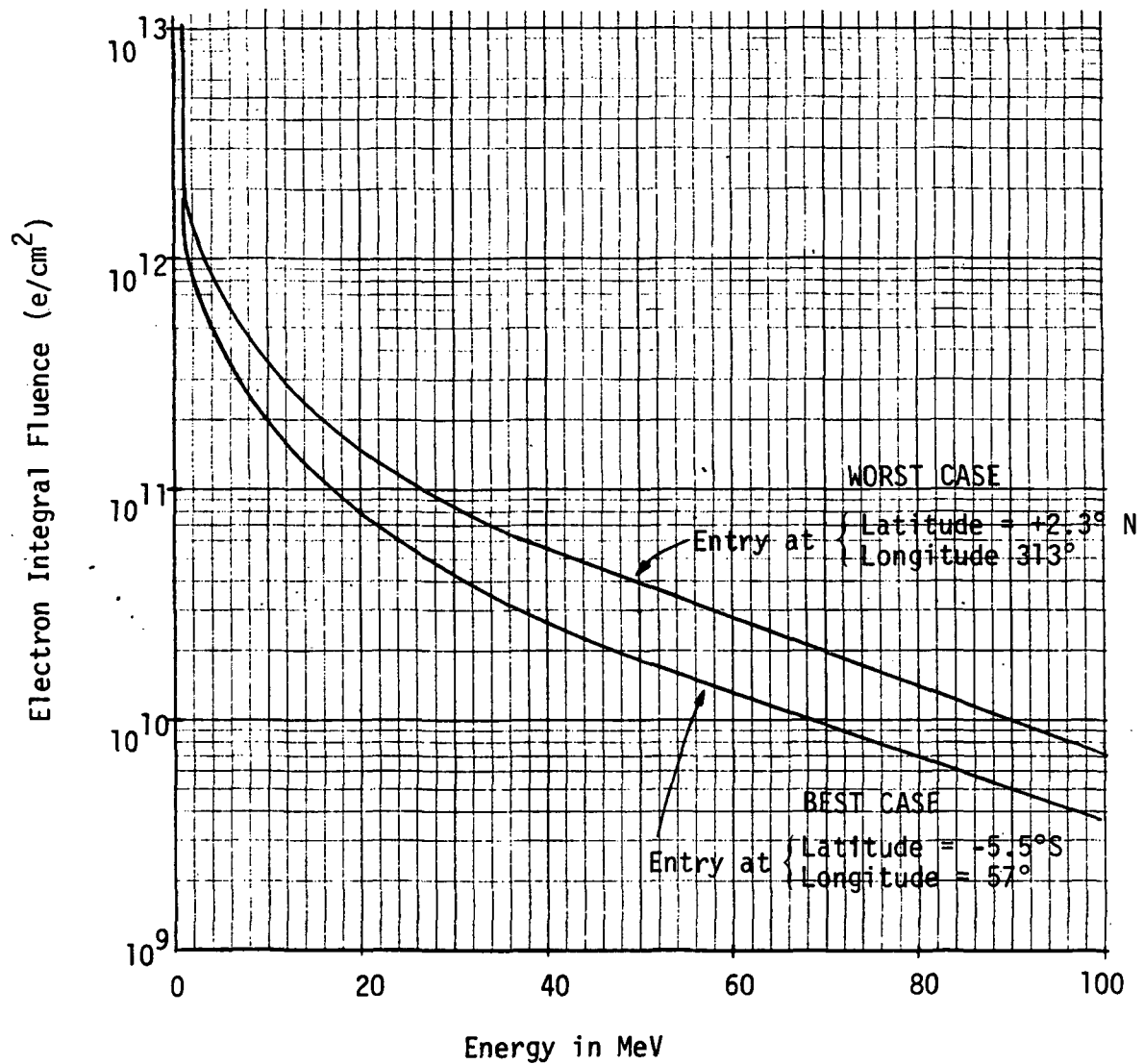


Figure 1.4: Electron Integral Fluence vs Energy for 2 Trajectories³
 Note: variations with entry trajectory do not necessarily represent worst-case model of Jovian environment.

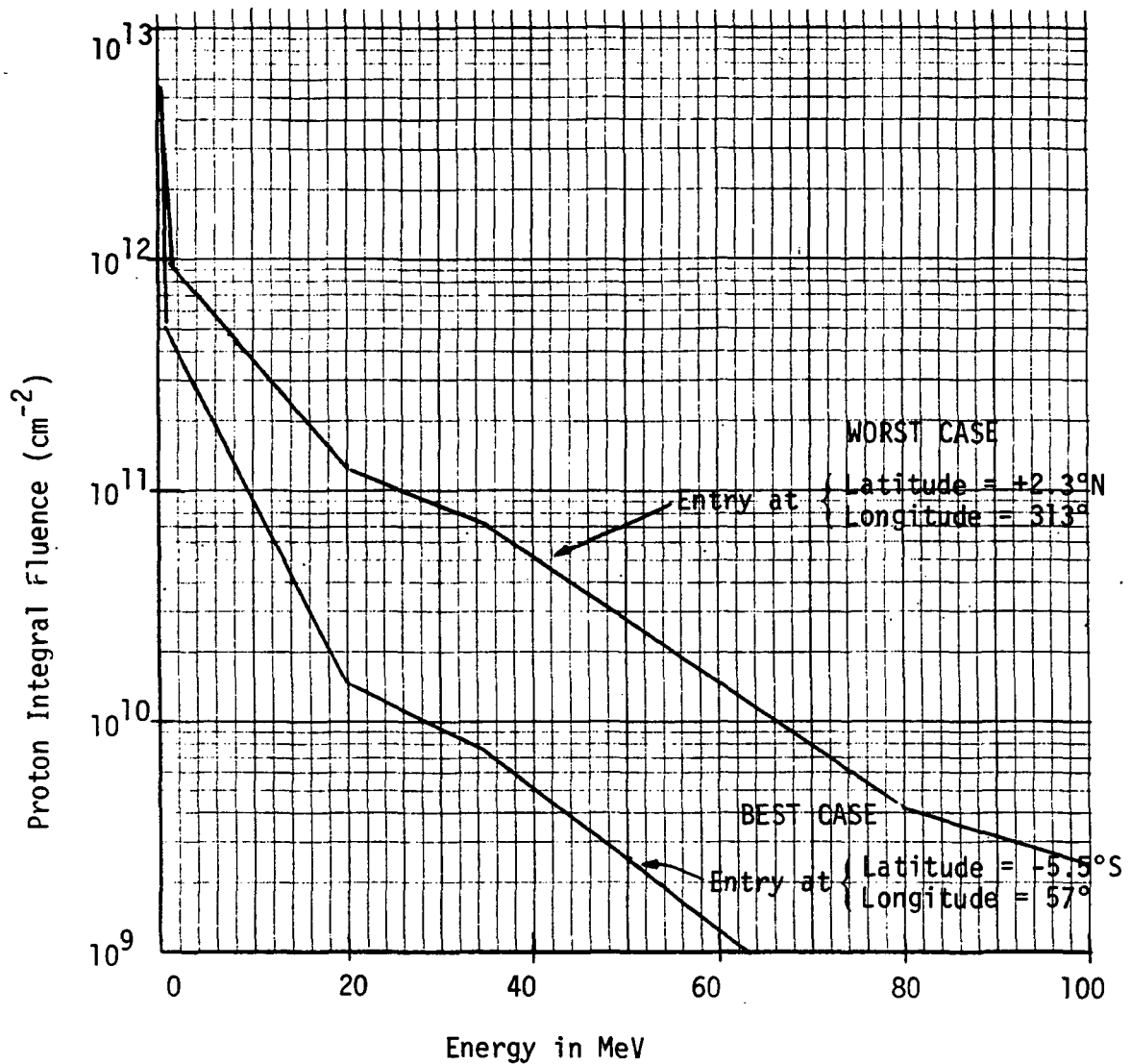


Figure 1.5: Proton Integral Fluence vs Energy for 2 Trajectories³
 Note: variations with entry trajectory do not necessarily represent worst-case model of Jovian environment.

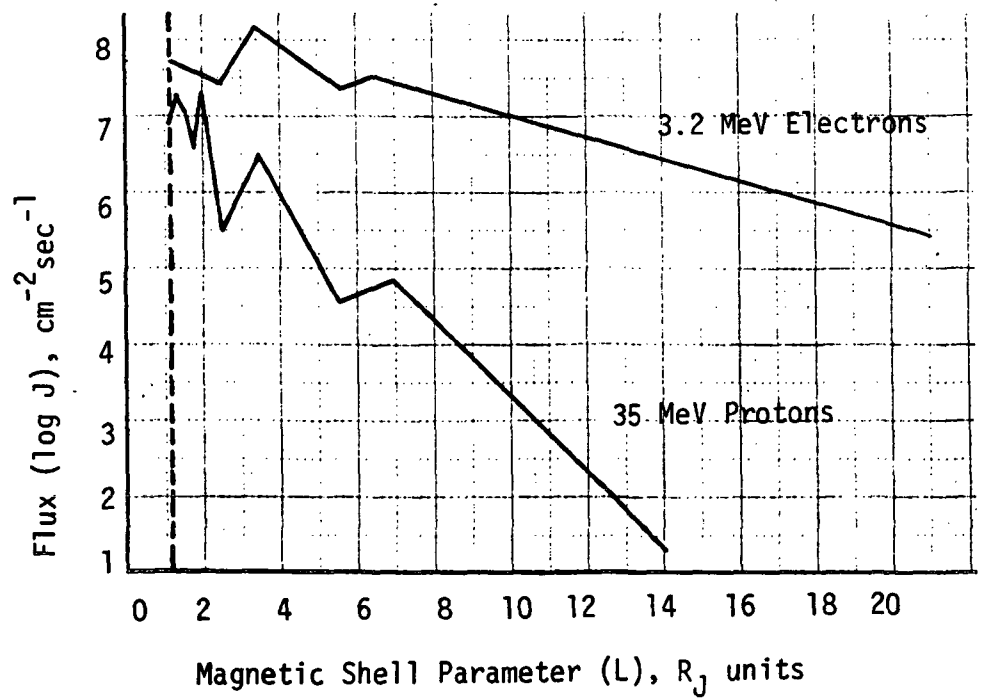
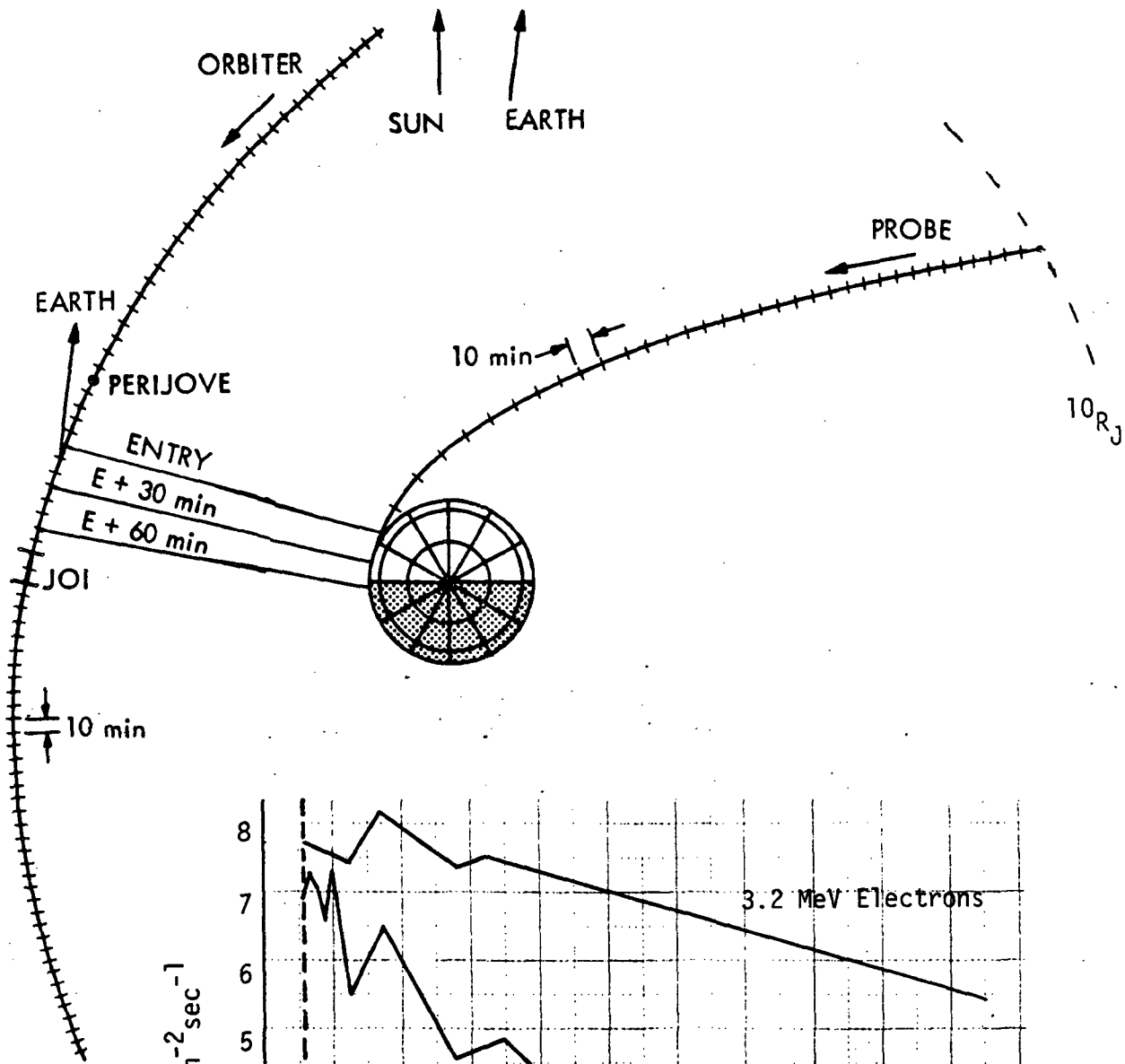


Figure 1.6: Probe Entry Sequence and Radiation Flux for Distances $\leq 10 R_J$

Data from both Pioneer 10 & 11 were used to obtain analytical models for calculating fluence and dose values under various probe entry conditions. Thus, once entry latitude, longitude (magnetic and geographical), entry velocity, and entry flight path angle are specified, the model allows one to calculate the electron and proton fluence and flux encountered by the Probe.³ For illustrative purposes, we have calculated radiation environment values for two probe trajectories chosen to be representative as best and worst case examples. Table 1.1 shows the electron and proton fluences for probe entry at

- | | | |
|-----|----------------------------------|------------|
| | 1) Latitude = -5.5° South | Best Case |
| | Longitude = 57° | |
| and | 2) Latitude = $+2.3^\circ$ North | Worst Case |
| | Longitude = 313° | |

Plots of these data are shown in Figures 1.4 and 1.5. According to the model described in Reference 3, the electron and proton flux are specified for L greater than 1.1 radii, which is considered the altitude where the energetic particle flux cutoff occurs. The flux of electrons and protons vs. distance from Jupiter in units of Jupiter radius is shown in Figure 1.6. In terms of the overall mission, the Jovian radiation environment is initially encountered far from probe separation ($\geq 20 R_J$) and terminates (for the assumed model) at about 1.1 Jovian radii.

The effect of these protons and electrons on electronic components is determined by two factors:

- 1) the incident radiation is attenuated by material between the affected component and the probe exterior.

and, 2) The relative effectiveness of electrons and protons of various energies must be evaluated by a weighting function for each damage mode. As discussed in Sections 1.2.1 and 1.2.2, the appropriate integrals over the radiation spectra are the energy deposition, expressed as absorbed dose, D , in rad(Si), and the displacement equivalent fluences, Φ_3 , for the 3 MeV equivalent electrons/cm² and Φ_{20} for 20 MeV equivalent protons/cm².

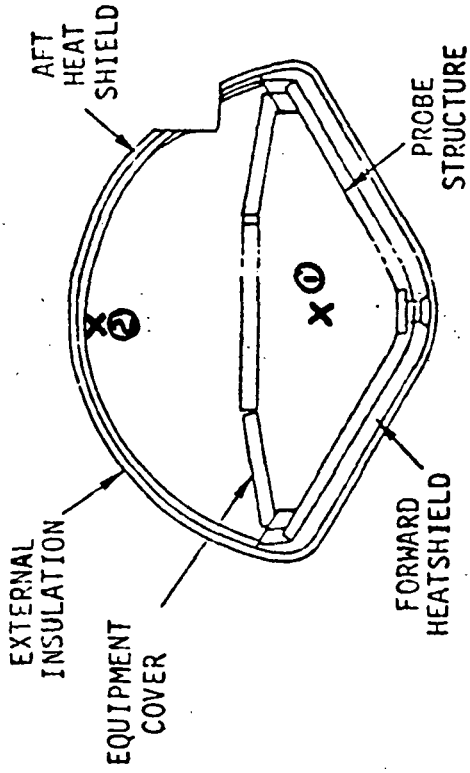
The effectiveness of overlaying materials can be measured by the product of thickness and density, expressed in g/cm². Estimated shielding thicknesses for a typical probe design are shown in Figure 1.7.

The first location chosen was inside the equipment bay, i.e., surrounded by the equipment cover, and approximately in the center; the second location was chosen as far away from the equipment bay as possible at the extreme aft edge inside the heat shield. Using the shield estimates shown in Figure 1.7, we calculated the proton dose, electron dose, 20 MeV equivalent proton fluence, and 3 MeV equivalent electron fluence, peak proton dose rate and peak electron dose rate at each point; results are shown in Table 1.2.

1.2 CRITICAL RADIATION EFFECTS

1.2.1 Long-term Ionization Effects

- Most critical concern for probe electronics, particularly MOS integrated circuits
- Environment defined by absorbed energy from electron and proton exposures in units of rads(material)



FORWARD			
EXTERNAL INSULATION	MULTILAYER MYLAR		0.11 g/cm ²
FORWARD ABLATOR	CARBON PHENOLIC		7.75 g/cm ²
HEAT SHIELD BACKUP	FIBERGLASS HONEYCOMB		0.05 g/cm ²
STRUCTURE	ALUMINUM		<u>0.42 g/cm²</u>
			8.33 g/cm ²
EQUIPMENT COVER			
INTERNAL INSULATION	URETHANE FOAM		0.16 g/cm ²
STRUCTURE	ALUMINUM		<u>0.22 g/cm²</u>
			0.38 g/cm ²
AFT			
EXTERNAL INSULATION	MULTILAYER MYLAR		0.11 g/cm ²
AFT HEAT SHIELD	FIBERGLASS HONEYCOMB		<u>0.49 g/cm²</u>
			0.60 g/cm ²

Figure 1.7: Probe Structural Shielding¹

TABLE 1.2: Dose/Fluence Calculated for 2 Locations Inside the Probe Encountered for Worst Case Entry Trajectory (but not necessarily worst-case environment model).

LOCATION	ELECTRON DOSE (Rads)	PROTON DOSE (Rads)	TOTAL DOSE (Rads)	20 MeV Proton Equivalent Fluence (cm ⁻²)	3 MeV Equivalent Electron Fluence (cm ⁻²)
1	2.5×10^4	9.2×10^3	3.4×10^4	3.8×10^{10}	1.7×10^{12}
2	4.0×10^4	2.7×10^4	6.7×10^4	8.8×10^{10}	2.4×10^{12}
	ELECTRON PEAK DOSE RATE (Rad(Si))/sec		PROTON PEAK DOSE RATE (Rad(Si))/sec		WORST CASE DOSE RATE (Rad(Si))/sec
1	4.0		5.2		9.2
2	6.2		13.3		19.5

Ionization effects are the consequences of radiation-induced events in which electrons are separated from their parent atoms. The resultant free charges are rapidly immobilized, but with persistent effects in the electronic components. Molecular changes produced by ionization, generally classed as radiation chemistry or chemical radiation effects, are not important for the Probe environment. The effects of electronic charge trapped in insulating layers in semiconductor devices is of critical importance for Probe applications.

The relative effectiveness for electrons and protons in producing ionization effects is proportional to their energy deposition, generally expressed in rad(material) units, where one rad corresponds to 100 ergs/gm of energy deposited in the reference material.* The reference material of most interest is silicon or silicon dioxide. For the Probe radiation environment there is no significant difference in rad(Si) and rad(SiO₂), so the former is generally used. The conversion of electrons and proton fluence of various energy into rad(Si) is shown in Figure 1.8.

Long-term ionization effects in semiconductor devices are of serious concern for the Probe. The energy levels of the electrons and protons in the Jovian radiation belts are easily high enough to penetrate through the electronics; shielding to radiation levels of no concern would require a prohibitive weight penalty.

There are two types of ionization effects in semiconductor devices: 1) generation of hole-electron pairs in the bulk semiconductor and 2) generation of hole-electron pairs in the silicon-dioxide passivation layer at the surface of any modern device. In the former case, the generated carriers

* Another measure of an ionizing radiation environment is the Roentgen (R), which represents ionization in air at standard temperature and pressure. Since the effects of concern are the result of ionization in a component, the use of units directly representing absorbed energy in the material of interest (rad) is preferable to specification of the ionizing radiation environment around the component.

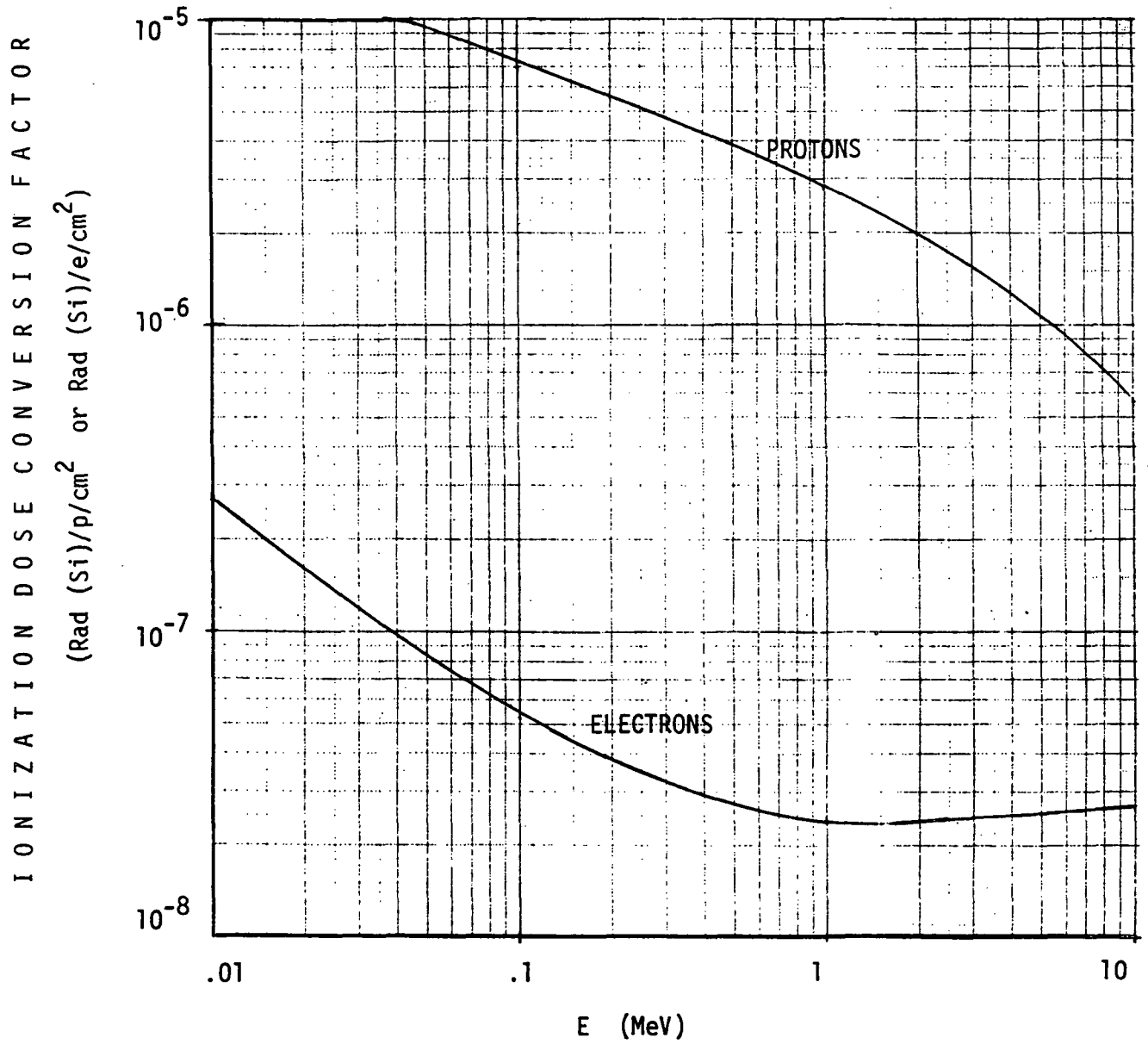


Figure 1.8: Ionization Dose Conversion Factors for Protons and Electrons.⁴

are free to move through the semiconductor and the effect is transient in nature causing no permanent performance degradation. On the other hand, holes generated in the silicon-dioxide passivation layer are trapped and appear as a permanent positive charge which can degrade device performance. The distribution of this positive trapped charge in the oxide is a function of the electrical bias on the oxide during radiation exposure. The density of trapped charge in the oxide affects the degree of device parameter degradation and requires consideration of bias conditions on the device during the mission.

Ionization effects are generally most severe in devices that depend on the silicon surface characteristics. For example, in a p-channel enhancement mode MOS transistor (PMOS), a negative gate potential produces sufficient positive charge at the surface of the bulk silicon to invert the n-type channel material to p-type and allow conduction between the p-type source and drain regions. The addition of radiation-induced positive charge in the gate oxide increases the potential required to invert the silicon. The threshold voltage is increased further by interface states created by irradiation. The magnitude of ΔV_T increases with increasing trapped charge (i.e., radiation exposure).

If a positive gate-channel bias is established on the gate oxide during radiation exposure, the positive trapped charge will accumulate near the silicon-oxide interface. Conversely, a negative bias during exposure will result in positive trapped charge near the oxide-metal interface. Thus, the observed threshold-voltage shift will be substantially greater for positive-gate bias during irradiation than that observed for negative bias.

Effects in n-channel MOS transistor elements (NMOS) are a little more complicated than those in p-channel devices. The effect of the oxide charge is still a negative shift in the threshold-voltage which, in this

case, reduces its magnitude. The effect of the interface states, however, is a positive shift in threshold voltage. The net observed effect for a typical n-channel enhancement MOS transistor is usually a decrease in the magnitude of V_T at low exposure levels, bringing the device toward depletion-mode operation, with a subsequent increase in V_T for larger radiation exposure. This subsequent increase in V_T , however, is generally observed with a decrease in channel transconductance.

The magnitude of threshold-voltage shift in MOS transistors is a strong function of device processing parameters. For highly susceptible devices, a threshold-voltage shift of 0.5V may be observed at radiation levels as low as 1 krad(Si). For hardened devices a radiation exposure of greater than 1 Mrad(Si) is required for the same threshold-voltage shift. The key processing parameters in determining hardness are the surface quality of the starting silicon surface, purity of the gate oxide, and minimized thermal stressing during all processing steps. Unfortunately, there are no electrical parameter measurements on processed devices which would screen out unacceptable parts. Required techniques at present are tight process controls and radiation testing during device procurement.

Bipolar semiconductor devices and microcircuits are also susceptible to long-term ionization effects but generally not to the same degree as MOS devices and microcircuits. As in MOS devices, effects are the result of positive trapped charge in the silicon passivation layer. In this case, however, the basic effect is typically an increased rate of surface minority-carrier recombination, which is observed as a degradation in transistor gain, and an increase in junction leakage currents.

Because the affected element of transistor gain is surface recombination, the overall gain degradation is most severe at low bias current levels. Under low bias current, the gain in a bipolar transistor is determined principally by carrier recombination in the emitter-junction depletion

region. Trapped positive charge in the oxide increases width of the depletion region at the surface in the p-region of the device and causes an increase in depletion-layer carrier recombination as well as bulk surface recombination.

Surface conditions are not as critical to high performance bipolar transistor devices as was the case for MOS devices. As a result, those processing parameters critical to long-term ionization effects are not consistently controlled and there may be a wide variation in effect between devices of the same functional type.

Variation in effect with applied bias during radiation exposure is also significant for bipolar transistors. The worst-case is that of reversed junction bias. Reverse bias on the emitter-base junction enhances transistor gain degradation and reverse bias on the collector-base junction enhances both collector leakage current and gain degradation.

The worst-case for bipolar transistor operation is exposure with both junctions reverse-biased, followed by operation at low bias currents where the gain will be dominated by emitter-base depletion layer recombination. Conversely, the best case would be exposure under high-current saturation (both junctions forward biased) and operation at, or above, the bias current corresponding to peak transistor gain.

Long-term ionization effects in microcircuits are the sum of effects in the individual elements. MOS microcircuits are susceptible as a result of the radiation-induced threshold voltage shift in the transistor elements. Bipolar microcircuits are generally less susceptible than MOS arrays, with their effects principally a result of transistor gain degradation.

The critical radiation failure level for a microcircuit is a function of the margin in the circuit design (e.g., excess transistor gain), electrical bias during radiation exposure, and system performance requirements (e.g., fan-out). At the low extreme in susceptibility are n-MOS dynamic

random-access-memories (RAM) and high performance operational amplifiers (OpAmp) that are seriously damaged at radiation levels of less than 10^4 rads(Si). At the high extreme are high-speed, high-power digital TTL and ECL arrays that perform at exposure levels greater than 10^7 rads(Si). For a given technology, microcircuits tend to become more susceptible with increases in array complexity.

1.2.2 Displacement Effects

- Serious, but not critical concern
- Effects in silicon devices normalized to convenient electron and proton energies
- Equivalent neutron damage effects defined to broaden available component data base

Displacement effects are the result of atoms being knocked out of their normal positions in the crystal lattice. The important effects appear as permanent damage, and the magnitude is a function of the integrated radiation exposure. For the Probe radiation environment, displacement effects are of concern only in semiconductor devices. The proton and electron environments both contribute to displacement damage.

The relative effectiveness of protons and electrons of various energies depends on the probability per unit path length for making a close encounter with an atom, resulting in an energetic recoil, and the relative effectiveness for creating permanent property changes as a function of recoil energy. Electrons and protons produce qualitatively different types of damage. Electrons tend to produce simple defects with an efficiency that depends sensitively on impurities present in the semiconductor before irradiation. Protons tend to produce defect clusters whose effectiveness is less dependent on subtleties in the starting material. The relative

effectiveness for electrons of various energies producing displacement damage in silicon has been studied theoretically and experimentally. Unfortunately, an accurate representation of the energy dependence of damage depends on the specific material (e.g., type, resistivity). However, for purposes of Probe design, a single relative damage curve can be used for silicon without causing undue error. This curve, normalized to unity at an electron energy of 3 MeV, is shown in Figure 1.9. Using this curve, any arbitrary spectrum, such as the external fluence described in Section 1.1.2, can be weighted and integrated to yield a fluence of 3 MeV electrons, Φ_3 , whose displacement damage effectiveness is the same (in silicon) as the original spectrum. In a similar manner, the curve of relative effectiveness of different energy protons, Figure 1.10, can be used to calculate the 20 MeV equivalent proton fluence, Φ_{20} . The normalization energies (3 MeV for electrons, 20 MeV for protons) were chosen because with a typical spectrum and thickness of overlaying material, the displacement-equivalent electron fluence is near the fluence of electrons of energy greater than 3 MeV, and similarly for protons of 20 MeV, but this rule is only approximate and does not hold for different spectra and shields. The spectrum at the affected silicon should be integrated over the damage curves, Figures 1.9 and 1.10, to deduce reasonably accurate values of the damaging influence.

A large fraction of the existing experimental data on displacement effects in semiconductors is for neutron irradiation. In this case, effects are generally normalized to that of a monoenergetic 1 MeV equivalent fluence. Thus, in evaluating experimental data, spectrum equivalences must be considered for both the proton and electrons of the Jovian environment and experimental results obtained from terrestrial simulators.

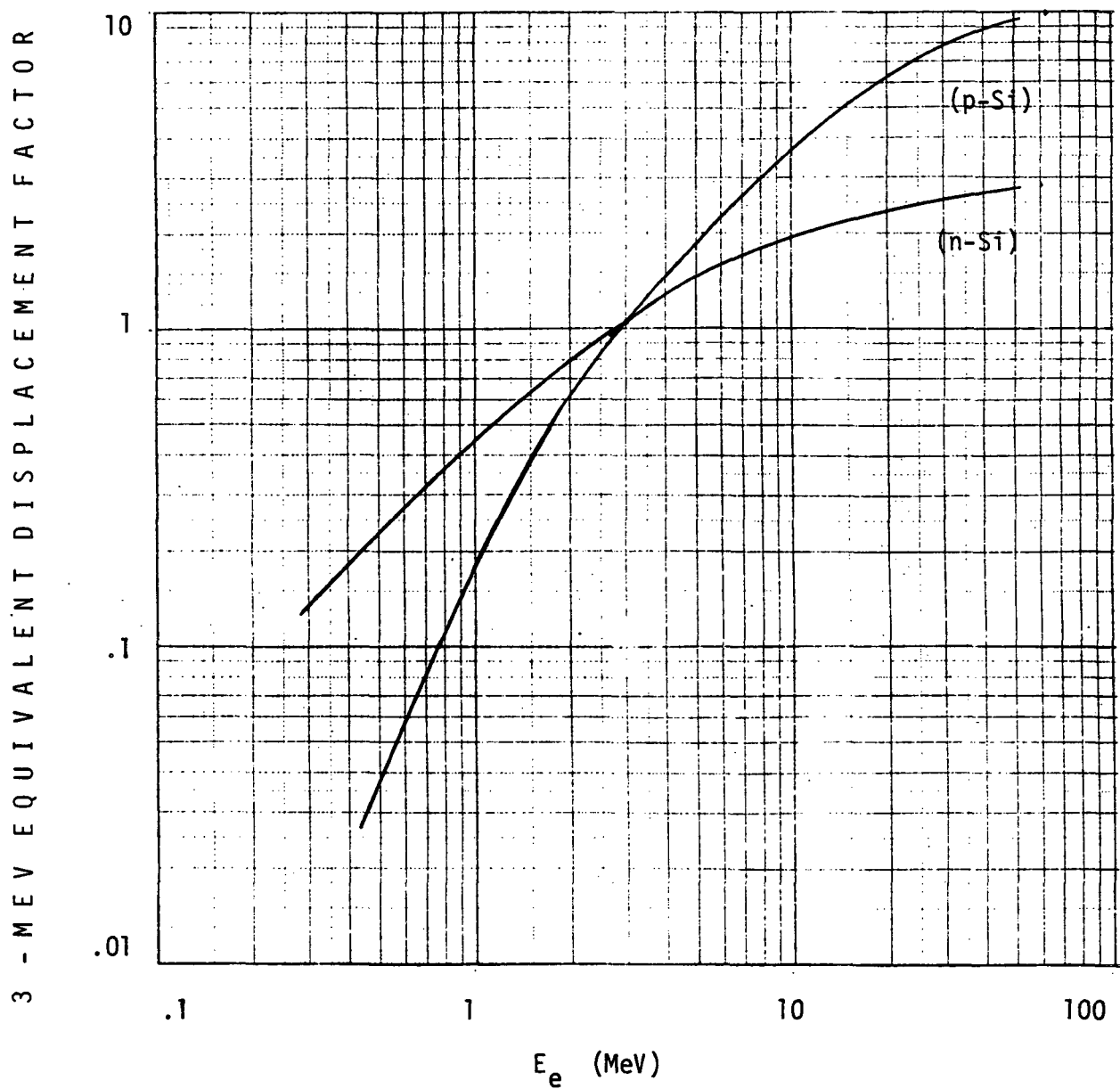


Figure 1.9: 3-MeV Equivalent Displacement Factors for Electrons of Various Energy Levels.⁴

20 - MEV EQUIVALENT DISPLACEMENT FACTOR

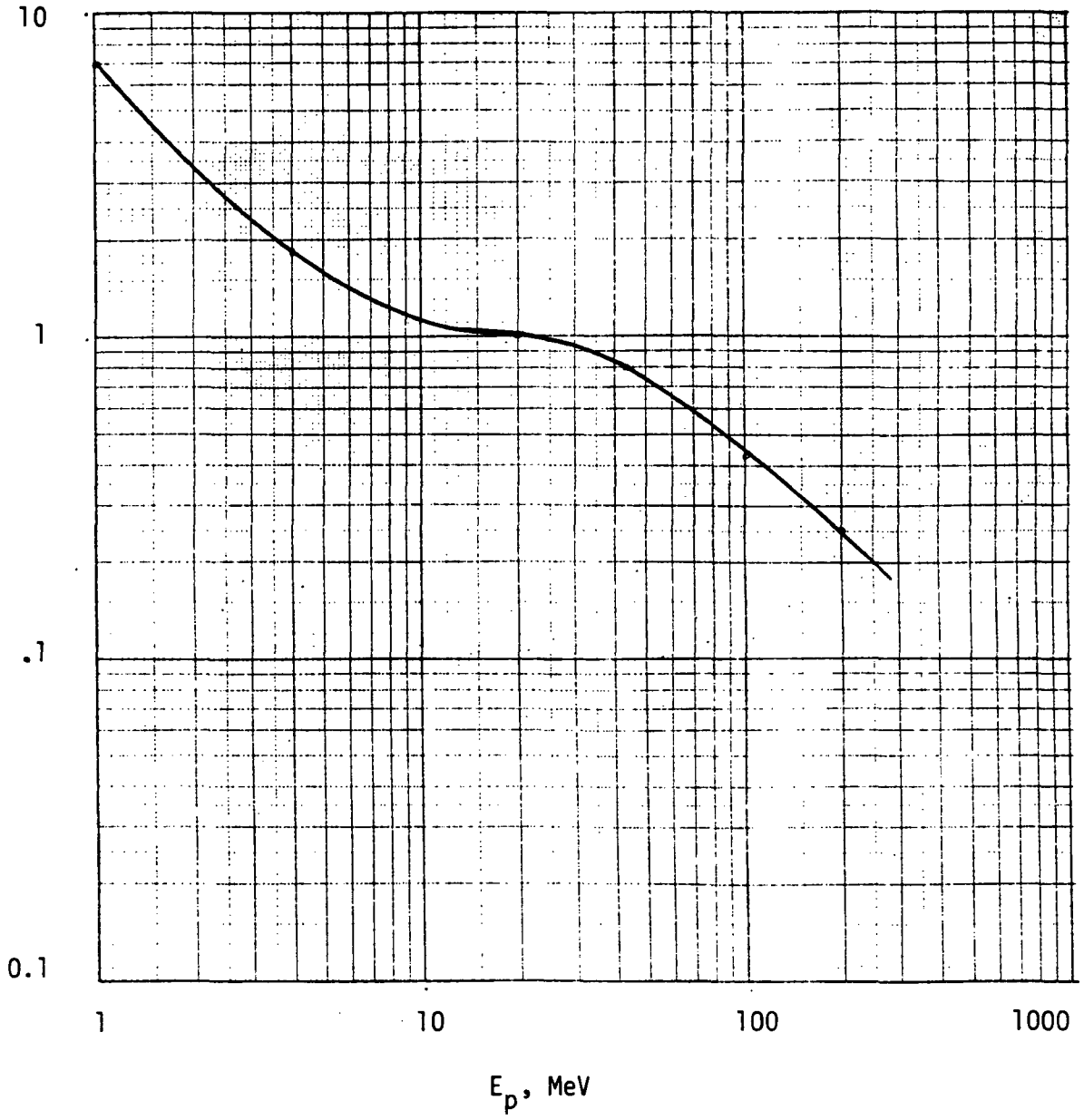


Figure 1.10: 20 MeV Equivalent Displacement Factors for Protons of Various Energy Levels.^{4,5}

The semiconductor material property that depends most sensitively on displacement effects is the minority carrier lifetime (τ). Therefore, devices whose useful characteristics do not depend on τ are insensitive to displacement effects damage. For Probe applications, displacement effects can be neglected entirely in MOS and JFET structures. The effect on bipolar transistors increases with increasing base width; therefore high-frequency transistors are less affected than low-frequency devices. Generally, the high-speed logic structures, such as TTL, use geometries in which displacement effects at Probe fluences are negligible. Displacement effects in rectifier and switching diodes can be neglected unless their application can be degraded by very subtle property changes, such as V_f . Voltage regulator diodes (VRD) ("Zeners") are often used in precision applications, in which a small change in voltage ($\sim 1\text{mV}$) can be significant. Such changes can occur, especially in the forward biased temperature-compensating diode that is frequently encapsulated with the VRD in a precision device. Efficiency of electro-optical transducers (LED, laser-diode, photo-diode, photo-transistor, solar cell, photoconductive cell, etc.) are particularly dependent on τ , and therefore are likely to be the most sensitive to displacement effects.

1.2.3 Transient Interference Effects

- Significant only in low current detector circuits and charge-storage microcircuits.

Ionizing radiation exposure can result in effects that interfere with experiment performance, but disappear with the end of exposure with no permanent damage. Ionizing radiation produces excess hole-electron pairs in the bulk semiconductor of a device at a rate proportional to the absorbed ionizing radiation dose rate. For silicon, this carrier generation rate, g , is given as

$$g = (4 \times 10^{13}) \dot{D} \text{ hole-electron pairs/second}$$

where \dot{D} is the absorbed ionizing dose rate in rads(Si)/s. For the particle energies of the Jovian radiation belts that penetrate to the silicon device chips, this carrier generation will be uniform throughout the bulk silicon of the device.

The effects of this carrier generation are primarily in a diode photoeffect at all p-n junctions. This photoeffect, just as in a solar cell, produces an increase in reverse-bias current, a short-circuit photocurrent or an open-circuit photovoltage.

For the Probe mission, the expected worst-case ionizing radiation dose rate is less than 100 rads(Si)/s which corresponds to a radiation-induced carrier generation of 4×10^{15} hole-electron pairs/s. At this radiation level, the carrier generation rate is comparable to thermal carrier generation rates at room temperature. In general then, transient interference effects will be negligible in semiconductor devices which have a comfortable design margin at elevated temperature (e.g., 100°C). The most critical semiconductor devices will be those that are critically dependent on extremely low junction leakage currents, such as dynamic MOS logic circuits, semiconductor image sensors and charge-coupled circuits. The effect in dynamic MOS logic circuits is an increase in the required refresh rate. In image sensors and CCD's the effect will appear as an increase in the dark current.

Transient interference effects may also be the result of ionization effects in non-semiconductor materials. Charge emission from metallic surfaces is on the order of 10^{-13} A/cm²-rad/s which would correspond to a worst-case of less than 10^{-11} A/cm² for the probe mission. This could have an effect in charge sensitive instruments and could result in electro-static charging of electrically-isolated metallic surfaces.

Optical materials will also luminesce during irradiation, generally re-emitting less than 1% of the absorbed energy in visible light. Sensors sensitive to low light levels must deal with this radiation-induced background.

1.2.4 Radiation Survivability

The Probe will encounter the Jovian radiation environment at approximately $20 R_J$ and the exposure will persist to the upper limit of the Jovian atmosphere at approximately $1.1 R_J$. In terms of the requirements on most of the Probe electronics, the radiation exposure will be over before operation is initiated. Unfortunately, however, the radiation exposure will cause significant permanent degradation in the performance parameters of critical electronic components. Displacement damage and long-term ionization effects are the result of interactions between the high energy particles and the bulk silicon and silicon passivation layer of the semiconductor devices. The parameter degradation accumulates with radiation exposure. For some critical semiconductor devices (such as MOS microcircuits) the degree of radiation damage is a function of electrical bias during exposure. Because of this bias dependence it is necessary to evaluate radiation effects under bias conditions representative of system operation, but significant parameter degradation can be expected for critical devices even under the most favorable bias conditions.

Operational calibration of instruments before Probe entry may be required while the Probe is still within the radiation environment. In this case the instrument design must account for additional post-calibration degradation in the critical electronic components and possible errors resulting from transient interference effects during calibration.

In summary, the high-energy Jovian radiation environment will cause significant performance degradation to critical semiconductor components even under conditions of passive, or turned-off operation during radiation exposure.

1.3 CRITICAL DESIGN CONSIDERATIONS

The radiation environment for the JOP is essentially another set of constraints on the normal design process. It is unique only in the unfamiliarity of many designers with the effects, and the relative scarcity of adequate radiation-response data on components of interest.

The overall design objective of the Probe is for a high probability of successful performance during an intense observation period following a long dormant ride. In general, overall probe performance has the highest priority. Failure of any experiment, for example, must be limited to that experiment alone.

Acceptable performance of the Probe electronics in the radiation environment can be obtained by a proper combination of design considerations. These include:

- a) Device hardening by component and material selection.
- b) Circuit hardening by making the circuit tolerant to expected changes in device parameters.
- c) Taking advantage of the inherent shielding of the structure and other electronic components by proper placing of sensitive devices.
- d) Deliberate shielding of sensitive devices.

It is important to apply quantitative estimates of the radiation-induced changes in order to properly select the optimum trade-off between

these different design options and to allocate the survivability budget between the potentially soft components.

1.3.1 Component and Circuit Design Applications

The sensitivity of a given component to radiation depends on the application. In general, radiation problems occur when a component is used close to its limits in operating range or precision. Examples of limits in operating range are very low p-n junction current densities, or very close match between parameters of junction pairs.

For the JOP radiation environment, long-term ionization effects in the surface layer of semiconductor devices are of prime importance, whereas bulk displacement damage is of less importance. Surface ionization effects produce leakage currents in semiconductor devices with back-biased junctions. Bipolar transistors suffer degradation in dc gain, particularly at low current levels. MOS devices are most likely to become nonfunctional in an ionizing radiation environment. Next most sensitive are the linear integrated circuits. Displacement damage is restricted to low-frequency bipolar devices causing a decrease in gain (transistors) or efficiency (solar cells). Table 1.3 shows types of devices affected by these environments.

The devices and materials of concern for long-term ionization are:

- a) MOS structure (threshold voltage shift, enhanced leakage in CMOS pairs).
- b) Bipolar transistors (h_{FE} degradation especially at low I_C), and junction field effects transistors (JFETs) (enhanced source-drain leakage current).
- d) Quartz resonant crystals (frequency shifts).
- e) Optical materials (coloration).

TABLE 1.3: Radiation Sensitive Components

	<u>Long-term Ionization Effects</u>	<u>Displacement Effects</u>
MOS Devices	I	V
Linear Bipolar IC's	I	III
Digital Bipolar IC's	IV	IV
I ² L	II	II
Bipolar Transistors	I	III
JFET's and JFET Type Analog Switches	III	V
Electro-Optical Devices	II	II
Crystal Oscillators and Filters	II	V
Precision Voltage Regulator Diodes	III	II
Other Diodes and Rectifiers	IV	IV
Optical Materials	II	V
SCR's, UJT's, Thyristors	II	I

Priorities:

I: Serious concern

II: Significant attention required, no serious constraints

III: Some attention required

IV: Review only

V: No attention needed

Displacement effects can affect the following devices and properties in the Probe electronics:

- 1) Bipolar transistors with low f_T (h_{FE} , $V_{CE_{SAT}}$, $V_{BE_{SAT}}$).
- 2) Precision voltage regulator (V_2).
- 3) Light emitting diodes (LED) (light emitting efficiency).
- 4) Semiconductor photodetectors (sensitivity).
- 5) SCR's, UJT's, thyristors (turn-on sensitivity, holding current).

The last radiation effect to consider is transient interference. There are five types of transient interference in electronics at these low dose rates:

- a) Primary photocurrents in low current sensitive input stages to the electronics.
- b) Components extremely dependent on low junction leakage currents such as dynamic MOS logic circuits and charge-coupled devices.
- c) Electron emission from cathodes of electron multiplier-type detectors.
- d) Ionization-induced conductivity in photo-sensitive materials, such as those in the VIDICON detector surface.
- e) Ionization-induced fluorescence in optical materials such as detector windows and lenses.

Devices whose normal operating point is at currents in the μA range or above will not be significantly affected by interference.

1.3.2 Shielding Design

It is clear that moving from an unacceptable design condition requires increasing parts (circuits) capability and/or reducing the radiation level at the parts locations. The latter effect can be obtained by relocating sensitive parts to areas of greater inherent shielding or by adding local shielding.

The addition of shielding can be used to reduce the radiation levels, with a resulting increase in weight as a penalty. Figure 1.11 presents the dose for the "worst" and "best" probe entry angles as a function of total uniform shield thickness. A reasonably accurate calculation of the dose at a device located inside a nonuniform shield geometry can be estimated by dividing the 4π solid angle into segments within each of which the overlying material is approximately of constant thickness (in gm/cm^2). The total dose is then calculated by summing the contribution from each solid angle, attenuated as given in Figure 1.11. An example is given in Table 1.4.

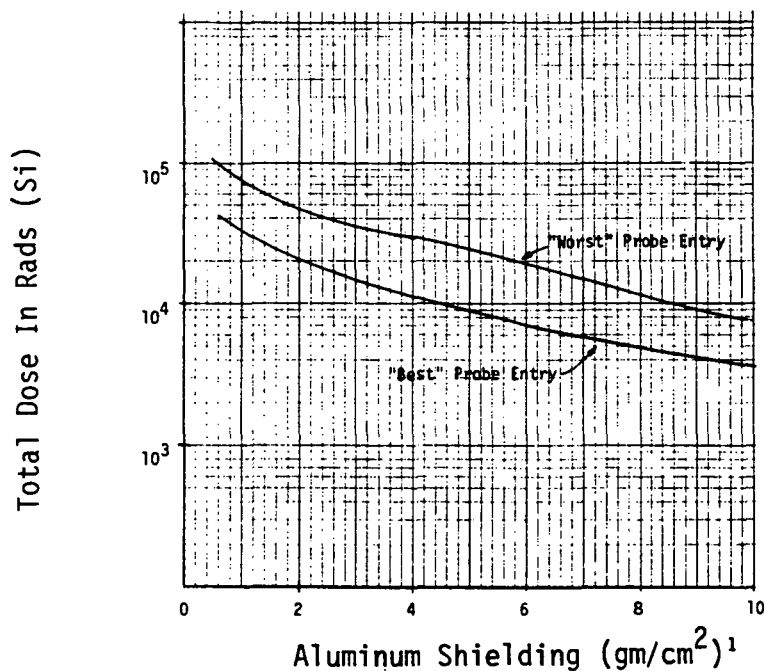


Figure 1.11: Total Dose vs. Shielding

TABLE 1.4: Example Calculation of Total Dose at an Arbitrary Location within the Probe.

Shield Density (gm/cm ²)	Solid Angle Segment ($\Omega/4\pi$)	Dose per 4 π Segment (rads)	Dose (rads)
0.60	.33	8.7×10^4	2.9×10^4
1.00	.48	6.5×10^4	3.1×10^4
3.60	.02	3.3×10^4	0.08×10^4
6.80	.10	1.4×10^4	0.14×10^4
9.6	.07	8×10^3	0.05×10^4
TOTAL DOSE = 6.2×10^4 rads			

Assume that for an arbitrary location inside the probe, an analysis reveals the shield segments and solid angle factors shown in columns 1 & 2 of Table 1.4. From Figure 1.11 we obtain the dose for the amount of shield material within each segment as shown in Column 3. The actual dose contributed per segment is the product of Columns 2 & 3 and is shown in Column 4. Finally, the total dose is the summation of each entry in Column 4 and is shown at the bottom of Table 1.4.

By analyzing locations within the probe in this manner as shown in Figure 1.12, it may be possible to add shielding in very limited amounts but still obtain a significant reduction in total dose (locations defined on Figure 1.7). Thus, from Table 1.4, entries 1 & 2 contribute over 95% of the total dose but only involve about 81% of the 4 π solid angle. Clearly, adding less than full spherical shielding can still obtain a considerable effect. This kind of analysis should be performed for determining any additional shielding.

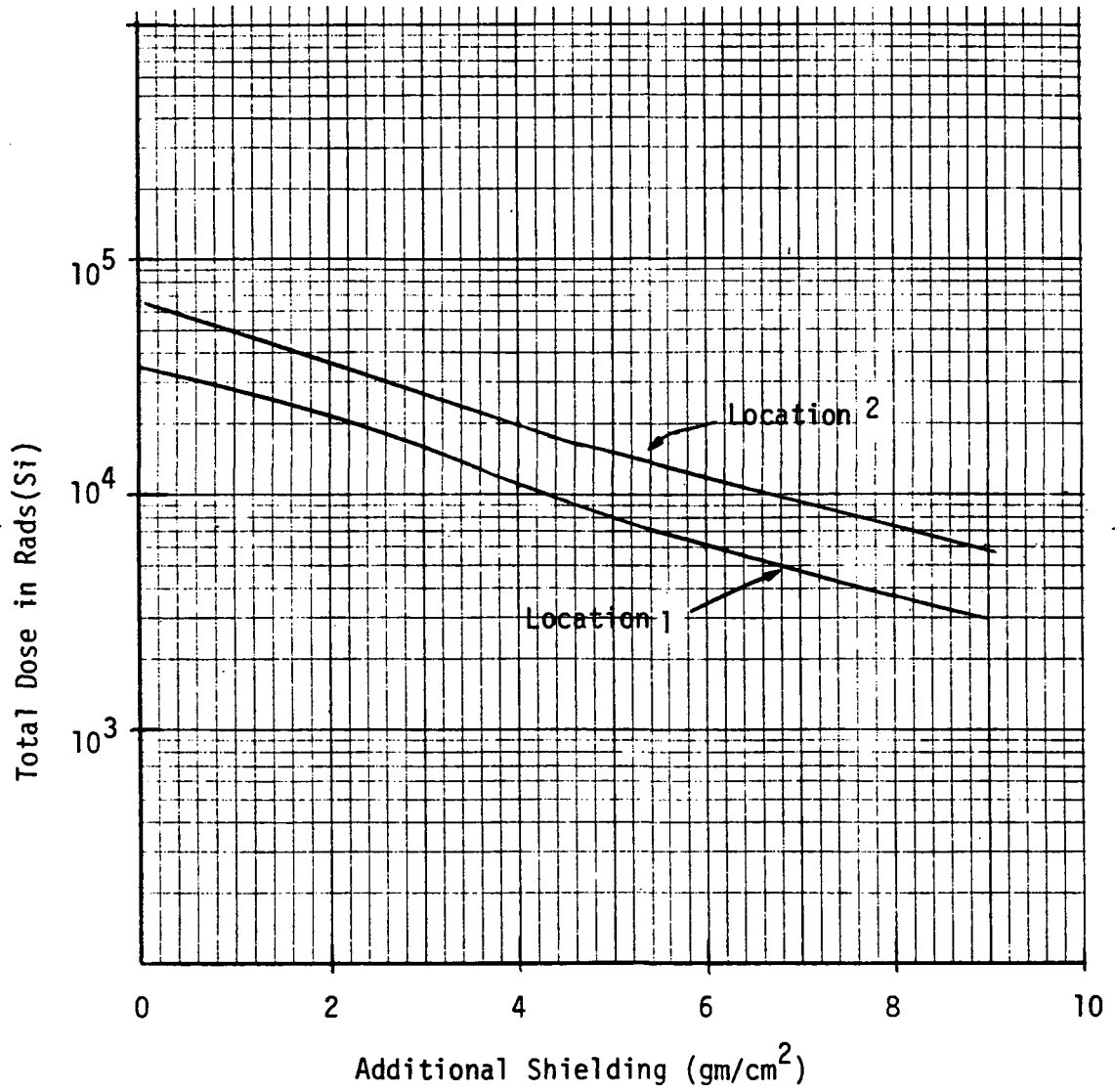


Figure 1.12: Effects of Additional Shielding

SECTION 2

2.0 COMPONENT RADIATION EFFECTS

In this section we will describe the three critical radiation effects (long-term ionization, displacement, and transient interference) in various electronic and optical components. Care should be exercised when using data shown in this section for design values since it represents a cross-section of data available to date. Other similar devices may be better or worse. The existing data will show how and by what magnitude the effects may be expected. Functional dependence on measurable parameters will be presented where they are known. Section 3 will provide methods to design systems and determine the actual radiation hardness of the devices used in the systems.

2.1 BIPOLAR TRANSISTORS

2.1.1 Long-Term Ionization Effects

<u>Bipolar Transistors - Long-Term Ionization Effects</u>
<ul style="list-style-type: none">- h_{FE} decreases- I_{CBO} increases- Noise (Current and Voltage) increase

The effects of long-term ionization on bipolar transistors are mainly in the degradation of the common emitter current gain (h_{FE}); particularly

at low collector bias currents due to a radiation-induced increase in base current (I_b). At the dose levels considered for this handbook, breakdown voltage effects need not be considered and switching response is affected only by the change in gain.

The decrease in common-emitter current gain, h_{FE} , can be represented at low doses by an increase in $1/h_{FE}$ proportional to dose. After the change is large ($h_{FE} < 20$) the response may saturate or become superlinear, producing catastrophic degradation of the device. Leakage current and noise in the transistor (noise current and noise voltage) can increase due to long-term ionization by more than 400% of their original pre-irradiation values. Both NPN and PNP transistor types have similar effects on electrical parameters with the differences being in the magnitude of the effects.

Figure 2.1 shows qualitatively how the gain changes with dose with approximate dose levels for a general PNP transistor. Bipolar transistors degrade in gain due to long-term ionization more for the active state than the passive state; the passive state transistor degrades more than transistors in saturation.⁶ This is the result of reverse bias junction showing a greater radiation effect than forward bias.

Since variations in manufacturing processes and device designs can influence the gain degradation even for the same device type, conservative estimates need to be made for design parameters.

Figure 2.2 presents data on the rate of degradation for a variety of transistors as a function of collector current, I_C . A first order correction can be made by normalizing the collector current values to the maximum h_{FE} current ($I_{C_{max}}$). The decrease in damage rate with increasing collector current is apparent in all devices. The dependence on I_C varies between devices, but averages $\sim \sqrt{I_C}$. For 150 krads, most devices fall

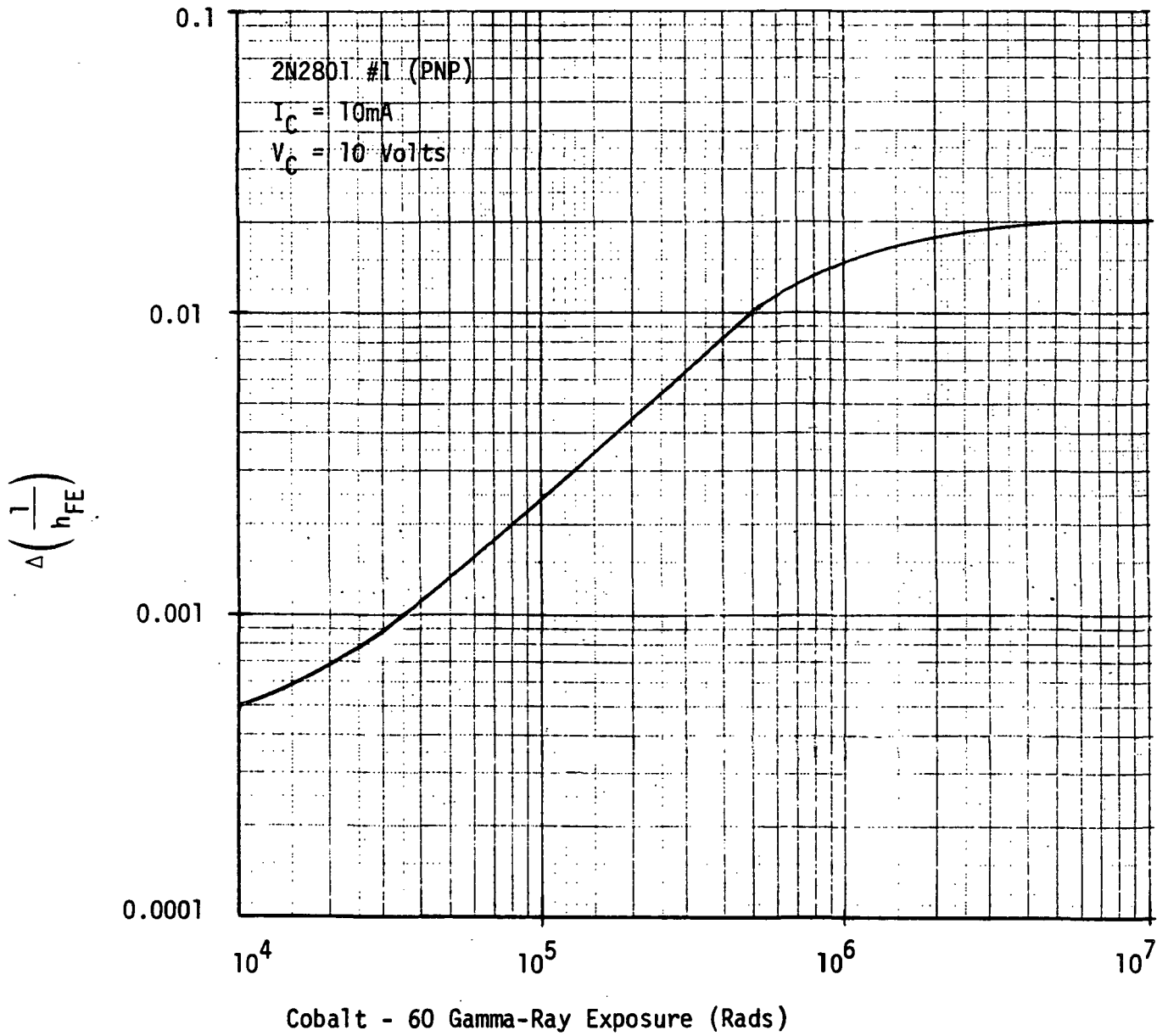


Figure 2.1: Damage Curve of Gain Vs. Ionization Dose⁷

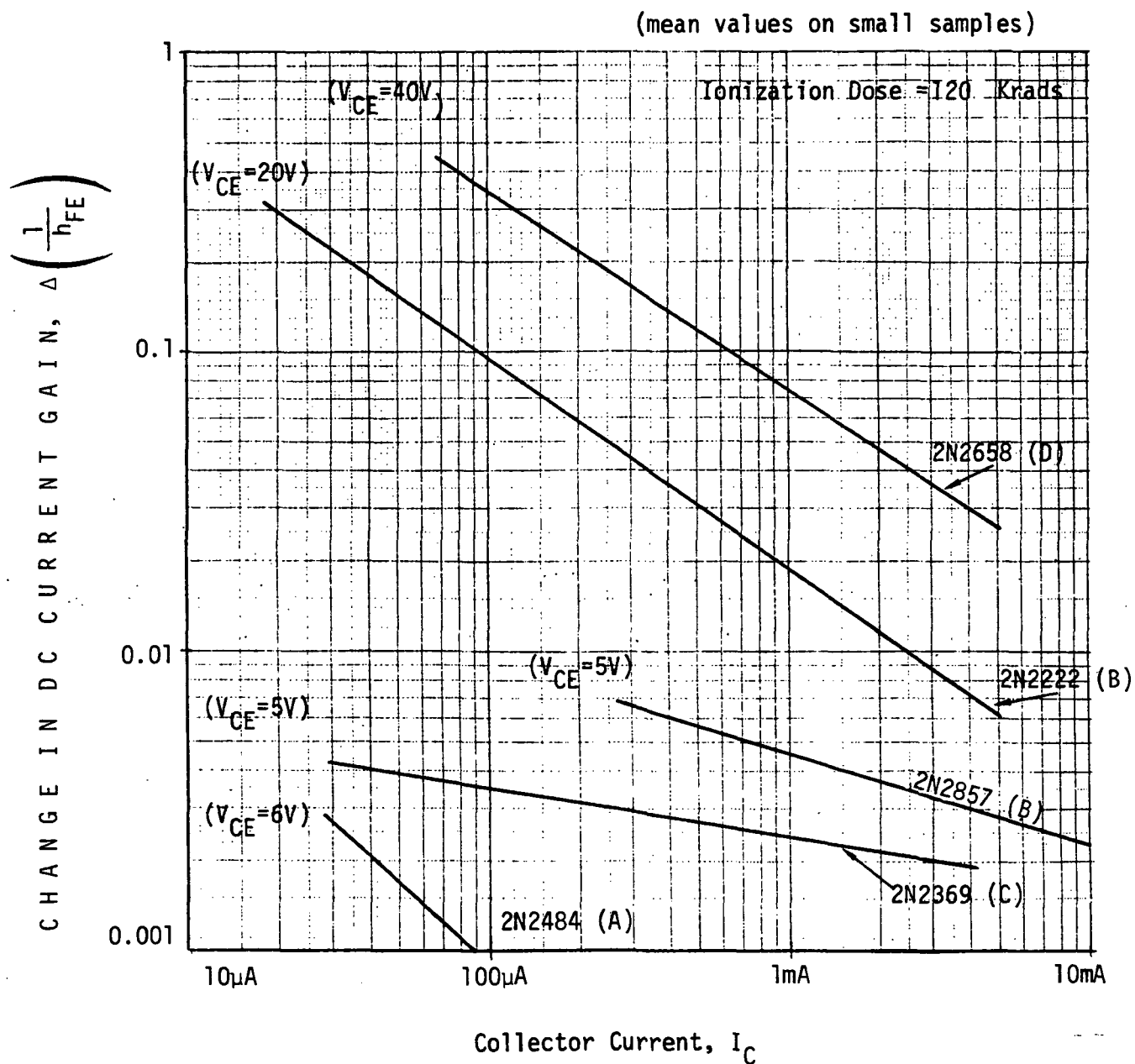


Figure 2.2: Typical Long-Term Ionization Effects in Several Types of Bipolar Transistors from Various Manufacturers (A, B, C, and D) Showing Wide Variations between Device Types.⁸

below the line

$$\log_{10} \Delta(1/h_{FE}) = -\frac{1}{2} \log_{10} (I_C) - 0.52$$

where I_C is in μ amps

but a few devices exceed this line considerably. At present we don't know of any means other than irradiation of samples from test lots of the devices to predict which devices will have the larger response. Even the same device type will exhibit a different response when manufactured by different vendors and even at different times by the same manufacturer. Both of these cases are shown in Figure 2.3 for the 2N2222A transistor type.

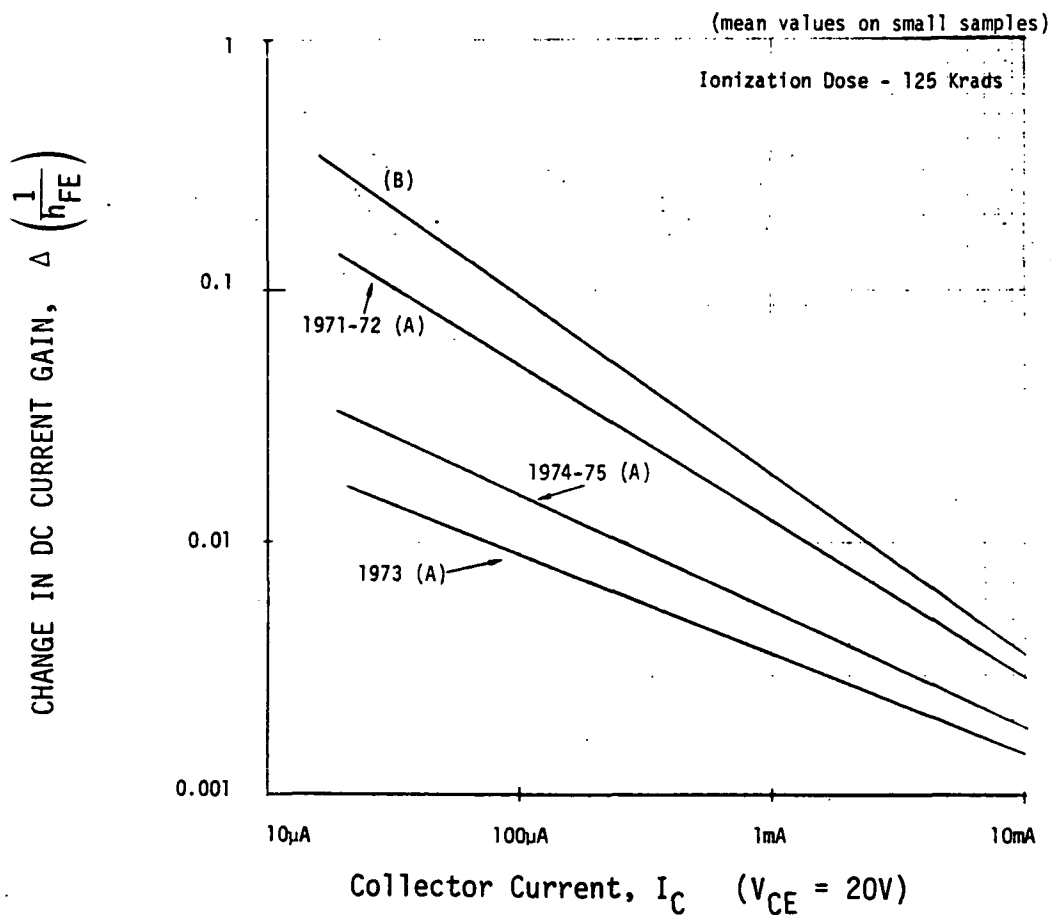


Figure 2.3: Typical Long-Term Ionization Effects in 2N2222 Bipolar Transistors from Two Manufacturers (A and B) Showing Variation with Date Produced and between Manufacturers.⁸

Figure 2.4 illustrates an attempt to establish worst case degradation rates from device specification data. There is reason to believe that for a given passivation process, the rate of degradation will depend on junction breakdown voltage (BV_{ebo}), emitter current density, and base width in a manner producing a linear relationship between the functions plotted in Figure 2.4. The extensive data taken by JPL for the MJS program⁸ are plotted. The worst-case data show a strong superlinear dependence on BV_{ebo} . Whether this is a real dependence or the result of variations in composition of the passivation-layer we cannot say. However, the evidence is clear that degradation rates as large as

$$\frac{\Delta(1/h_{FE})}{\Delta D} \left(\frac{I_c}{I_{c_{max}}} \frac{\sqrt{f_t}}{BV_{ebo}} \right)^{1/2} \sim 10^{-4}$$

have been observed, where I_c is the collector current, $I_{c_{max}}$ is the

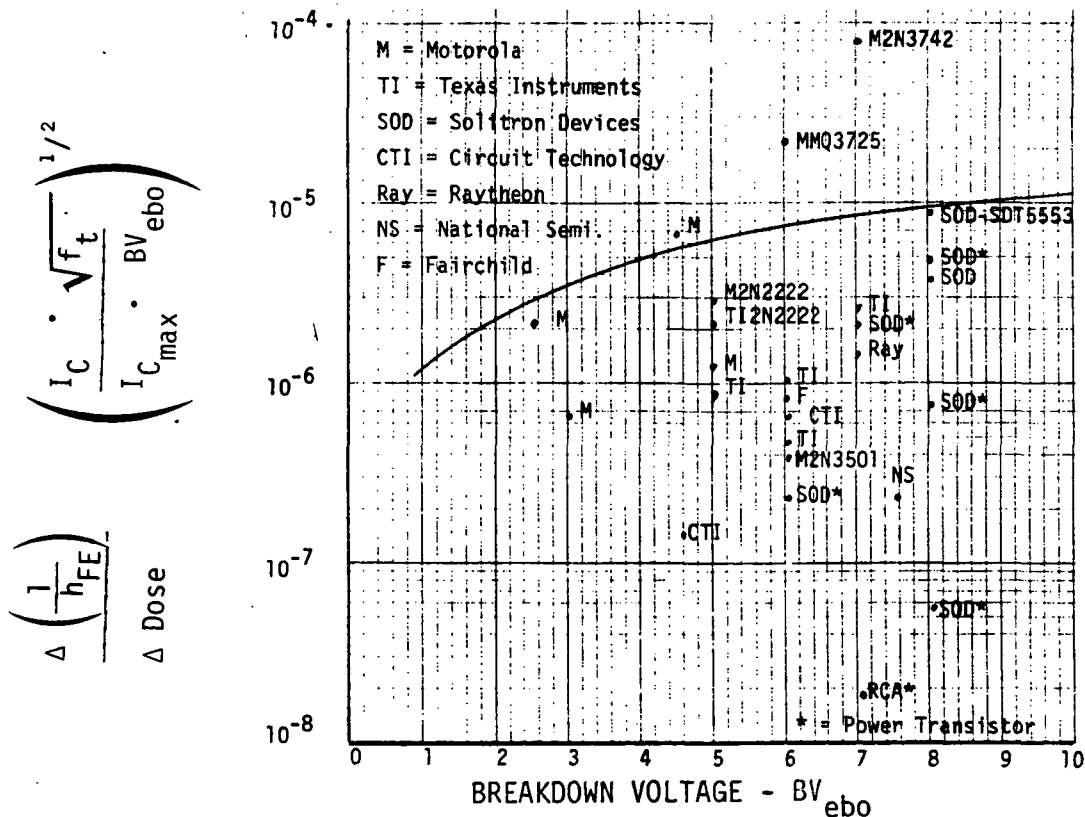


Figure 2.4: Long-Term Ionization Degradation Rates for NPN Transistors Normalized for Emitter Current Density Dependence. (3 MeV electron effects only).

collector current at peak h_{FE} , and f_T is the gain-frequency product in Hz. For a device with $f_T = 10^8$ Hz, $BV_{ebo} = 7V$ and $I_c/I_{c_{max}} = .01$, this corresponds to $\Delta(1/h_{FE}) = 3 \times 10^{-5}$ D(rad). In other words, h_{FE} would decrease to less than 10 at 3000 rad(Si). At this time it is not clear whether the envelope of the highest points in Figure 2.4 can be used as a safe design criterion. It is clear that lower values of degradation rates cannot be assumed without experimental data to substantiate them.

For leakage current (I_{CBO}), an initial sharp rise at low doses is followed by a stable region over higher dose level.⁶ Both NPN and PNP transistors show this same initial increase. Figure 2.5 is an example of the I_{CBO} increase that can be expected, although the increase is not large enough to be worrisome in most applications.

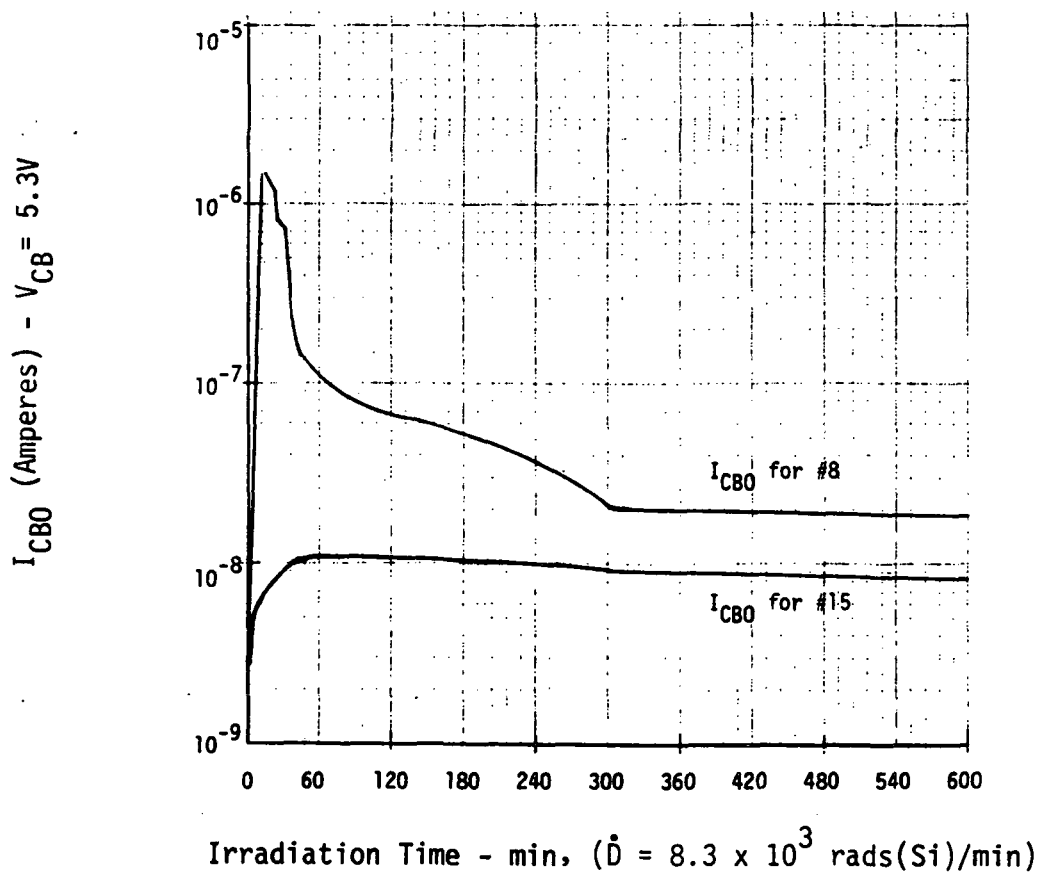


Figure 2.5: I_{CBO} vs. Irradiation Time.⁶

Both PNP and NPN transistors show an increase in noise current and noise voltage for dose levels down to 10^5 rad(Si). PNP transistors generally degrade faster in noise at lower doses than NPN transistors.⁹ The noise increase levels off at approximately $10^6 - 10^7$ rad(Si) for both types. The magnitude of change of the noise current usually determines the change in noise voltage. Tables 2.1, 2.2, and 2.3 show some experimental data demonstrating the possible magnitude of the effect.

The changes described depend on the device type, manufacturer, date of production of the devices and the bias condition during irradiation. Each can be the most important factor in any one case. The main factors which control the changes in the electrical properties of bipolar transistors for the long-term ionization effect are the build-up of trapped positive charge in the oxide near the silicon surface and creation of surface states at the silicon-silicon dioxide interface. The manufacturer's processing steps and resultant oxide quality have therefore a major impact on the resultant radiation hardness. This is why two manufacturers supplying the same part type can have such wide variations in radiation hardness between each other's product, and even within a manufacturer's own product over a significant length of time there can be large differences in radiation hardness.

The chip design of the device and the way it is used (bias condition) is also a major factor in the hardness of a device. This is one area that the system designer can control. As shown in Figure 2.4, there was quite a spread of worst case data even for the same breakdown voltages.

Gain degradation from long-term ionization is known to depend on bias conditions. Examples of the effect of bias in the active region of the transistor is shown in Figures 2.6, 2.7, and 2.8; and compared with the passive case.

TABLE 2.1 Noise Current Corner Frequency,⁹ $f_1(\gamma) = f_1 + \Delta f_1(\gamma)$

Device Type	f_1 (kHz) $\gamma = 0$	f_1 (kHz) $\gamma = 10^5 \text{ Rad(Si)}$	f_1 (kHz) $\gamma = 1.1 \times 10^6 \text{ Rad(Si)}$	f_1 (kHz) $\gamma = 1.1 \times 10^7 \text{ Rad(Si)}$
8883	12	30 - 38	79 - 94	250 - 188
2N5332	10	9 - 32	40 - 56	152 - 121
SN14021	5	7 - 19	24.4 - 26.5	40 - 40
X416S	5	5 - 10	17.5 - 38.4	48 - 46
X416L	0.7	1.0 - 0.8	2.5 - 2.3	14.4 - 15.2
A	0.49	0.71	2.3	5.16
B	0.87	1.27	3.2	7.2
C	0.13	1.4	6.4	7.5
D	4.2	11.2	48	43
E	0.2	1.97	9.1	9.1

Note: Two numbers shown for the first 5 device types are values of f_1 obtained by extrapolating from 100 Hz and 1000 Hz respectively. Accuracy of f_1 determination is $\pm 20\%$ for the serial group devices.

TABLE 2.2 Transistor Types in Parallel-Irradiation Group⁹

Device Designation	Type	h_{FE}	Base Depth (Na Lines)	Emitter Geometry	Number of Transistors
8883	PNP	52	< 5	Stripe	30
2N5332	PNP	51	< 5	Stripe	40
X416S	PNP	42	< 5	Stripe	40
X416L	PNP	35	< 5	Stripe	21
SN14021	PNP	40	< 5	Stripe	21

TABLE 2.3: Transistors in Serial-Irradiation Group⁹

Device Designation	Type	h_{FE}	Base Depth (Na Lines)	Emitter Geometry	Emitter Area (Mil ²)	Emitter Periphery (Mils)	Number of Transistors
A	NPN	140	1	Stripe	54	54	13
B	NPN	303	28	Circle	12.6	12.6	12
C	NPN	449	4	Circle	3.1	6.3	9
D	PNP	112	9	Stripe	15	35	12
E	PNP	457	4	Stripe	2.8	9.4	20

Note: Two type E units and one type C unit are on a single chip
 parallel-irradiation devices differ from serial-irradiation devices by the method of irradiation and measurement of noise figure. Parallel refers to one exposure level - one measurement per device and no device used again for the next higher radiation level while serial refers to one group of devices subjected to higher and higher radiation levels with measurements of noise figure taken between exposures.

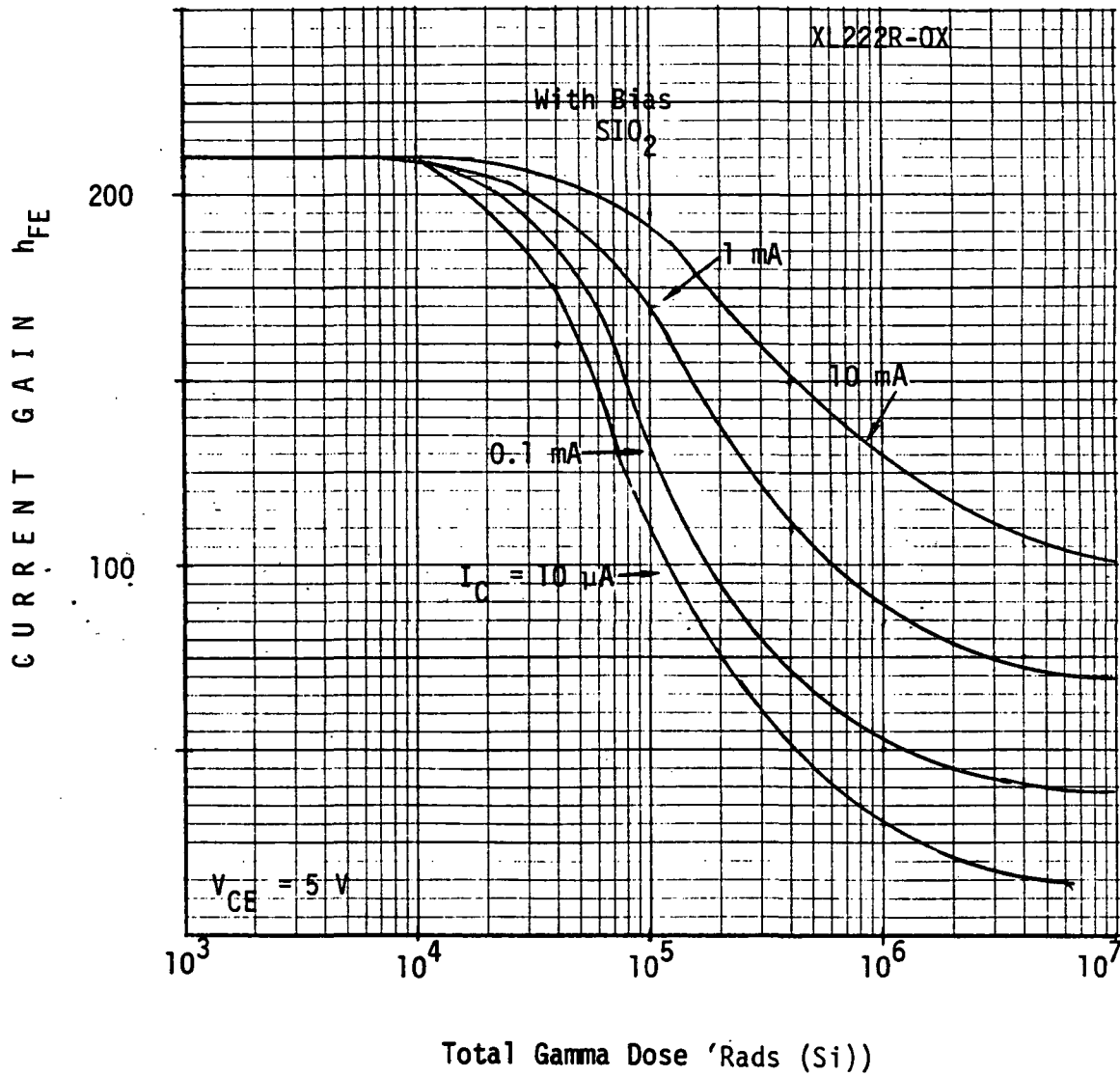


Figure 2.6: Device Current Gain vs. Gamma Dose for a PNP Device with Oxide Passivation Irradiated With Bias.¹⁰

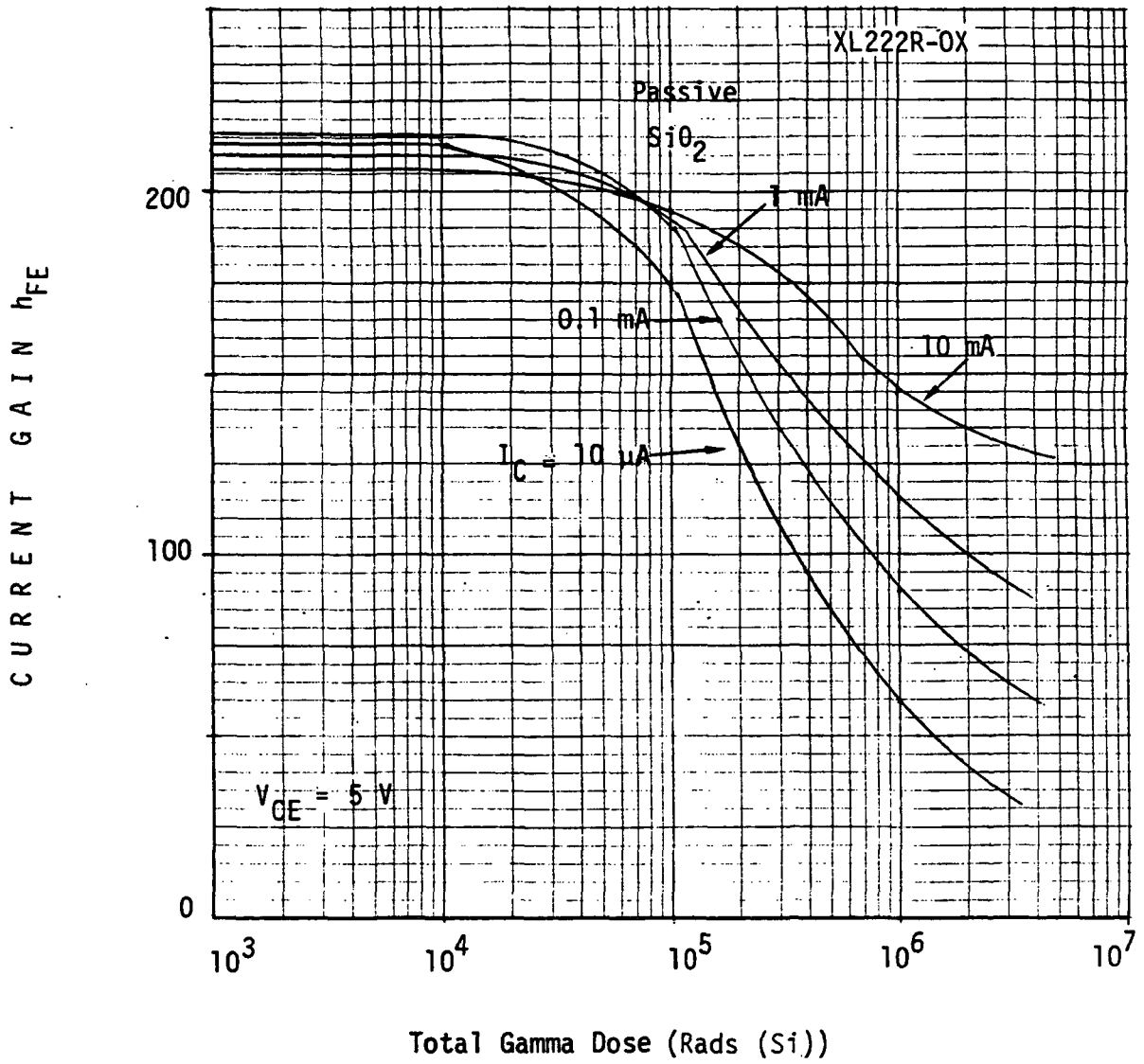


Figure 2.7: Device Current Gain vs. Gamma Dose for a PNP Device with Oxide Passivation Irradiated with No Bias.¹⁰

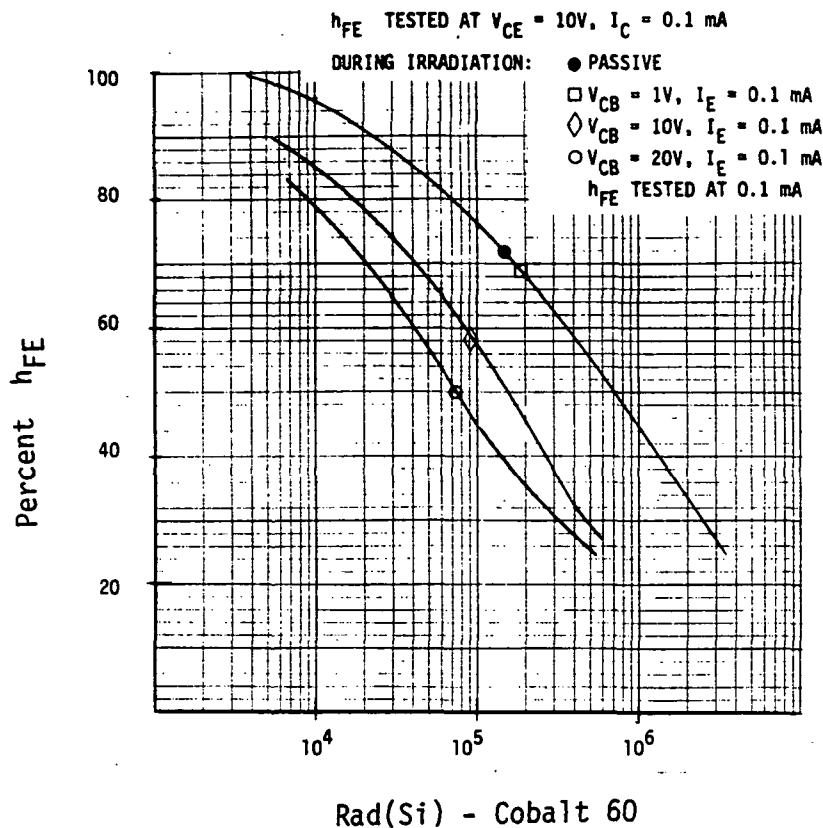


Figure 2.8: 2N1613 Transistor Voltage Dependence of Degradation.¹¹

Low emitter (or collector) currents and high collector bias voltages increase the gain degradation.^{6,10} Thus, for low base-emitter voltages (V_{BE}) corresponding to low emitter currents and for high collector-base voltages (higher reverse bias), the gain decreases faster with increasing dose. As shown in Figure 2.9, I_{CBO} versus dose is also dependent on bias conditions of the collector-base junction. More change in I_{CBO} occurs initially for collector-base bias than for a passive state; but the long term total dose effect appears to be similar.

Additional insight into the gain degradation of bipolar transistors is presented in an extensive JPL study of the 2N2222.¹² Substantial samples were obtained from several manufacturers and exposed under a variety of bias conditions. Perhaps the most significant was the conclusion that almost all of the data could be collected in a log normal distribution with a standard deviation of a factor of 1.8 in $(1/h_{FE})$. If we assume $\Delta(1/h_{FE})$ is proportional to dose for sufficiently low doses, this corresponds to a standard deviation in the failure dose distribution of a factor of 1.8 also.

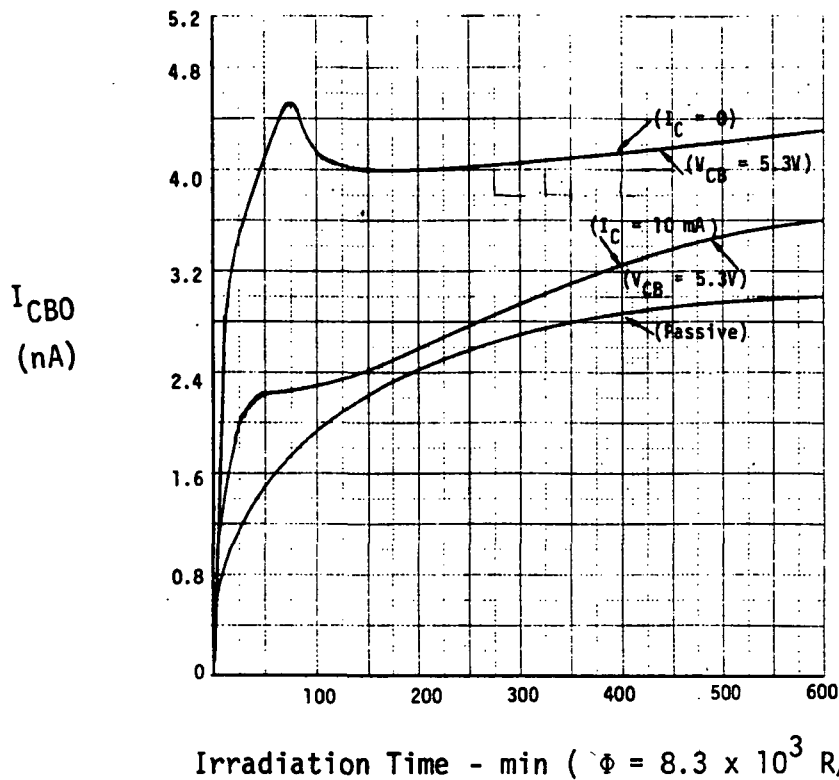


Figure 2.9: I_{CBO} as a Function of Exposure Time for Various Biases during Irradiation.⁶

2.1.2 Displacement Effects

Displacement effects produce long term degradation in semiconductor devices primarily by decreasing the minority-carrier lifetime. In bipolar transistors, the principal result is a decrease in current gain (h_{FE}) although subtle changes in voltages (e.g., V_{BE} , $V_{CE_{SAT}}$) can also occur.

As discussed in Section 1.2.2, the displacement damage effectiveness of a spectrum of particles can be related to a standard energy for each particle type (e.g., 3 MeV for electrons, 20 MeV for protons, 1 MeV for neutrons). With larger uncertainty they can also be converted from one particle type to another as shown in Section 3.1.

Displacement damage induced degradation of h_{FE} in bipolar transistors can be represented by the equation:

$$\frac{1}{h_{FE}} = \frac{1}{h_{FE_0}} + \frac{0.2 K_d \Phi}{f_T}$$

where h_{FE_0} , and h_{FE} are the gain before and after irradiation, respectively, Φ is the radiation fluence, f_T is the unity-gain roll-off frequency, and K_d is a damage constant derived from minority-carrier damage:

$$1/\tau = 1/\tau_0 + K_d \Phi$$

The value of K_d depends on the particle type and energy, on the resistivity and injection level (e.g., emitter current density) of the semiconductor material, and in some cases on the impurity type. Typical values of K_d at low injection levels are $K_{de} \approx 3 \times 10^{-8}$ to 3×10^{-7} cm²/sec for 3 MeV electrons, $K_{dp} \approx 10^{-5}$ to 10^{-4} cm²/sec for 20 MeV protons and $K_{dn} \approx 2 \times 10^{-6}$ to 2×10^{-5} cm²/sec for 1 MeV neutrons.⁵

A few examples of proton-irradiation data are given in Reference 13. For example, the rate of degradation of a 2N1613 transistor irradiated with the case removed with 20 MeV Protons at $I_c = 10\text{mA}$ is given as:

$$\frac{d(1/h_{FE})}{d(\Phi_{20})} = 3.5 \times 10^{-14} \text{ cm}^2$$

Given the nominal value of $f_T \sim 300$ MHz for a 2N1613, this value corresponds to $K_{dp} \sim 5 \times 10^{-5}$ cm²/sec, which falls within the range given above.

There exist large quantities of neutron data.¹⁴ However, if we combine worst-case proton and electron radiation levels with worst-case damage conversion levels the equivalent neutron fluence becomes appreciable

for lower frequency devices. For example, using the factors from Reference 14 and the worst case fluence from Section 1.1.2,

$$\Phi_3 \sim 3 \times 10^{12} \text{ e/cm}^2$$

$$\Phi_{20} \sim 9 \times 10^{10} \text{ p/cm}^2$$

$$\Phi_1 = 30 \times 9 \times 10^{10} + .06 \times 3 \times 10^{12} \cong 3 \times 10^{12} \text{ n/cm}^2$$

Neutron irradiation data on the 2N1613 indicate at $I_c = 10\text{mA}$, $\Delta(1/h_{FE})/\Delta\Phi_1 = 2.6 \times 10^{-15}$, or a damage constant of $K_{dn} = 3 \times 10^{-6} \text{ cm}^2/\text{sec}$. which again falls within the range of K_{dn} given above.¹⁴

We can now use various data to derive worst case values for $\Delta 1/h_{FE}$ for a transistor with $f_T = 300 \text{ MHz}$ (e.g., 2N1613) as follows:

- a) For protons from $K_{dp} \leq 10^{-4} \text{ cm}^2/\text{sec}$, $\Delta(1/h_{FE}) \leq 7 \times 10^{-3}$
- b) For protons from Reference 13 data, $\Delta(1/h_{FE}) = 3.5 \times 10^{-3}$
- c) For electrons from $K_{de} \leq 3 \times 10^{-7} \text{ cm}^2/\text{sec}$, $\Delta(1/h_{FE}) \leq 6 \times 10^{-4}$
- d) For neutron equivalent for $K_{dn} \leq 2 \times 10^{-5} \text{ cm}^2/\text{sec}$, $\Delta(1/h_{FE}) \leq .04$
- e) For neutron equivalent from Reference 14 neutron data,
 $\Delta(1/h_{FE}) \leq 6 \times 10^{-3}$

This example illustrates two important points:

- 1) The equivalent neutron fluence is dominated by the assumed proton fluence. It decreases rapidly with extra shielding, since the proton fluence is rapidly attenuated.
- 2) The equivalent neutron fluence is useful for comparing with experimental neutron data (e.g., item e above) not for calculation with worst-case damage constants (e.g., item c above).

It can be safely assumed that significant changes in saturation voltages do not occur until the h_{FE} has decreased markedly. For example, in Reference 13, on a 2N834 at $\Phi_{p20} = 3 \times 10^{12}$ protons/cm², $\Delta V_{CE_{SAT}} = 10$ mV, whereas $\Delta(1/h_{FE}) = .03$. At $\Phi_{p20} = 10^{11}$ protons/cm², the $\Delta V_{CE_{SAT}} < 1$ mV. It can be safely assumed that $\Delta V_{CE_{SAT}} < 10$ mV as long as $\Delta(1/h_{FE}) < .01$. If such changes are significant to a circuit application, test data on the actual device should be sought.

It is recognized that variations of displacement effects occur within a device type manufactured at a given time, with time of manufacture, and between manufacturers. This subject has not been studied sufficiently to derive confident conclusions. It is clear that the most important, but not the only causal variable is the transistor base width, which can be controlled by a screen on minimum value of f_T . A study of transistors procured as JANTX equivalent devices revealed variances over a period of years corresponding to a log-normal standard deviation of up to a factor of 1.5, although the distributions for most device types fell within a factor of 1.2.¹⁵

2.1.3 Transient Interference Effects

By calculating the carriers generated in a typical bipolar transistor for a dose rate of 100 rads(Si)/s using the expression found in Section 1.2.3,

$$g = (4 \times 10^{13}) \dot{D} = (4 \times 10^{13}) (10^2) \cong 4 \times 10^{15} \text{ carriers/second}$$

For a good transistor using standard packaging techniques, the minority-carrier lifetime = $\tau \cong 10^{-6}$.

Therefore, the carriers available due to transient radiation = $5 \times 10^{15} \times (10^{-6}) \cong 10^{10}$ which is about the thermal generation rate in silicon. The transient radiation effects appear to be no larger than the normal leakage currents found in all bipolar transistors.

2.2 OTHER DISCRETE SEMICONDUCTOR COMPONENTS

2.2.1 Junction Field Effect Transistors (JFETs)

<u>JFETs - Silicon - Long-Term Ionization</u>

- I_{GSS} increases

The two most common materials used in JFETs are Silicon (Si) and Gallium Arsenide (GaAs). Silicon has been the only material used until recently in commercially available JFETs but GaAs is now becoming available. Silicon will be emphasized since it represents the most mature process and consequently the most reliable; even though it may not have the best potential electrical advantages of the two.

In the case of long-term ionization effects, standard silicon JFETs develop increases in leakage currents (I_{GSS}), especially in n-channel devices. Any change in pinch-off voltage is not appreciable until dose levels well above those considered in this handbook. I_{GSS} can change as much as an order of magnitude for dose levels down to 6×10^4 rad(Si). Table 2.4 gives some examples of the effects. Pinch-off voltage does not decrease more than 50% until well above 10^6 rad(Si).¹⁶

For both silicon and GaAs JFETs, displacement effects are negligible to levels beyond those considered in this handbook. Proton fluence effects

on g_m , I_{GSS} and pinch-off voltage in JFETs do not become significant (i.e., > 1%) until $>10^{11}$ p/cm² (20 MeV equivalent) for silicon^{16,17,18} and $\approx 10^{13}$ p/cm² (20 MeV equivalent) for GaAs.^{16,19}

Dose rates of $< 10^2$ rad(Si)/sec will produce excess leakage currents in cut-off JFET switches of $\lesssim 10^{-9}$ A. This is negligible for most applications.

GaAs JFETs appear to be much less affected by long-term ionization than Si devices. The limitation of these devices in the Jupiter Probe appears to be determined more by reliability due to the immaturity of the technology.

TABLE 2.4: Behavior of I_{GSS} of N-Channel JFETs²⁰

Device Type	Gate Bias During Irrad.	I_{GSS} (A)	
		Pre-irradiation	Post-60 krad(Si)
2N4093	-20V	10^{-10}	10^{-9}
2N4391	-20V	10^{-10}	3×10^{-10}
2N4391 (unscreened)	-20V	10^{-10}	9×10^{-10}
2N4392	-20V	10^{-10}	10^{-9}
2N4393	-20V	10^{-10}	5×10^{-9}
2N4856	-20V	10^{-11}	4×10^{-9}
2N5196	-10V	5×10^{-11}	7×10^{-11}
2N5520	-10V	5×10^{-11}	7×10^{-11}
2N5556	-15V	10^{-10}	3×10^{-10}

2.2.2 Silicon Controlled Rectifiers (SCRs)

SCRs - Displacement & Long-term Ionization

- Saturation voltage increases
- gate trigger current increases

The large base regions of the SCR require a long carrier lifetime even at the relatively low JOP levels, displacement damage effects may cause substantial performance degradation.

A typical SCR is sensitive to displacement damage at 10^{10} p/cm² (20 MeV equivalent). The "on" voltage increases by as much as 50% (resulting from the "on" resistance increasing); and the gain is significantly reduced at this level. The effects are strongly dependent on the dopants and dimensions used by each manufacturer.

For long-term ionization effects, the device is dependent on the surface junction bias condition. The gate trigger current can increase by as much as 100% at 10^4 rad(Si)¹⁶ due to increased leakage; but since the reverse biased junction is located in the bulk material and the surface junction is forward biased, SCR long-term ionization effects on gain would not be as great as for planar transistors.

2.2.3 Diodes

Diodes - Long-Term Ionization and Displacement

- Zener voltage decreases slightly in precision applications

The effect of the Probe environment on semiconductor diodes is at most small changes in leakage current and forward voltage. Therefore, only diodes used in precision applications need be considered.

The breakdown voltage of voltage-regulator diodes (VRD), ("Zener diodes") is a function of the semiconductor resistivity, which depends only insensitively on displacement effects. However, temperature compensated VRD's usually include a forward-biased diode in series with the reverse-biased Zener or avalanche breakdown unit to accomplish a first-order cancellation of the temperature coefficient of breakdown voltage. The voltage across the forward-biased diode has a dependence on minority-carrier lifetime, and can produce a small shift in total voltage across the series combination.

The voltage in temperature compensated devices usually decreases with displacement damage. The exact magnitude of the change depends on the construction of the temperature compensating element, and does not depend in a simple way on the rated breakdown voltage. It tends to increase with increasing current, but this dependence is not useful since these devices are temperature-compensated at only one value of current.

Electron irradiation data on a few VRD's has been presented⁸ indicating that $\Delta V_Z/V_Z \lesssim 0.3\%$ at $\Phi_3 = 3 \times 10^{12} \text{ e/cm}^2$. Many devices exist in which $\Delta V_Z < 2 \text{ mV}$ at $\Phi_3 = 3 \times 10^{12} \text{ e/cm}^2$. A proton fluence of $\Phi_{20} = 10^{12} \text{ proton/cm}^2$ (more than 10 times the Probe environment), produced only $\sim 1\%$ changes in V_Z .^{8,14} Neutron data indicate changes of $\Delta V_Z/V_Z \lesssim 1.5\%$ at $\Phi_1 = 3 \times 10^{12} \text{ n/cm}^2$.¹⁶

The changes in non-temperature-compensated devices are generally smaller and may be positive rather than the negative change in temperature-compensated VRD's.

Other types of diodes using heavily doped semiconductors (e.g., tunnel, microwave, avalanche) are essentially unaffected by the Probe environment.

2.2.4 Electro-Optical Devices

Electro-Optical Devices - Displacement

- GaAs LED's - decreased output
- Si photodetectors - decreased sensitivity
- Optical isolators - decreased coupling

Electro-Optical Devices - Interference

- Increased dark current

This section discusses the displacement and ionizing effects on semiconductor devices that measure or use optical information. The types of devices to be discussed are:

- Silicon diode imaging sensors
- photo conductor and photo voltaic detectors (infrared)
- silicon surface barrier detectors
- optical isolators
- GaAs and Si LEDs
- GaAs Laser Diodes

Within this general class of optical detectors and filters there are multiple types of devices and materials available. The effects of protons on these devices and materials shows that in general above 10^{12} p/cm² (20 MeV equivalent) the damage is severe except for infrared devices.²¹ Infrared devices are very radiation resistant to proton fluence. For proton fluence below 10^{11} p/cm², fewer types of these devices are affected (those affected would include Silicon diode imaging sensors used in vidicon arrays and silicon detectors). A summary of proton effects on several filters, lenses and detectors is shown in the Table 2.5.

TABLE 2.5: Summary of Proton Irradiations. ^a ²¹

Component	Ionization dose ^b RAD(Si) (Minimum)	Displacement Damage (20 MeV Eq.)	Comments ^b
Calcite (CaCO ₃)	6.6 (5)	3.0 (12)	SBRC, no damage in IR Region.
Channel Multiplier	7.5 (5)	3.4 (12)	EMR-648F, no damage (Serious damage expected if powered).
HgCdTe Detectors (2)	1.1 (6)	5.2 (12)	No Effect.
HgCdTe Detectors (2)	7.1 (5)	3.3 (12)	No effect, LN ₂ temperature in vacuum.
LiF	8.5 (5)	3.9 (12)	EMR, 1216Å (68% + 48% transmission; 1470Å (88% + 63%).
Magnetometer - Cell B	1.2 (6)	5.6 (12)	Helium filled pyrex tube ~ 5% transmission loss (1.08μ)
Magnetometer - Polarizer B	1.2 (6)	5.6 (12)	~ 5% transmission loss (1.08μ).
Magnetometer Sensor Unit	1.5 (4)	5.8 (10)	Active test, no interference or damage in least sensitive mode, PBS.
MgF Crystal	8.5 (5)	3.9 (12)	EMR, 1216Å (52% + 50% transmission); 1470Å (80% + 82%).
PbS Detector	5.5 (4)	2.2 (11)	Actively monitored, no interference or damage ($\phi_p \approx 10^8$ p/cm ² - sec).
Photomultiplier	1.2 (6)	5.6 (12)	EMR 531E-01-14; loss of Q.E. and radiant sensitivity.
Photomultiplier	8.3 (5)	3.8 (12)	RCA-C70114M, bias 1.7 KV, 67% gain and 2.5% resolution losses.
Photomultiplier (2)	1.9 (0)	8.4 (6)	Active test, dark current up 2 to 4 orders of magnitude
Photomultiplier	2.1 (0)	8.1 (6)	Dark current up 2 to 4 orders of magnitude, no damage at max. current ratings.

a) All devices were tested passively (i.e. nonpowered electrically), at room temperature and in air unless otherwise noted.

b) Numerical notation example: 3.7 (11) - 3.7 x 10¹¹. Ionization dose calculated from proton fluence using Figure 1.3 in Section 1.2. Flux was typically 10⁸ p/cm² - sec.

Component	Ionization dose ^b RAD(Si) (Minimum)	Displacement Damage (20 MeV Eq.)	Comments ^b
Si Detector (2)	1.2 (6)	5.6 (12)	Intrinsic IR (1.08μ), S/N decrease by an order of magnitude.
Si Detector	5.5 (4)	2.2 (11)	Intrinsic IR (1.08μ), actively monitored, $\phi_p = 0.9$ to 1.2 (8) p/cm ² ; total interference and significant permanent damage.
Thermopile	2.2 (1)	8.4 (7)	Active +30 mV offset 15 to 60 mV noise; no permanent damage.
Vidicon, SE-S	9.0 (4)	3.5 (11)	SBRC, no effect.
Vidicon, Si	1.1 (6)	5.6 (12)	G. E. 1341-02, slight effect.
Vidicon, Si targets (9)	1.1 (6)	5.6 (12)	RCA 4532, seriously damaged.
Vidicon, Si (3)	7.8 (4)	3.6 (11)	RCA, serious damage.
Vidicon, SIT	2.3 (2)	9.0 (8)	RCA 4532, damage at lowest level.
AS ₂ S ₃ lens	6.9 (3)	2.7 (10)	RCA 4804; significant damage.
BG-23 glass	9.4 (5)	4.3 (12)	Lens cracked (thermal stress?) < 5% transmission loss.
Ge (IR Filter)	9.5 (5)	4.4 (12)	SBRC, no damage in IR region.
IR Filters (9)	6.3 (4)	3.3 (11)	SBRC, no effect in IR.
Magnetometer Filter	3.5 (3)	1.8 (10)	SBRC, different materials, no effect.
Schott Filter glasses (6)	1.3 (6)	5.7 (12)	No effect.
Si IR Filter	6.6 (5)	3.0 (12)	SBRC IR different types, no effect.
Silicon resin block	8.5 (4)	3.3 (11)	SBRC, no effect.
Silicon resin between two fused silica pieces	1.0 (6)	5.5 (12)	SBRC, no effect in IR.
	1.0 (6)	5.5 (12)	SBRC, no effect in IR.

From comparison of this data with other studies²²⁻²⁷ the following conclusions were drawn:

- a) HgCdTe and PbS detectors (infrared) showed little damage or effects up to the level of concern in this handbook. InSb detectors could be affected if they were photo-voltaic rather than photoconductive²⁷ but only at 10^{11} p/cm² or above.
- b) Silicon detectors and silicon vidicons were very sensitive to proton radiation.²⁸
- c) Infrared and visible region filters showed no effect (for Silicon or Germanium).
- d) Photomultipliers were extremely sensitive to interference.

The data currently available is insufficient to allow too many generalizations on radiation effects. Most decisions will have to be made by comparison with available examples.

Let us examine one of the semiconductor devices found to be most sensitive; silicon vidicon. For the silicon diode imaging sensors (vidicon type array application) the proton and electron fluence effects depend on the temperature of the device.²⁸ Figures 2.10 and 2.11 show how the dark current and quantum efficiency can change due to proton and electron fluence.

The response of the silicon sensor is also dependent on the energy of the particle (electron, proton, gamma, or X-ray) and its fluence. The radiation effects for these high energy levels are summarized in Table 2.6. The information is at room temperature conditions.

Photomultipliers appear to have no permanent damage due to either displacement or ionization but are very susceptible to dose rates even as low as considered for this handbook. A peak anode current of as much as

Curve No.	T_M ($^{\circ}k$)	V_T (Volts)	Electron Energy (MeV)	ϕ (e/cm^2)
I	217		11.0	6.4×10^{14}
II	300		1.0	3×10^{12}
III	300	8	11.0	Zero
IV	300		1.0	Zero
V	300		11.0	1.5×10^{13}
VI	300		1.0	10^{15}
VII	300		11.0	1.5×10^{14}

QUANTUM EFFICIENCY (%)

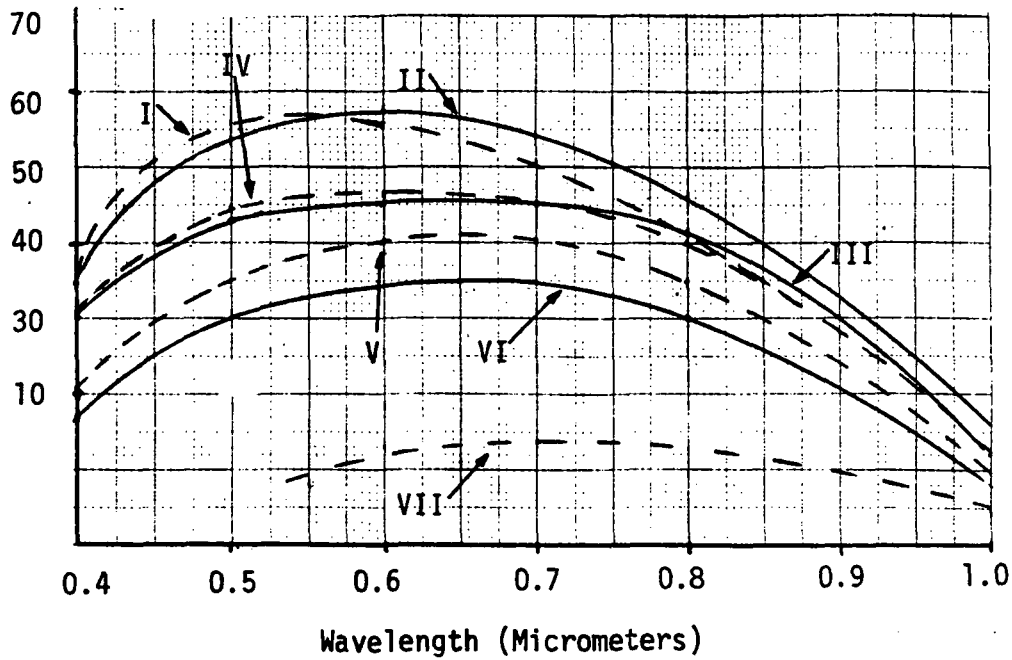


Figure 2.10: Quantum Efficiency Versus Wavelength of Incident Light of an Array Irradiated by 1 MeV Electrons and Arrays Irradiated by 11 MeV Electrons.²⁸ Measurements at Temperatures of 300 $^{\circ}k$ and 217 $^{\circ}k$.

Curve No	T_M ($^{\circ}K$)	Electron Energy (MeV)	ϕ (e/cm^2)
I	300	11.0	6.4×10^{14}
II	217	11.0	6.4×10^{14}
III			10^{15}
IV			1.5×10^{14}
V	300	1.0	1.5×10^{13}
VI			3×10^{12}
VII			Zero

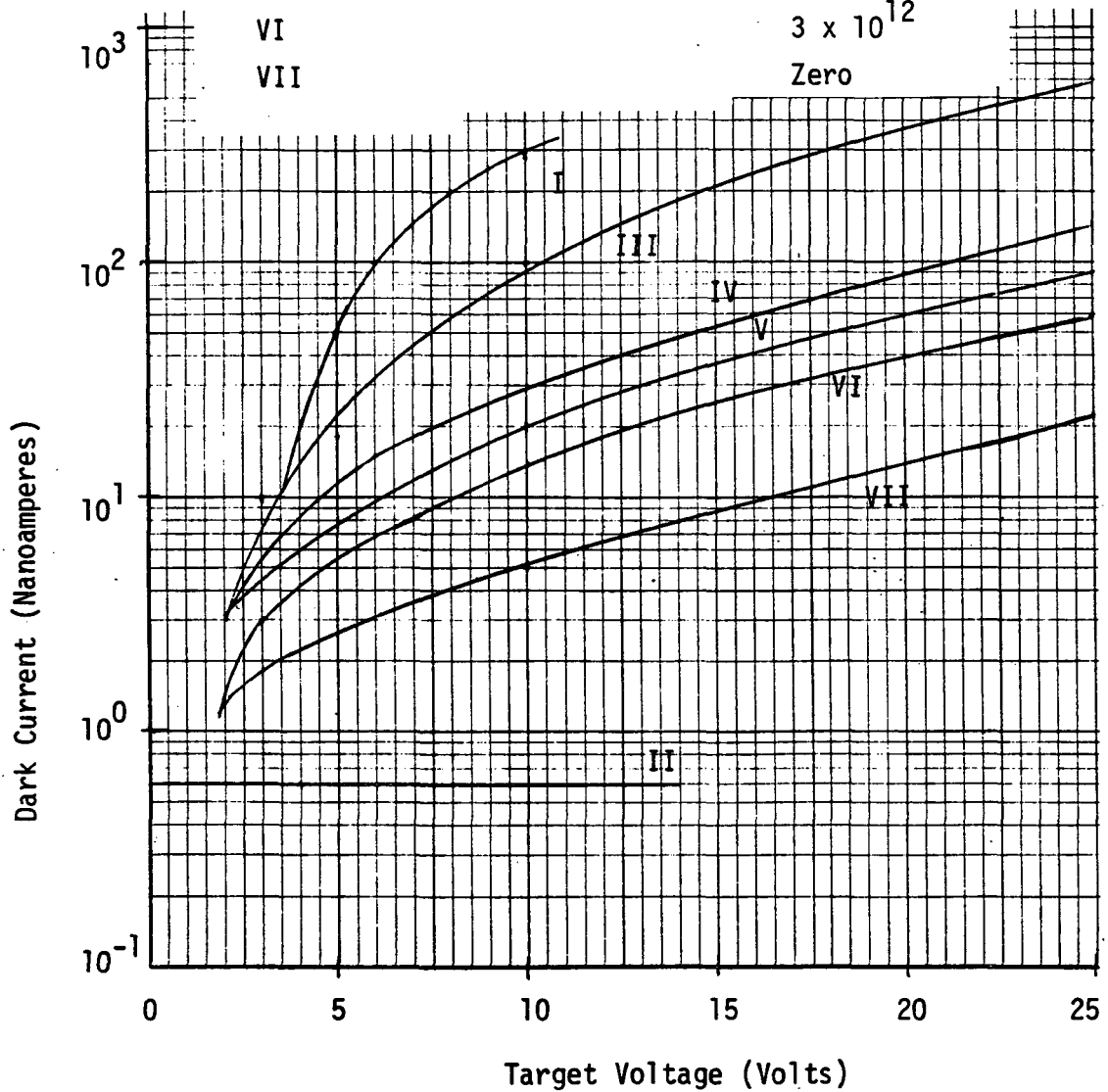


Figure 2.11 Dark Current Versus Target Voltage of an Array Irradiated by 1 MeV Electrons and 11 MeV Electrons.²⁸ Measurements at 300 K and 217 K.

10^{-2} amps can be generated by the 100 rad(Si)/s transient ionizing radiation.²⁹ The interference effect in phototubes is due to luminescence of the window and electron emission from the cathode and first dynode.

TABLE 2.6: Threshold Limits of Particle Fluence and Flux²⁸

	11 MeV	3 MeV	142 MeV
Dark Current	10^{12} e/cm ²	10^9 p/cm ²	10^{12} p/cm ²
Spectral Response	3×10^{12} e/cm ²	10^{10} p/cm ²	10^{12} p/cm ²
Glass Darkening	4×10^{12} e/cm ²	8×10^{10} p/cm ²	10^{12} p/cm ²
Cerenkov and Fluorescence	2×10^8 e/cm ² -sec	4×10^6 p/cm ² -sec	8×10^7 p/cm ² -sec
Electron-Hole Pair Current and Charging Effects	3×10^6 e/cm ² -sec	6×10^4 p/cm ² -sec	10^6 p/cm ² -sec

Another group of devices to be discussed under optical devices is the group using Gallium Arsenide (GaAs) for the bulk material. This group includes light emitting diodes (LEDs), optical Isolators and Laser diodes.

The emission efficiency of GaAs LED's is significantly reduced by electron and proton irradiation. The magnitude of the change depends on the particular device. Figure 2.12 shows how much relative effect was found in silicon amphoteric GaAs LEDs made by Texas Instruments.

Figure 2.13 presents data from electron irradiation of three types of GaAs LED's. The large change produced by even 5×10^{12} electrons/cm² (25 MeV) is evident.

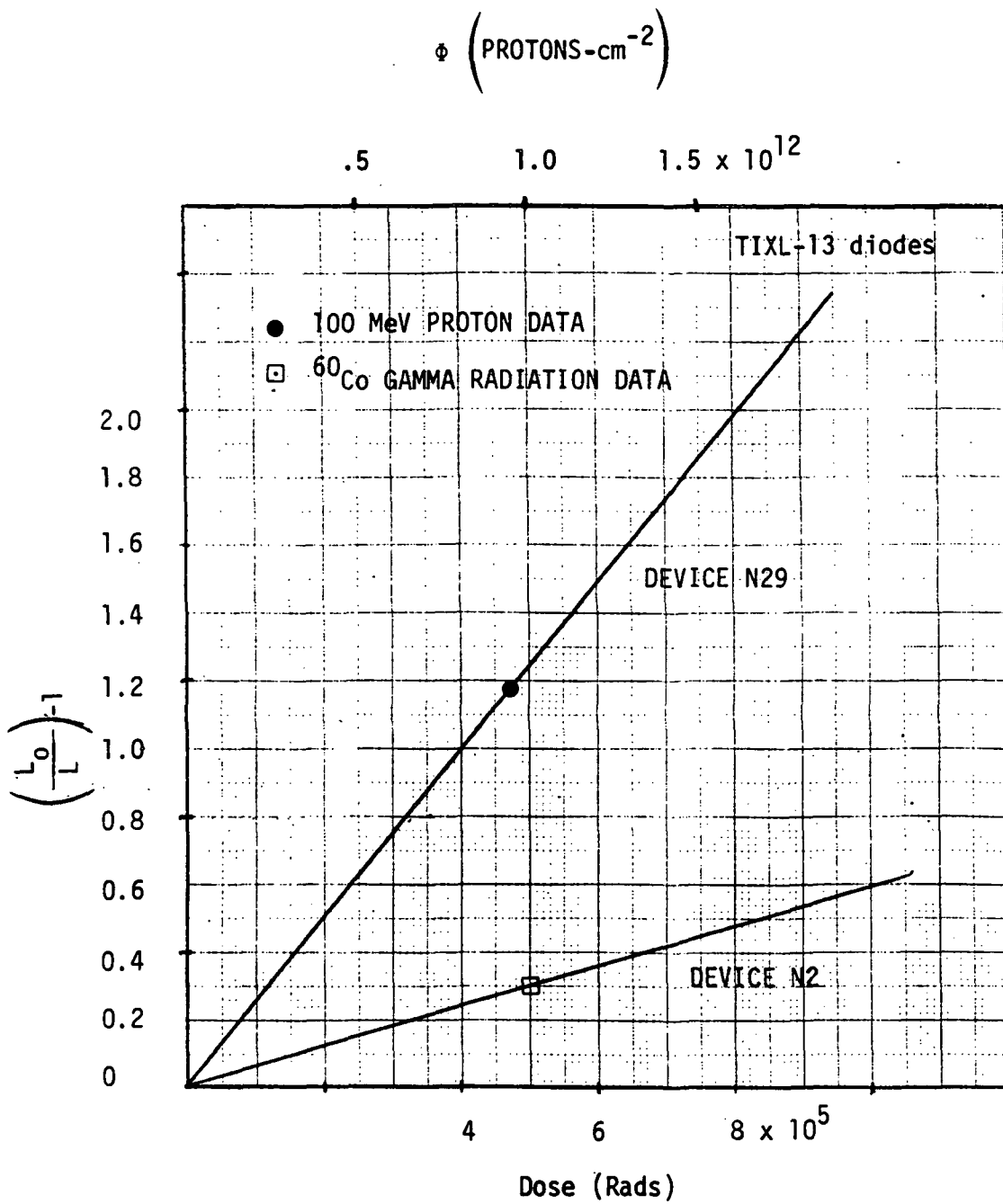


Figure 2.12: Light Intensity Degradation for Protons and ⁶⁰Co Gamma Radiation for GaAs LEDs.³⁰

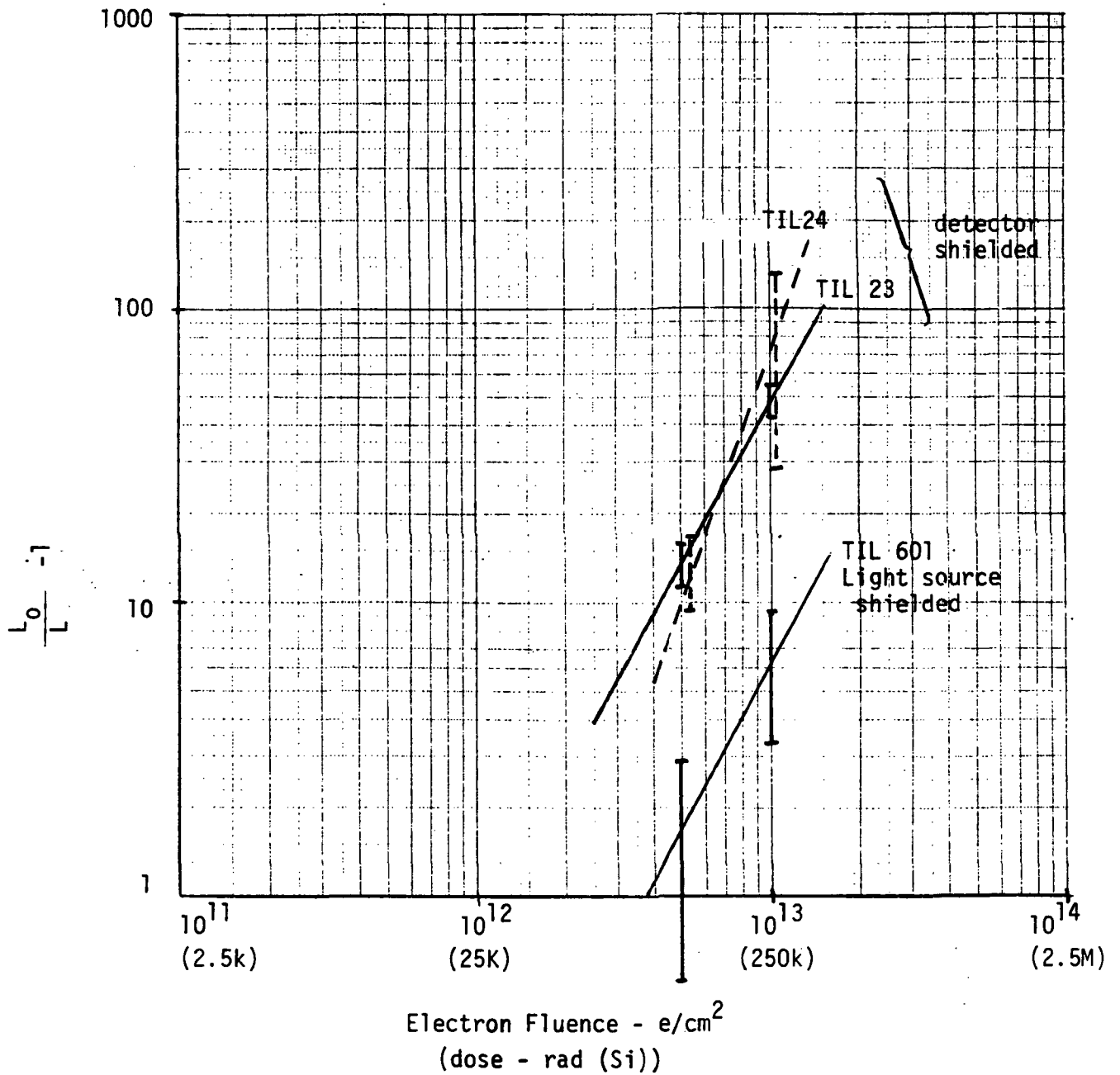


Figure 2.13: Effects of Electron Irradiation on Light Output⁸ of GaAs Light Sources (TIL23 and TIL24) and Light Detectors (TIL601).

Optical isolators are actually a combination of a GaAs LED and either a photo-diode or photo-transistor. The isolators containing photo-diodes were more radiation resistant than those containing photo-transistors.³¹ (This is mainly the result of having a more sensitive LED in the photo-transistor isolator). In the photo-diode isolator, the LED was the limiting factor while the bias (V_{CE}) on the photo-transistor determined whether the LED was the limiting factor in the photo-transistor isolators. For permanent damage due to displacement or long-term ionization, at low V_{CE} , the high input current of the LED will cause the LED to produce the major portion of degradation. If low input current of the LED is used with high V_{CE} on the photo-transistor, then the photo-transistor will be the limiting factor.

GaAs laser diodes do not appear to be sensitive to radiation fluences of protons discussed in this handbook.³² This is especially true at low temperatures and for currents significantly above threshold.

Although solar cells are not used on the Probe for power, they might be candidates for other photodetector applications. Displacement damage in N-on-P cells is less than in P-on-N cells, but is still significant at fluences of interest. Figure 2.14 illustrates typical damage rates for a variety of particles.

2.3 INTEGRATED CIRCUITS

Characterization of radiation effects on microcircuits has become a routine aspect of component qualification for hardened systems. As microcircuit technology has evolved, complex MSI/LSI digital arrays have been developed to supplement the single-function microcircuits as system components. These complex arrays are the blend of semiconductor device technology with the performance capability of digital subsystems. As a

J_{SC} (mA/cm²) under 135 mW/cm²

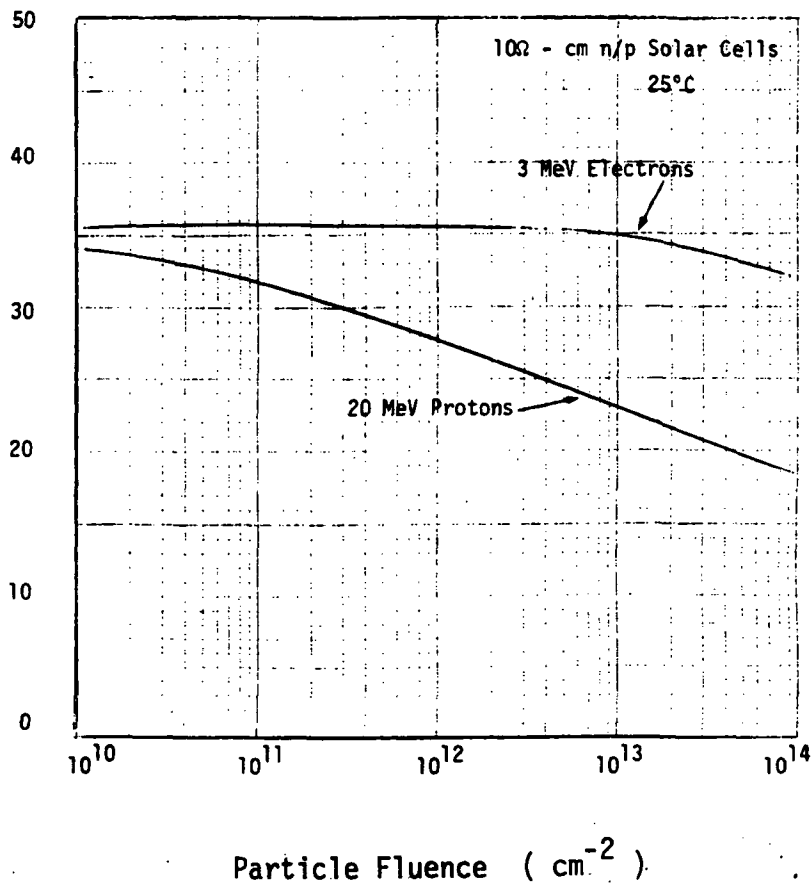


Figure 2.14: Variation of Solar Cell Short Circuit Density with Fluence for Protons and Electrons.³³

direct evolution of microcircuit technology there are many similarities in radiation vulnerability between the simpler SSI (Small-Scale-Integration) and MSI/LSI (Medium/Large-Scale-Integration) devices. There are also however, unique aspects that critically distinguish MSI/LSI. These are principally the technology, circuit performance, and radiation response of the basic logic cells, as well as the requirement for evaluation of overall array performance and radiation vulnerability assessment without access to direct measurements on the internal logic cells.³⁴

The basic MSI/LSI logic cell, free from the constraints of external loading and noise margin, has evolved into circuit realizations that have little or no correspondence to a single-function microcircuit. This is

illustrated most strongly by the development of memory cells of both bipolar and MOS memories, and in the logic cells of dynamic-logic MOS arrays. With the evolution in the circuit realization of the basic logic cell, the nature and critical failure levels must also change.

Results are presented on radiation effects of DTL, TTL, ECL, I^2L , and Schottky-clamped TTL arrays of bipolar technology as well as the static p-MOS, dynamic p-MOS, C/MOS, C/MOS/SOS, n-MOS and charge-coupled-device arrays, focusing more on the nature of radiation effects rather than on the levels of radiation hardness attainable.

Given the measured radiation vulnerability of the logic cells of a digital subsystem, the subsystem vulnerability can be determined with little difficulty, subject to a few confirming experiments at the overall subsystem level. Application of MSI/LSI arrays as system components, however, makes a vital difference in the component characterization due to the lack of access to the performance characteristics and radiation vulnerability of the basic logic circuits (cells). This distinction might seem fairly subtle, but it has a first-order impact on the experimental characterization; particularly in the required analytical techniques and mathematical models necessary to support the experimental study. Techniques of simplified modeling and logic simulation, which are useful but not necessary for small scale microcircuit study, become critical in support of MSI/LSI experimental characterization.

Study of radiation effects on microcircuits has included the measurement of transient photoresponse as a function of ionizing radiation pulse width, as well as the permanent damage effects resulting from neutron/electron exposure. Results indicate that the basic-radiation-induced failure mechanisms in complex devices are essentially the same as those well known for single-function digital microcircuits,^{35, 36} that is, 1) displacement-induced gain degradation in bipolar transistor elements, 2) long-term ionization-induced threshold voltage shift in MOS transistor elements,

and 3) increase in the p-n junction thermal leakage currents. No significant interference effects are expected in digital microcircuits. Potential interference effects may be expected in analog microcircuits with high-impedance inputs at which $\Delta I \lesssim 1 \text{ nA}$ may affect circuit performance. Failure levels observed are consistent with those expected from studies on basic semiconductor elements and microcircuits, but as reflected through the specific logic cell technology and overall array performance characteristics.

2.3.1 Bipolar Digital

Bipolar Digital - Long-Term Ionization and Displacement
- Slight fanout decrease in I^2L at low gate currents.

Radiation vulnerability of junction-isolated digital bipolar arrays is generally similar for single-function microcircuits, MSI and LSI arrays. Displacement-degradation effects observed in the bipolar LSI arrays reflect the general evolution to high-speed transistors, with the corresponding reduction in degradation. Gains obtained by the use of high-speed transistor elements, however, can be offset by reducing the allowable margin of gain variation in the cell design. Typical failure levels observed for the LSI arrays are $\Phi_1 \approx 10^{15} \text{ n/cm}^2$ indicating that, on balance, there has been some natural hardening of the LSI devices in the process of evolution from the single-function microcircuits. Clearly these levels are of no concern in the Probe.

Bipolar digital devices have a long-term ionization effect threshold from $10^4 - 10^7 \text{ rads(Si)}$ depending on the device type and the bias conditions used during radiation exposure. Table 2.7 shows examples of several complex devices and their levels of failure in radiation environments.

TABLE 2.7: Complex Microcircuit Radiation Hardness Examples³⁷

Technology	Device	Displacement Damage (n/cm ²)	Long-Term Ionization [rad(Si)]
T ² L/SC	MMI6701D	10 ¹⁴ (Sink current)	≈ 10 ⁶ (Sink current)
I ² L	TIX0400	5 x 10 ¹¹ (Sink current)	≈ 10 ⁶ (Output levels)
T ² L/SC	MMI6340D	10 ¹⁴	> 10 ⁶
T ² L	IM5533A	> 10 ¹⁴ (output gain reduced)	> 3 x 10 ⁷
T ² L/SC	AM2901	Unknown	> 2 x 10 ⁷

ECL technology was tested and found to be functional at radiation levels greater than 3×10^7 rad(Si) and 10^{15} n/cm².³⁸ An important exception to this trend in bipolar microcircuits is I²L. The use of lateral pnp and inverted npn transistors in the basic logic cells substantially reduces the basic displacement damage hardness. I²L is a new and evolving technology, however, and the radiation hardness is generally increasing with the technological maturing. It is expected that degradation may be observed at 10^{12} n/cm² in well designed arrays, damage will be substantial at 10^{13} n/cm² and array performance at 10^{14} n/cm² cannot be expected. I²L tests show susceptibility levels in the range 6×10^4 to greater than 10^6 rads(Si) for all device types at injection currents of 60 microamps per gate. Techniques for hardness improvement by process control are known.³⁹ The fanout required also affects these levels significantly. For example, by changing the fanout from 6 to 2, the dose for failure increases by a factor of 10. The worst-case for long-term ionization effects in I²L arrays is operation at minimum injection current. At exposure levels as low as 10^4 rads(Si), significant increases in minimum current of operation have been observed.⁴⁰

2.3.2 Bipolar Analog

Bipolar Analog

- large offset voltage increase
- large offset current increase
- loss in open-loop gain
- sink current decrease

OpAmps are particularly susceptible to surface effects because the input transistors are frequently operated at low collector current to increase the input impedance. Again the quality of the passivation layer controls the response, rather than the design of the semiconductor circuit.

Experimental data using electron irradiation of 1974-1975 devices to generate ionization effects indicate that 150 krad exposure of unhardened OpAmps may produce large offset voltage changes, ΔV_{OS} as shown in Figure 2.15, and offset current changes ΔI_{OS} as shown in Figure 2.16, and even catastrophic failures. Hardened versions seem to be able to achieve $\Delta V_{OS} < 2$ mV and $\Delta I_{OS} < 1$ nA. Effective hardening requires diffusion lot sampling to check on oxide quality. Hardened LM108 are also compared to unhardened LM108 in Figures 2.15 and 2.16.

Comparisons are also made for ΔI_B as shown in Figure 2.17.

Similar effects occur in other linear microcircuits, many of which incorporate some version of an OpAmp (e.g., voltage regulators). Generally these circuits are less demanding than low current OpAmps.

Figures 2.15, 2.16, and 2.17 give several indications of the magnitude and variation among devices within a manufacturer's product. The mean

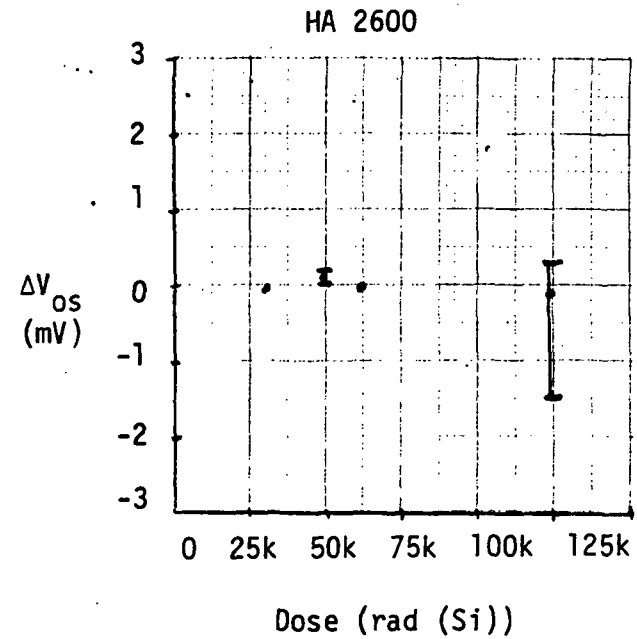
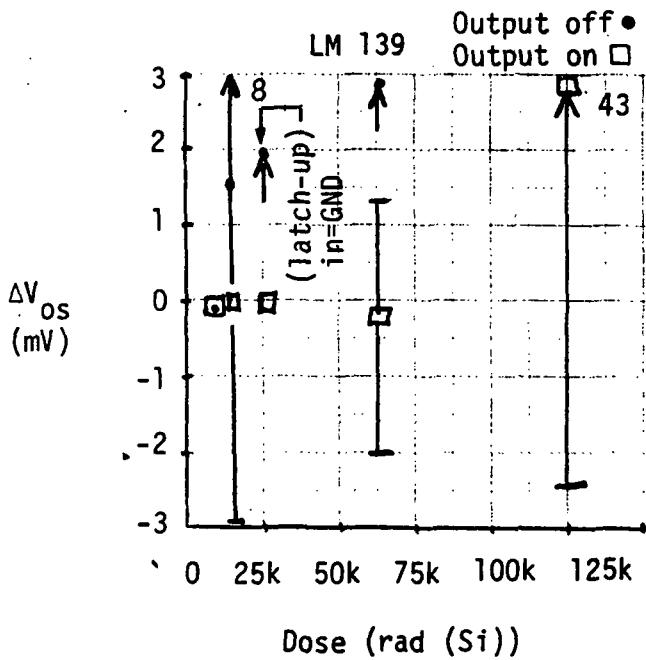
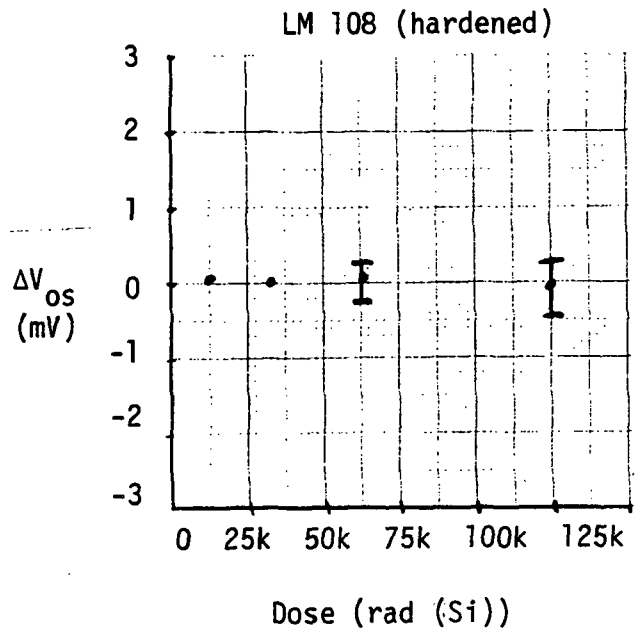
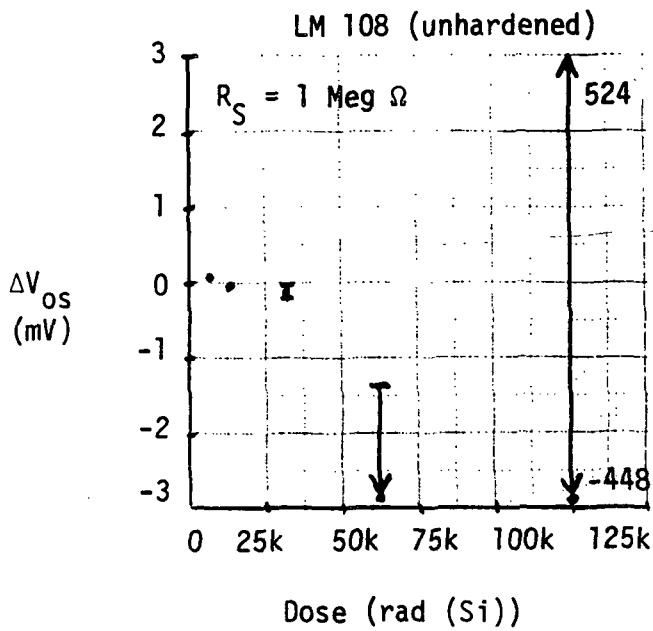


Figure 2.15: Range in ΔV_{OS} for Increasing Dose and for Several Device Types. Graphs Show Mean and Max-Min for Devices in Tests.⁸

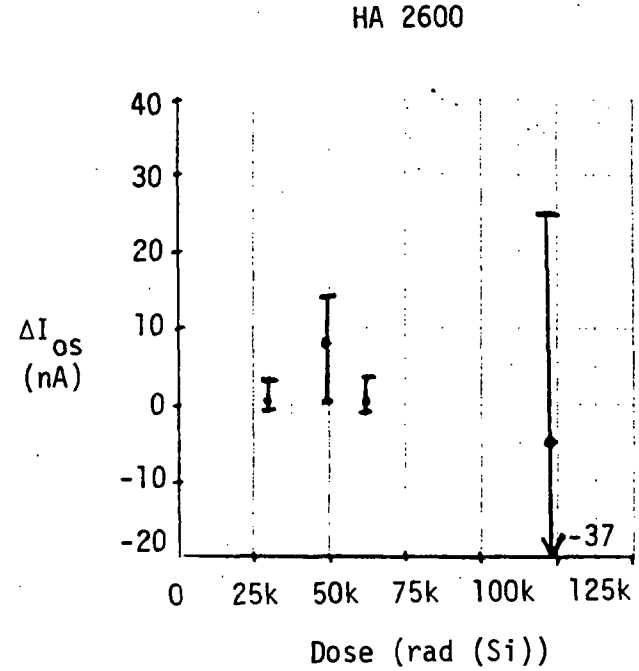
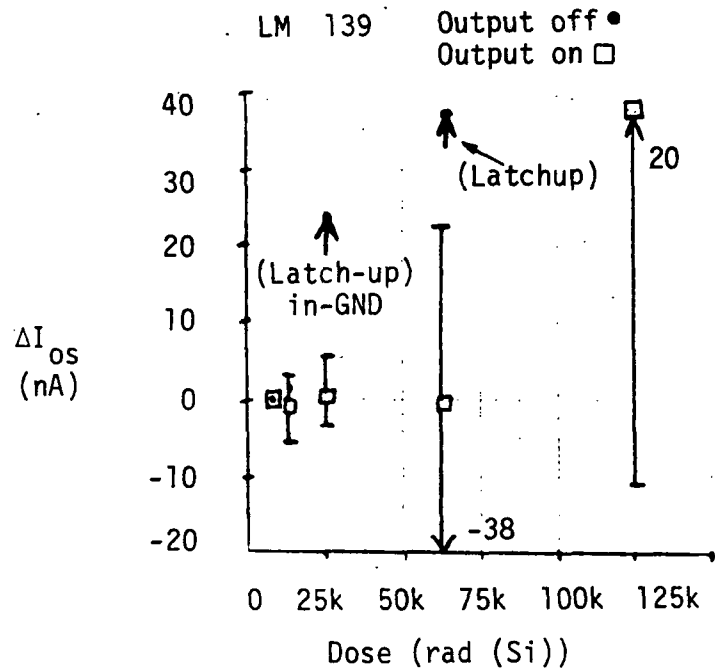
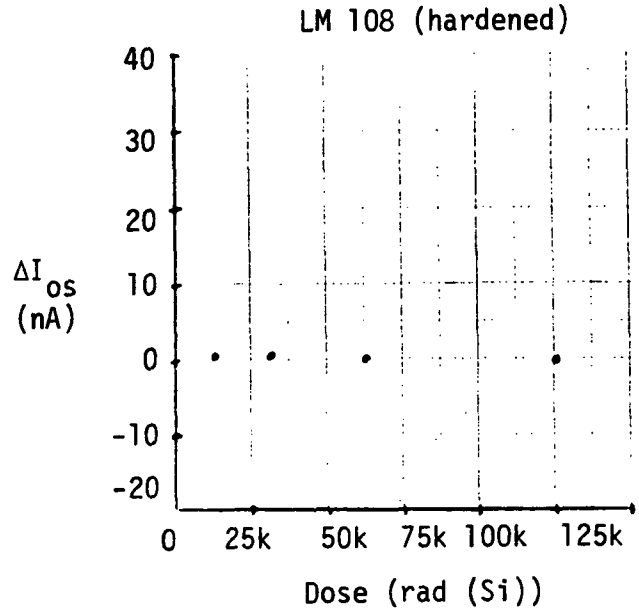
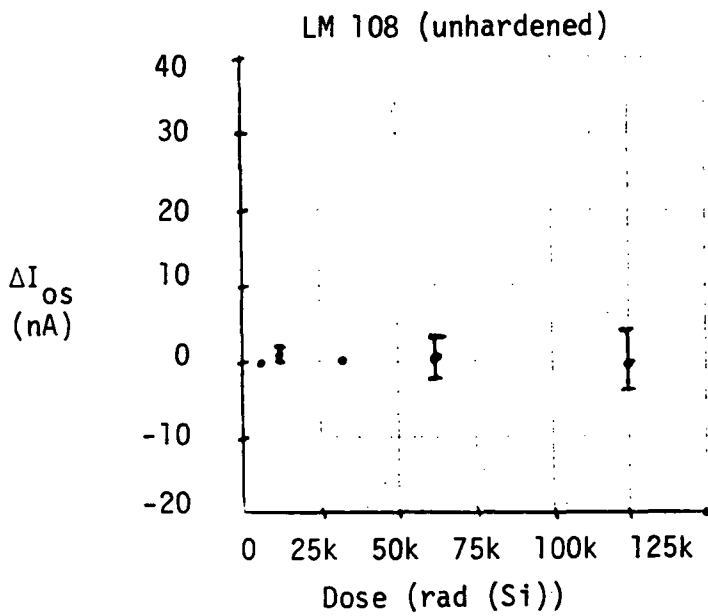


Figure 2.16: Range in ΔI_{os} for Increasing Dose for Several Device Types. Graphs Show Mean and Max-Min Values for Devices in Tests.⁸

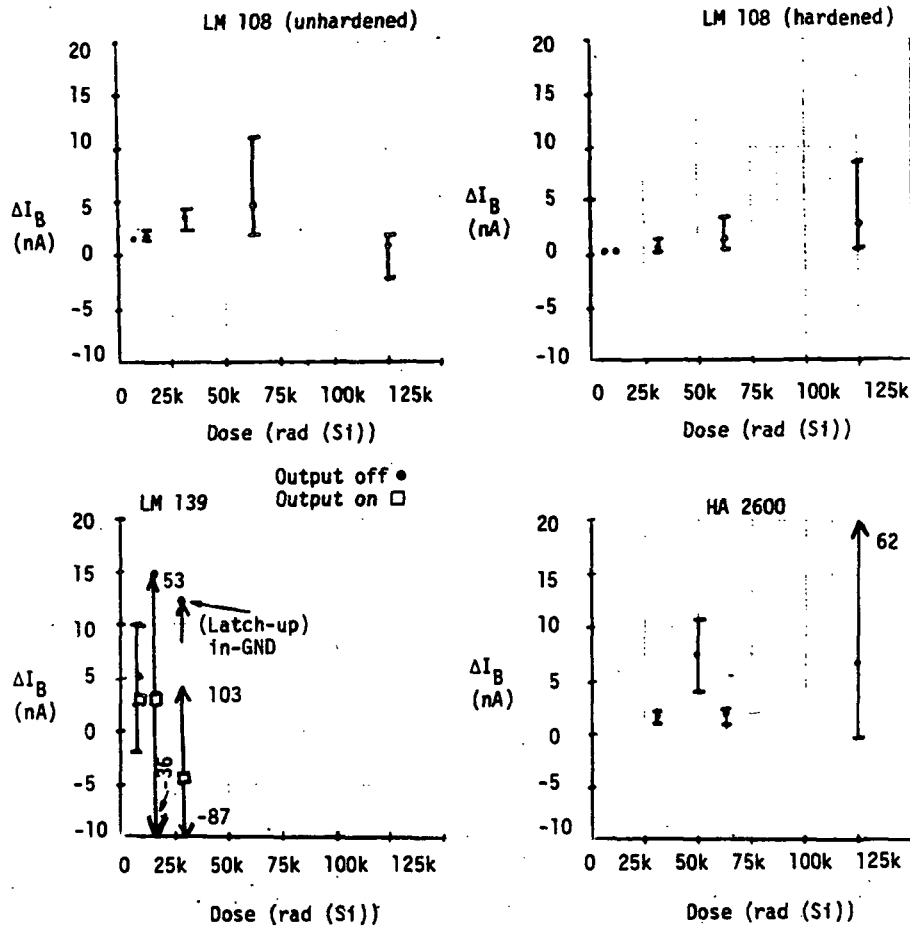


Figure 2.17: Range in ΔI_B for Increasing Dose and for Several Device Types. Graphs Show Mean and Max-Min for Devices in Tests.⁸

value of change for each parameter may stay within the allowable range for the design but the variation among devices from the same manufacturer indicate that the probability of obtaining at least one device that will have a wide variation from the mean is high. Also the type of application has an influence on the failure level. For the LM139 example, if the output is off and the input is grounded, then latch-up to the positive supply voltage occurs at radiation dose levels as low as 25 krad(Si). If the input is kept at -130 mV then latch-up is prevented but the magnitude of variation approaches 0.6 volts. The data also indicate the strongly nonlinear dependence of parameter change on dose.

The hardening of the LM108 improved the response of all parameters, with slightly less success for I_B .

Other manufacturers were also tested, showing as great or greater variations. These variations can be related to the date of production and not necessarily to the manufacturers (i.e., all manufacturers are capable of producing soft and hard linear ICs). The behavior of the LM108 (hardened) shown in Figures 2.15 through 2.17 is comparable to the best achieved.

Some specific examples of proton effects on bipolar linear circuits are shown in Table 2.8.

TABLE 2.8: Proton Damage in OpAmps²¹

<u>Device</u>	<u>(#)</u>	<u>MeV</u>	<u>P/cm²</u>	<u>Effect</u>
HA-2-2500-2	(6)	20	1.5×10^{12}	7% loss of gain at 10 and 10^2 Hz, OK at 10^3 and 10^4 Hz.
HA-2-2700-2	(7)	20	1.5×10^{12}	11% loss of gain at 10 Hz, 7% loss at 10^2 Hz, 8% loss at 10^3 Hz.
LM101AN	(6)	20	1.5×10^{12}	9% loss of gain at 10 Hz, 11% loss at 10^2 Hz, 12% loss at 10^3 Hz.

The above data therefore shows a large dependence of linear circuits on long-term ionization effects but small changes in gain for proton displacement damage.

2.3.3 MOS

MOS - Ionization

- critical total dose threshold voltage shifts
- failure levels from 10^3 to 10^7 rads(Si)
- critical dependence on bias during radiation exposure

Long-term ionizing radiation effects on MOS microcircuits are probably the most critical problem of the JOP electronic components. Because the radiation effects are determined by device parameters which do not directly appear in electrical performance characteristics or reliability, critical steps in processing are often uncontrolled. As a result there is a tremendous variation in the long-term ionizing radiation susceptibility of MOS microcircuits. Arrays can be obtained from today's technology with failure levels that range from close to 10^3 rads(Si) to greater than 10^7 rads(Si).

The basic radiation effect in all bulk silicon MOS arrays is the radiation-induced shift in threshold voltage. Characteristically, the threshold voltage of p-channel transistor elements increases monotonically with radiation while the threshold voltage of the n-channel elements initially decreases to a point which may bring the enhancement device to the undesired depletion mode, and then increases. Typical threshold voltage shifts are shown in Figure 2.18. The cases shown as unhardened represent effects observed in high-reliability commercial devices where the critical parameters affecting the radiation hardness have not been controlled. In hardened microcircuits, special attention has been paid to the quality of the starting material, minimizing thermal stress at the gate silicon-silicon-dioxide interface, cleanliness of the gate oxide from alkali impurities, eliminating ionizing radiation exposure during processing steps such as gate metallization, and elimination of high-temperature forming gas annealing.

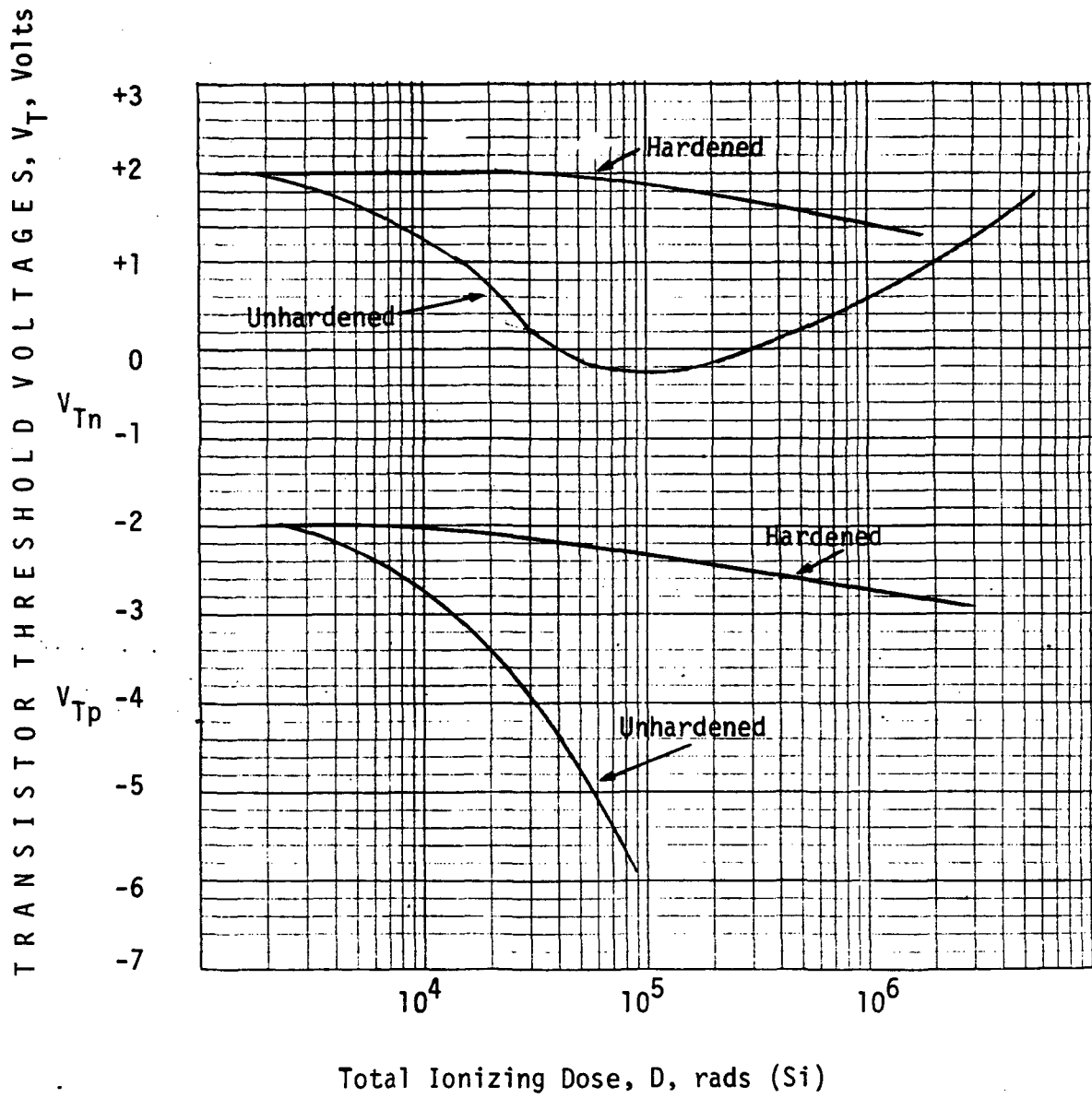
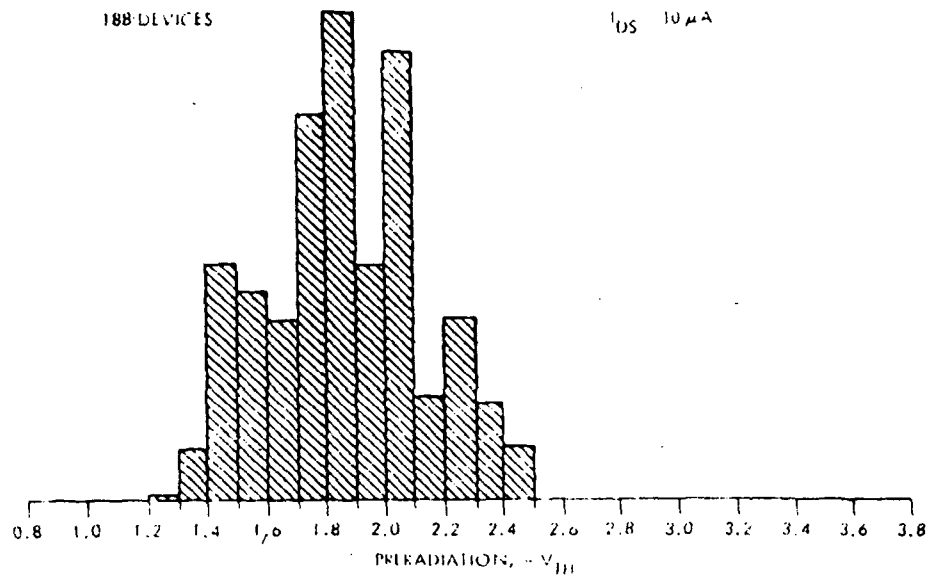


Figure 2.18: MOS Transistor Threshold Voltage Shifts.

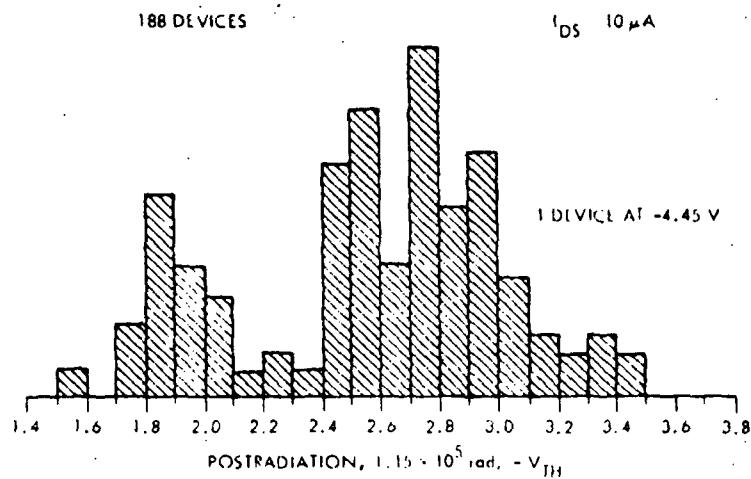
Hardened [i.e., failure levels greater than 10^6 rads(Si)] bulk CMOS arrays have been successfully demonstrated by Sandia, RCA, Hughes Semiconductor, and Rockwell International.

While it has been demonstrated that hardened MOS is realizable, the additional process controls and modifications in logic cell layout rules are not naturally compatible with the optimization of a high-performance minimum cost LSI array designed principally for commercial applications. For example, n-MOS dynamic random-access-memories are at the state-of-the-art in LSI technology. To realize these complex arrays, clever logic cell designs are used which use a minimum number of active elements, each one of which is carefully controlled to operate at a minimum margin in variations in threshold voltage, (typically less than 200 mV). This results in a complex array which can be produced at high yield for restricted temperature ranges in operation and with total ionizing dose failure levels between 1.7×10^3 and 3.5×10^3 rads(Si) for 4k dynamic random-access-memories.⁴¹ These results on the dynamic 4k memories probably represent the worst-case conditions of cell design and processing in which commercial processing goals are diametrically opposed to radiation hardness. Unfortunately, this trend is continuing in the semiconductor industry and application of commercial n-MOS LSI arrays (memories, controllers, microprocessors, etc) in JOP electronics must be discouraged. When necessary, these arrays must be considered among the most susceptible and critical system components.

The long-term ionization radiation hardness of MOS arrays will tend to decrease with increasing array complexity even for technologies adequate for small/medium-scale logic arrays. Studies of an 8-bit CMOS microprocessor,⁴² for example, indicated a failure level of about 1×10^5 rads(Si) which was about a factor of four less than that typical of the SSI/MSI microcircuits of the same design and processing technology. These results are consistent with the statistical variation in pre- and post-irradiation threshold voltages as illustrated in Figure 2.19. These results as well as a thorough characterization of CMOS microcircuit radiation susceptibility are presented in the JPL Radiation Design Criteria Handbook.⁸



(a) Threshold voltage of P-channel transistor on test pattern TA 6372, 950°C gate oxide anneal in forming gas, preradiation



(b) Threshold voltage of P-channel transistor on test pattern TA 6372, 950°C gate oxide anneal in forming gas, postradiation

Figure 2.19: Statistical Variation of MOS Transistor Threshold Voltages.⁸

An additional critical consideration in long-term ionizing radiation effects on MOS microcircuits is the variation in failure level with bias conditions on the microcircuit during radiation exposure. From extensive studies on individual transistor elements, maximum threshold voltage shift occurs with a positive d-c bias gate-substrate for both p-channel and n-channel transistors. This bias condition is generally most severe for p-channel devices, but fortunately does not typically occur in most operating conditions. Bias conditions which can lead to positive gate bias on the p-MOS elements are found in CMOS arrays under unfavorable leakage current conditions in NOR gates and in transmission gates.

In determining long-term ionizing radiation effects on MOS microcircuits the most severe operating condition is static bias during exposure, but it is difficult to identify or control the bias conditions on each internal transistor element. This uncertainty leads to some of the spread in experimentally observed failure levels.

Operation of a microcircuit under clocked or dynamic operating bias conditions significantly reduces the total dose failure level as illustrated in Figure 2.20. The increased hardness is in part due to the time-dependent variations between worst- and best-case bias conditions on the individual transistor elements. If the array is to be used dynamically during radiation exposure, experimental qualification under static bias conditions will probably lead to an unnecessarily harsh worst-case condition. Dynamic operation of an MOS array following exposure under static bias conditions will not gain any radiation hardness. If operation of the array is not required during radiation exposure, the most favorable bias condition would be dynamic operation, or if the power dissipation required cannot be allowed, the next best would be to insure that all power supply voltages are zero.

Additional technological development of MOS technology has led to the fabrication of arrays on insulating substrates (such as CMOS on sapphire).

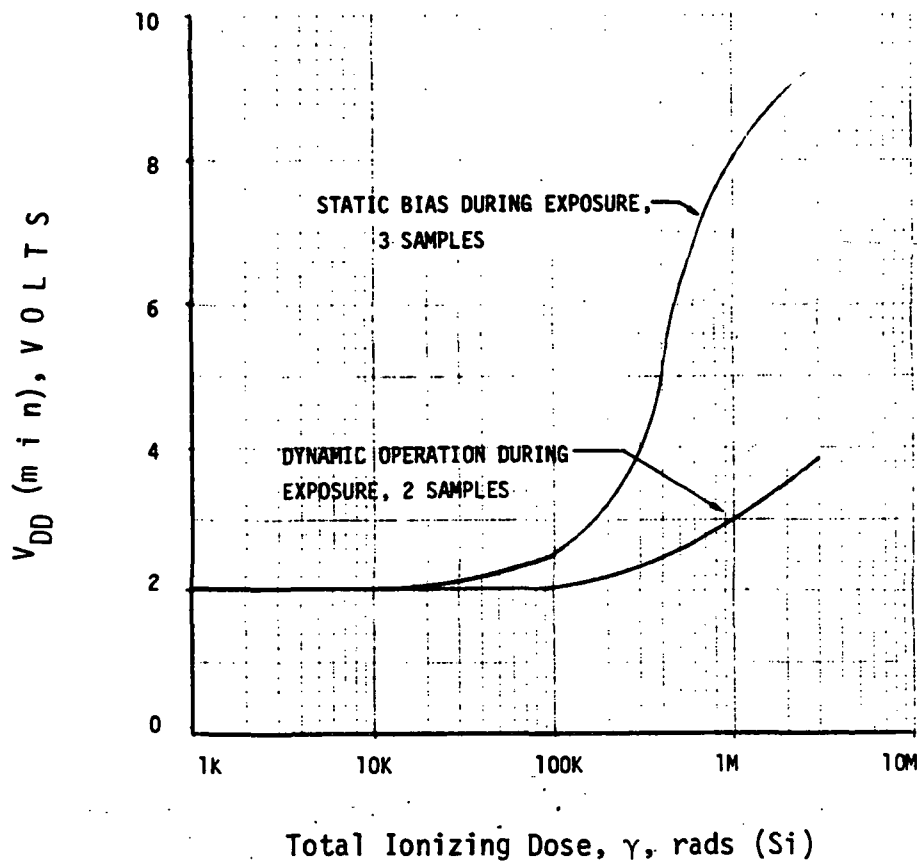


Figure 2.20: Variation of C/MOS CD4024 Total Dose Vulnerability with Bias During Exposure.³⁴

In terms of radiation effects, these arrays have all the susceptibility mechanisms of arrays fabricated on bulk semiconductor substrate, plus the addition of radiation-induced leakage paths at the interface between the silicon and the sapphire substrate. The principal advantages of CMOS/SOS over bulk CMOS are electrical switching speed, elimination of electrical and high-intensity pulsed ionizing radiation-induced latch-up, and hardening to high-intensity transient ionizing radiation-induced photoresponse effects. For the JOP electronics the only relevant advantage is the increase in electrical switching response with a trade-off required in the decrease in radiation hardness. If required, CMOS/SOS arrays would be very critical components in the system in limiting survival of the radiation environment.

Displacement damage effects in MOS arrays of all variations and technologies will be dominated by ionization effects for the JOP radiation exposure.

Transient interference effects are of no concern for static MOS logic arrays (that is, those that store data only in flip-flop cells). Dynamic arrays (those that store data on p-n junction capacitors) will require an increase in refresh data rate to insure reliable operation for applications required performance during ionizing radiation exposure.

2.3.4 CCD's Image Sensors and Other Complex Types

CCD's - Long-Term Ionization

- charge transfer efficiency degraded
- reduction in dynamic range

CCD's - Interference

- increased leakage current
- refresh rate increase required

The recently developed charge-coupled devices (CCD's) have applications in optical imaging, signal processing and serial memories. There are basically two approaches to CCD's: surface (SC) and buried (BC) channel. A CCD is basically a string of MOS transistors which have the same general reaction to radiation but since the mode of operation is different, the CCD's are affected in a different way.⁴³ CCD's are affected by the device threshold shift and the increase of surface state densities (which affect the threshold and transfer efficiency) due to ionizing radiation.

Considering displacement radiation, the main effects were bulk crystal damage producing leakage current at a linear rate of about a factor

of 6 for each decade increase in fluence for both types of CCD structures (SC and BC). This effect becomes significant around 10^{11} n/cm² to 10^{13} n/cm². Above 10^{12} n/cm² the charge transfer efficiency is also significantly degraded.⁴⁴ Transient interference from continuous ionizing radiation will fill the wells of a BC device in times ranging from 50 mseconds at 5 rad/sec to 5 mseconds at 100 rad/sec.

The most serious degradation is the very large leakage current increase and the resulting reductions in storage time and dynamic range. Also there is an increase in noise. Wide variations were seen from device to device in the charge transfer inefficiency changes. The limitations on leakage current changes were such that at 10^5 rads(Si) they were too high to meet the requirements on storage time, dynamic range and noise. The effects from ionizing radiation are a strong function of gate oxide quality.

The only significant difference found between aluminum and polysilicon gates is a larger threshold voltage shift with polysilicon for long-term ionization effects. Figures 2.21 to 2.25 show these effects.

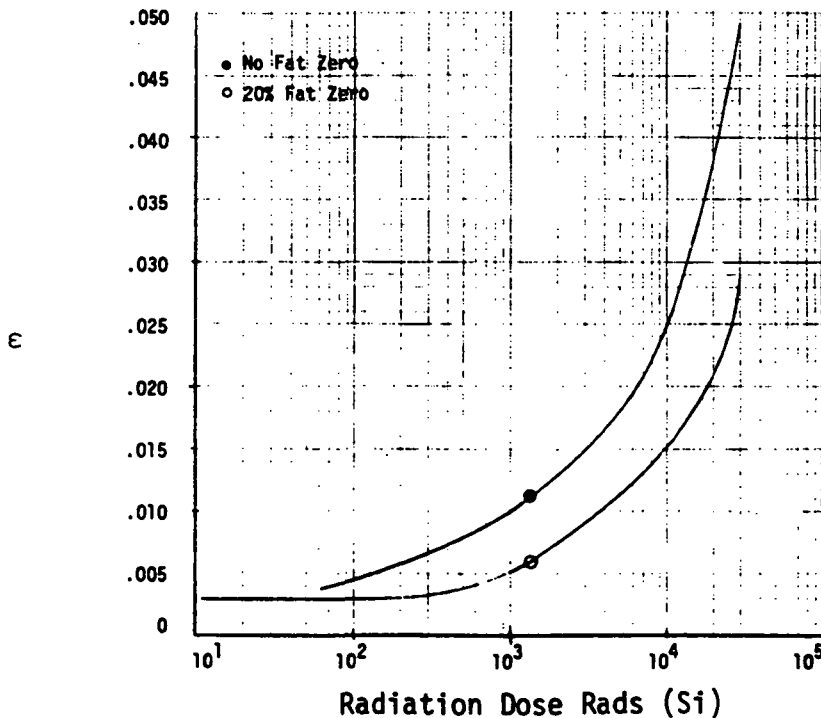


Figure 2.21: ϵ vs Total Dose for 500 x 1 CCD.⁴⁵

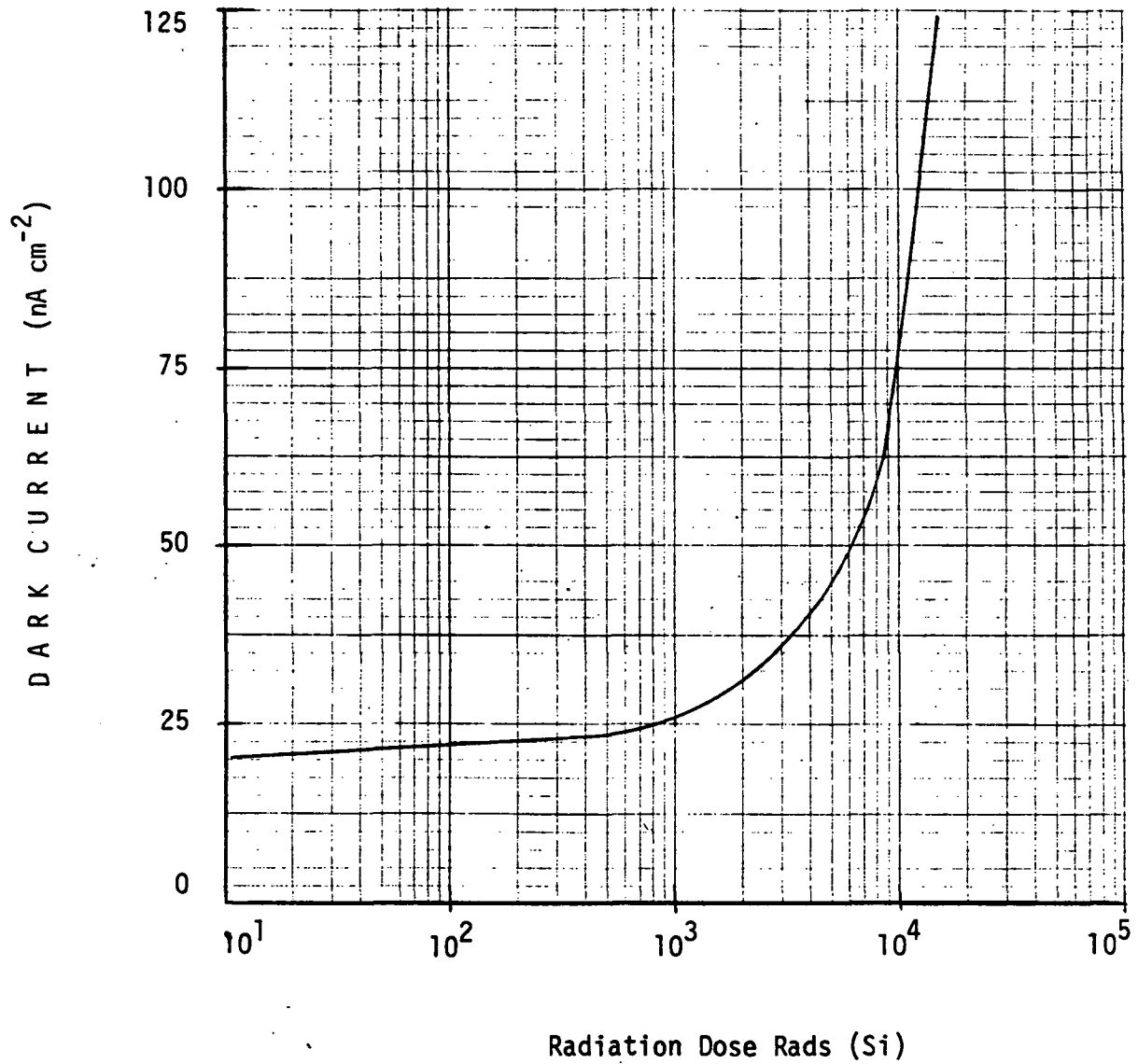


Figure 2.22: Dark Current vs Total Dose for 500 x 1 CCD.⁴⁵

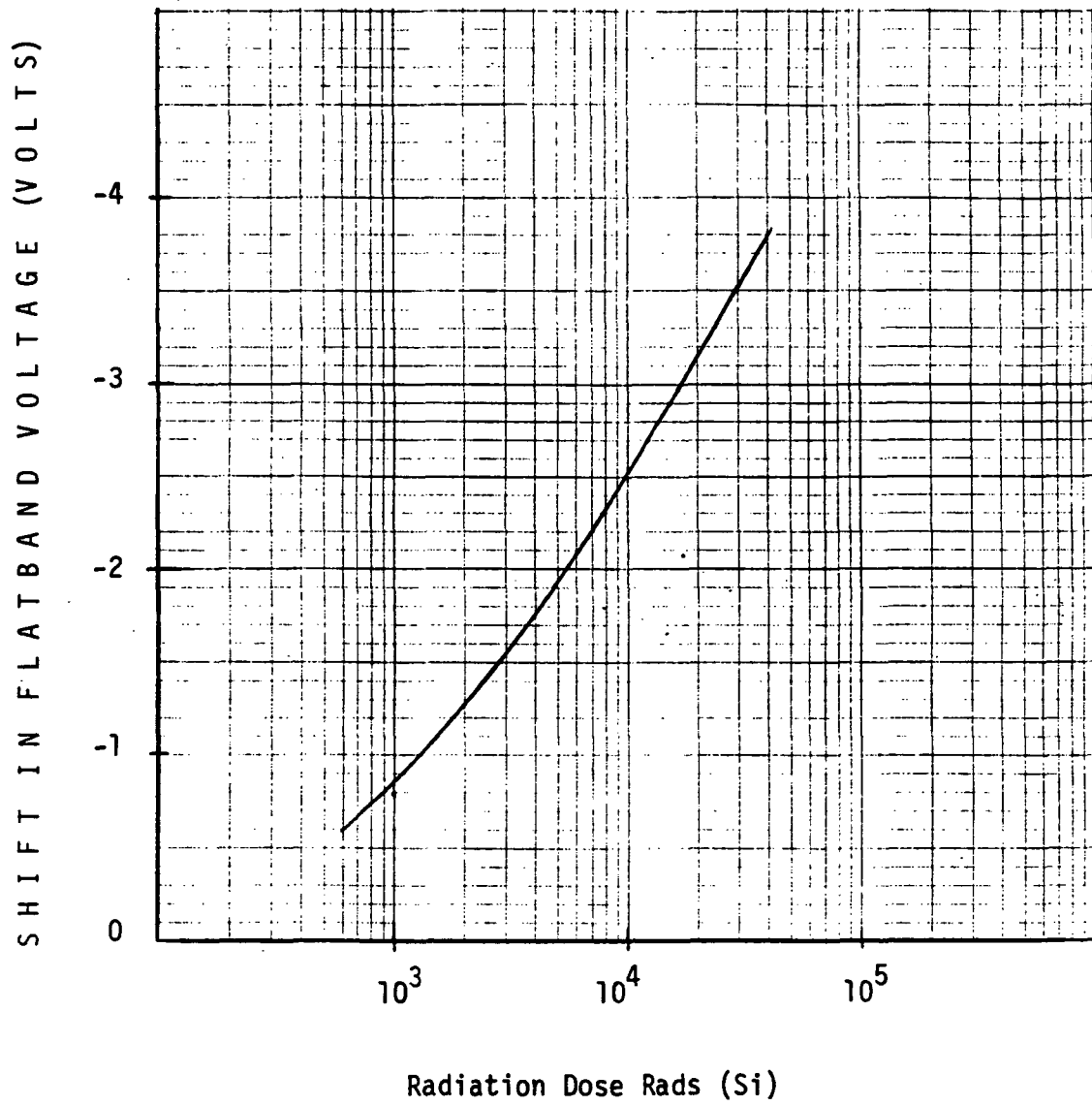


Figure 2.23: ΔV_{FB} vs Total Dose for the 500 x 1 CCD.⁴⁵

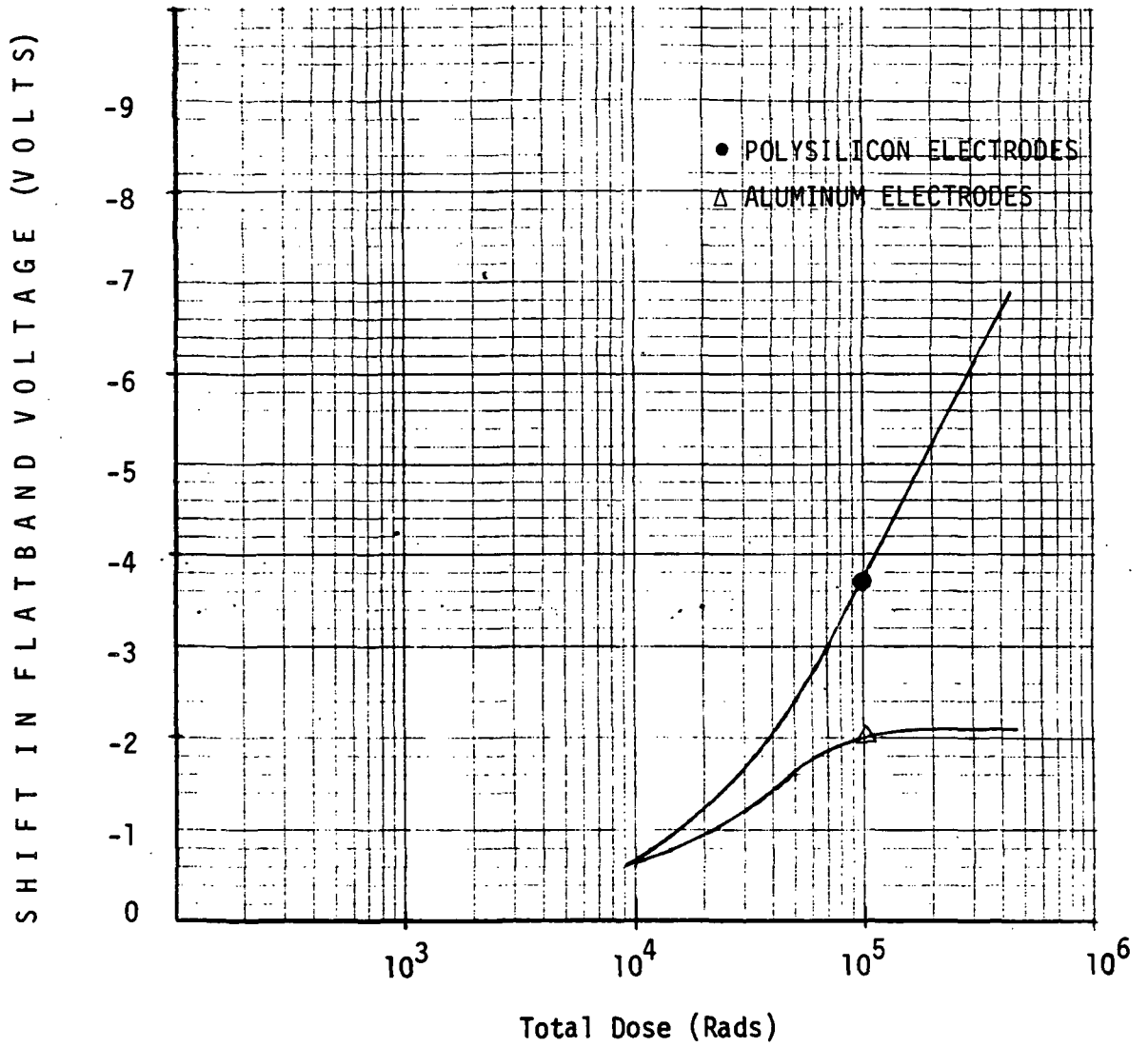


Figure 2.24: ΔV_{FB} vs Total Dose for 64 x 1 CCD.⁴⁵

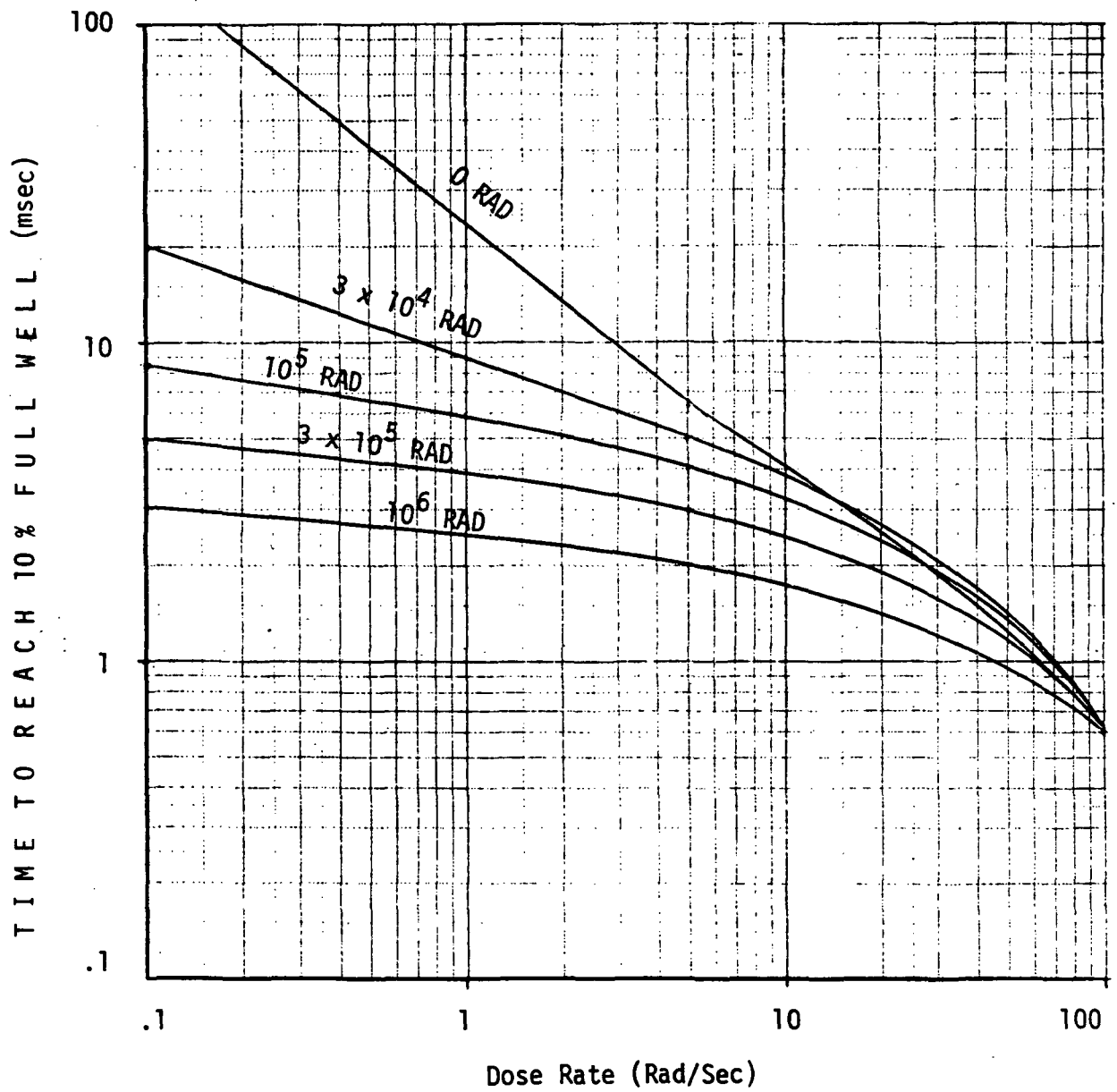


Figure 2.25: Effects of Low Rate Gamma Radiation on CCD Storage Time after Various Total Dose Levels.⁴⁴

2.3.5 Interference Effects

Transient interference effects on static logic microcircuits of bipolar and MOS technologies (i.e., TTL, S/C TTL, ECL, I²L, p-MOS, n-MOS and CMOS) are not significant at radiation dose rates below 10⁵ rads(Si)/s, and no problems are anticipated in JOP application. Transient interference effects may, however, be of concern for dynamic arrays and charge-coupled device arrays. The potential problem may be evaluated by determining the total ionizing dose necessary to compromise the stored charge in the array representing a single bit of information. This value has been reported as low as 0.1 rad(Si) for a dynamic MOS shift register. At a peak exposure rate of 100 rads(Si)/s it follows then that information in the CCD array must be refreshed at least every millisecond and at least every 10 milliseconds for the dynamic MOS array. These refresh times are only for the radiation-induced carrier generation and must be reduced further for thermal carrier generation. It is anticipated that above room temperature, thermal carrier generation will dominate for all but the highest performance arrays. An example of the increase in required refresh rate in a dynamic MOS array is presented in Table 2.9.

f_{ϕ} Hz	Failure Level rads(Si)/s	
~ 0.2	0.0	} Co ⁶⁰
4	1.1 x 10 ¹	
200	1.0 x 10 ³	
1k	4.8 x 10 ³	} Reactor
4k	1.6 x 10 ⁴	
10k	3.8 x 10 ⁴	
40k	1.6 x 10 ⁵	
100k	3.8 x 10 ⁵	

TABLE 2.9: I 1402 Dynamic MOS Shift Register Failure Level as a Function of Refresh Frequency.^{4,6}

2.4 OPTICAL MATERIALS

Optical Materials - Long-Term Ionization

- Coloration

Optical Materials - Interference

- Luminescence

Ionizing radiation produces color centers in optical materials (glassy or crystalline). The rate at which color centers are produced is a strong function of the material impurity content. As a general rule the purest glasses are least sensitive to radiation-induced coloration.

For reasonably low optical absorption the effect of radiation can be described as an incremental absorption coefficient proportional to radiation dose. For example, the transmissivity for light of wave length, λ , through a sample of thickness, χ , is:

$$\frac{I(\lambda)}{I_0(\lambda)} = \exp[-\mu(\lambda)\chi]$$

where $\mu(\lambda) = \mu_0(\lambda) + \mu'(\lambda) D$

and $\mu'(\lambda)$ is the rate of change of μ with dose, D , and has units of $\text{cm}^{-1}\text{rad}^{-1}$.

Table 2.10 presents some typical values of μ' over the visible spectrum for a variety of materials.⁴⁷ From theoretical consideration, a worst case value of $\mu' \approx 5 \times 10^{-4} \text{ cm}^{-1}\text{rad}^{-1}$ can be deduced.

For internal Probe applications, $D \lesssim 10^5$ rads, and the maximum

absorption for Suprasil 1, Corning 7940, or Suprasil W1 is less than 10^{-3} cm^{-1} .

TABLE 2.10: Absorption in Optical Materials⁴⁷

<u>RELATIVE RATING</u>	<u>MATERIAL</u>	<u>μ' ($\text{cm}^{-1} \text{ rad}^{-1}$)</u>
EXCELLENT	SUPRASIL 1	$\sim 10^{-10}$
VERY GOOD	CORNING 7940	$\sim 10^{-8}$
	SUPRASIL W1	$\sim 10^{-8}$
GOOD	POLYSTYRENE	$\sim 3 \times 10^{-8}$
	AMERSIL TO-8	$\sim 10^{-7}$
	LEAD SILICATE (ORDINARY GLASS)	$\sim 2 \times 10^{-6}$
	CORNING 5010 FIBER	$\sim 10^{-5}$

For external optical elements the dose in the outermost layer can be very large due to the deposition of lower energy protons. In effect the absorption coefficient, μ , can become very large, but only over a very thin layer, χ , of the outer material. This effect can be estimated from the total energy fluence in low energy protons, which is $\sim 2 \times 10^{12} \text{ MeV/cm}^2$. The integral of the dose over the thickness of the absorption layer is then $\sim 3 \times 10^4 \text{ rad-cm}$. This is equivalent in absorption to a material thickness 0.3 cm exposed to the internal dose of 10^5 rad .

Optical materials also luminesce when exposed to ionizing radiation. The emission is generally broad spectrum, with some increase toward short

wavelengths.²⁴ The emission efficiency (light output energy per unit radiation deposited energy) varies from a low value of $\sim 10^{-5}$ in pure materials to $\sim 10^{-3}$ in less pure materials. With reasonable confidence we can assume that luminescence efficiencies will be less than 1% in all materials except those deliberately used as scintillators (e.g., NaI(Tl), Pilot B plastic).

2.5 QUARTZ CRYSTAL OSCILLATORS AND FILTERS

Quartz Crystals - Long-Term Ionization

- Small frequency shifts

Ionizing radiation will produce very small changes in the resonant frequency of quartz crystals. These changes can be significant if the crystals are used in precise frequency applications.

Natural quartz, which is frequently used in high Q applications, exhibits relatively large changes, as shown in Figure 2.26.

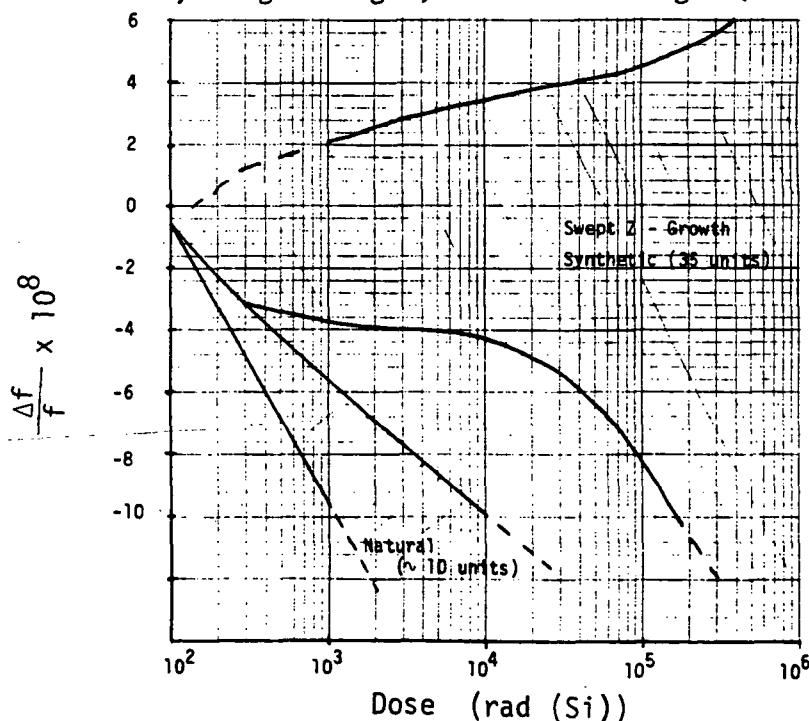


Figure 2.26: Composite Steady-State Frequency Shift Data vs Dose for Quartz Crystal Resonators.⁴⁸

Even a dose as low as 10^3 rad(quartz) can produce a frequency shift of 0.1 ppm. This problem can be overcome by using swept Z-growth synthetic premium - Q quartz, in which the frequency shift at 10^5 rad(quartz) is less than 0.1 ppm.

For further improvement in response, we can make use of the observed uniformity of radiation response over the central portion of a quartz bar from which the oscillator crystals are cut. Figure 2.27 illustrates this uniformity.^{4,8} It can be used to select a bar with minimum response, and to correct data for the known frequency shifts.

2.6 MISCELLANEOUS DEVICES AND MATERIALS

2.6.1 Surface Acoustic Wave Devices

These do not appear to be susceptible to change of any parameters below 10^{11} p/cm² (20 MeV equivalent) displacement damage and 10^5 rad(Si) long-term ionization.

2.6.2 Magnetic Bubble Domain Memories

Rare earth iron garnet films showed no significant changes in saturation magnetization, wall energy, wall mobility, coercivity and saturation velocity following neutron and gamma irradiation for levels at least two orders of magnitude above those of concern for this handbook. Therefore, no problem is expected for these device types.

2.6.3 Cabling

The Probe radiation environment will not produce any significant permanent degradation in cabling and wiring.

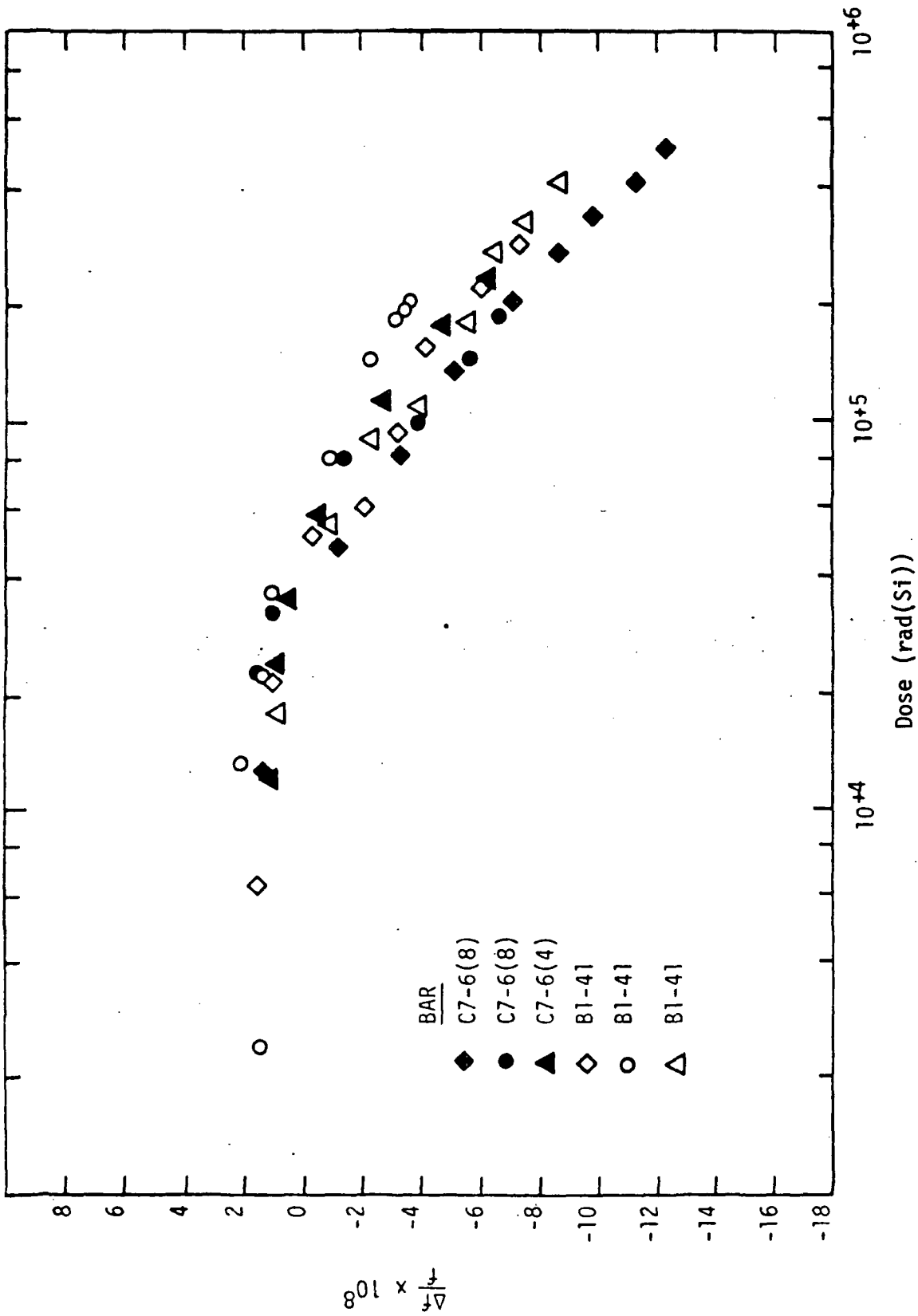


Figure 2.27: Frequency Offsets for 5-MHz Resonators of Swept Synthetic Quartz, Showing Behavior for Units Cut from the Same Bar. Irradiation Is by 35-MeV Electrons.⁴⁸

The wiring connecting low-current sensors to high impedance preamps can possibly be subject to interference during radiation exposure. It can be assumed that a current, I , is generated:

$$I = K_c \dot{D} L$$

where K_c is a constant dependent on the wire and the radiation spectrum, \dot{D} is the instantaneous dose rate and L is the length of irradiated wire.

The worst-case value of K_c is $\sim 5 \times 10^{-12}$ Asec/rad-cm, corresponding to the incident electrons all stopping in the insulator of ~ 1 cm thickness cable. In practice the actual value of K_c is smaller by a factor of 10-100, depending on the degree to which the electron spectrum has been hardened by intervening shielding.

2.6.4 Other Materials

For the Probe radiation environment, displacement effects can be neglected in all materials except semiconductors.

Chemical radiation effects even in long-chain polymers, can also almost surely be neglected. If in doubt the following numerical estimate can be performed. The most efficient radiation-chemistry processes produce a reaction (one chemical bond change) for ~ 30 eV of energy deposited. Therefore, a dose of D (rad) produces a change in the fraction, f , of molecules;

$$f = 3 \times 10^{-12} (D)M$$

where M is the molecular weight. For example, if we expose a long-chain polymer (Molecular weight $\sim 10^5$) to a dose of 10^5 rads a maximum of 3% of the molecules will have a bond altered by the radiation.

SECTION 3

3.0 DESIGN GUIDELINES FOR RADIATION EFFECTS

The first step in the design process is the selection of the general types of components which are desirable for the system based on performance characteristics under non-radiation conditions (i.e., a feasibility design to make sure the system can be designed). Now, the system designer must select the actual device types and specify modifications in the system so that the system will survive the severe environments of temperature, acceleration and radiation, among others. The following will provide the designer with the necessary guidelines so that the system will satisfy the radiation requirements of displacement effects, long-term ionization effects and transient interference effects. Section 2 of this handbook provides the designer with an overview of how radiation effects electronic system components and materials, and an appreciation of which types of components and effects are the most severe in the radiation environment.

The following sections show how to qualify devices for use in the radiation-hardened system.

At the outset the system survivability budget in the Probe must be known (0.99 probability of success for an experimental system is an example). Next, the experimental system failure budget must be broken down into the component failure budgets. This means that the types of parts in the system are defined and the number of each type is determined. Then a probability of successful operation must be defined for each type of

component such that the overall system probability is satisfied (this will probably require a reliability specialist to make the necessary breakdown using established rules for general reliability).

The biggest failure budget should be given initially to the components suspected of being most radiation sensitive as determined in Section 2 of this handbook. If a worst case number for failure budgets of component types is desired, take the system probability of failure and divide by N , where N is given by the total number of components in the system. Using this method, some devices will be easily qualified while other device types, which will have a harder time meeting the radiation requirements, could have used the added failure budget. A small improvement can be effected by using redundancy. Generally, the use of redundancy does not help to qualify a group of devices by changing the survivability budget unless the group is close to being qualified anyway; then a redundancy approach may be a viable and quick technique to obtain the added margin.

In addition to the failure budget the designer must have a radiation environment specified for the location of interest in the Probe. This radiation environment is determined primarily by the electron fluence and proton fluence and spectrum, as modified by the shielding between the external environment and the location of interest, as well as the bremsstrahlung generated in the shield. As a design input, however, the radiation environment should be defined as a 20 MeV equivalent proton and a 3 MeV equivalent electron fluence, which can be used for evaluating displacement damage effects, a total ionizing radiation absorbed dose for evaluating of long-term ionization effects, and a peak ionizing radiation absorbed dose rate for evaluating transient interference effects. The radiation environment presented in this Handbook

is based on the nominal model of the Jovian radiation environment and is intended to represent the general range of the expected environment. Definition of the uncertainties in the radiation model and worst-case levels will be made available through NASA Ames Research Center. Uncertainties, at present, could result in an increase in the radiation environment of up to a factor of five from that as presented in the Handbook.

It is essential in efficient design that the radiation level must be established as an input parameter of the design process. At that point, the component evaluation, design techniques and hardening can be implemented to realize a survivable and successful system.

In Section 3.1, we will present general design considerations that should be used to select devices, materials, and operating conditions for preliminary design. In Section 3.2 we present the statistical method for treating radiation response data leading to requirements for hardness assurance specifications on device procurement, where needed. In Section 3.3, we present factors to be incorporated into the definition of radiation effects tests on devices and subsystems.

3.1 DESIGN CONSIDERATIONS

3.1.1 Bipolar Transistors

3.1.1.1 Displacement Effects

The most important parameter for displacement effects is the proton fluence at the device with a relatively minor contribution from the electron fluence. The shielding provided by Probe structure, device placement, and the device case will in most instances make displacement effects negligible. Therefore, the first step in estimating the displacement effects contribution to bipolar transistor damage should be to make an

estimate of the equivalence proton fluence, Φ_{20} , and the equivalent electron fluence, Φ_3 at the device. For this purpose, the first calculation can use a worst case value of $\Phi_3 \sim 3 \times 10^{12}$ e/cm², but Φ_{20} should be for the specific component location.

The first estimate of an upper limit to h_{FE} degradation can then be performed using the specified minimum value of f_T :

$$\begin{aligned} \Delta(1/h_{FE}) &= \frac{0.2}{f_T} (K_p \Phi_{20} + K_e \Phi_3) \\ \Delta(1/h_{FE}) &\leq \frac{0.2}{f_T} (10^{-4} \Phi_{20} + 3 \times 10^{-7} \Phi_3) \\ &\leq \frac{0.2}{f_T} (10^{-4} \Phi_{20} + 10^6) \end{aligned}$$

If proton and electron data are available, they can be used to make a better estimate. However, their variance must be taken into account, as in the procedure discussed in Section 3.2.

If only neutron data are available, calculate an equivalent neutron fluence:

$$\Phi_1 \simeq 30 \Phi_{20} + .06 \Phi_3 \cong 30\Phi_{20} + 2 \times 10^{11}$$

The worst case value of $\Delta(1/h_{FE})$ is then deduced by calculating $\bar{X}S^{\pm(w+u)}$ at Φ_1 , using the methods of Section 3.2.

If this value is not acceptable for required circuit performance, the next step is to determine if the type of transistor, resistivity (from BV_{eb}) or injection level (from I_e) allows a lower conversion factor from proton/electron to neutron fluence.⁴

If this result is still not acceptable, the available alternatives are to relocate or shield the part, change the circuit requirements on the part [i.e. tolerate the larger $\Delta(1/h_{FE})$] or measure the proton/electron response of a sample of the part population to be used.

3.1.1.2 Long-Term Ionization Effects

There is no analytical form for long-term ionization effects on bipolar transistor to relate gain degradation to electrical parameters and a radiation damage constant:

Similarly, the selection of the device exhibiting minimum long-term ionization response is not governed by normal specifications. Evaluation of these effects must be based on irradiation test data as discussed in Section 3.2.

The use of the transistor in the circuit can minimize the degradation by providing adequate base current and operating the device at higher collector currents (optimally near the maximum of the h_{FE} vs. I_C curve).

3.1.2 Other Discrete Semiconductor Components

3.1.2.1 Junction - FETs

The increase in leakage current is strongly dependent on the bias at the gate junction; higher negative gate bias on a n-channel

device causes greater change in leakage current.⁴⁹ As with bipolar transistors, the designer has therefore some control over the resultant radiation hardness level of the device type but the hardness level is primarily dependent on the manufacturer's process.

3.1.2.2 SCRs

Performance degradation in SCR's is typically similar to that of bipolar transistors of low f_T . This is particularly the case with high voltage, high current devices. It is desirable to eliminate their application in the Probe electronics unless critically necessary. No analytical guidelines are available for either displacement damage or long-term ionization effects. Device selection must be made from experimental test data. Some parameter derating of gate turn-on and sustaining current parameters is necessary, but the principal consideration should be in device selection.

3.1.2.3 Diodes

For temperature-compensated voltage-regulator diodes it can be assumed that

$$\left| \frac{\Delta V_Z}{V_Z} \right| < 1.5 \times 10^{-12} \phi_{20} + 1 \times 10^{-15} \phi_3$$

and ΔV_Z is generally negative.

If these changes are not tolerable, neutron-irradiation data on the same device made by the same manufacturer can be used to establish limits for proton damage, using an assumed ratio of 30 for neutron/proton fluence. For confidence limits a population standard deviation of a factor of 1.5 should be used, unless data are taken on the same date - code lots as used for manufacture.

For other diode applications parameter changes are usually negligible. If a sensitive application occurs (e.g., $\Delta V_f < 100$ mV), the applicable data should be reviewed for the particular device type.

3.1.2.4 Electro-Optical Devices

The requirements on electro-optical devices depend very strongly on their application. Selection of devices and applications should be governed by the rules that semiconductor devices whose efficiency depends on long carrier-recombination times (e.g., solar cells, LED's) will degrade in efficiency. The application should provide adequate gain margin.

Vacuum tube photodetectors (e.g., electron multipliers) are undegraded by the Probe exposure, but may exhibit an increase in dark current due to transient interference.

An upper limit on interference effects can be estimated by assuming the following:

- 1) PN junctions will produce a dark current of less than $5\mu\text{A}$ per cm^2 of junction area.
- 2) Cables, wiring, and circuit boards will produce a current of less than 0.5 nA per cm^2 of projected area that can couple into a circuit.
- 3) The cathode of electron-emission devices (e.g., electron multipliers) will emit less than 10^{-11} A/ cm^2 of radiation induced dark current.
- 4) Optical materials will luminesce, emitting less than 1% of the radiation energy deposited in them.

3.1.3 Integrated Circuits

Design parameter flexibility on microcircuits is generally more limited than those of discrete circuit elements. For digital microcircuits, selection of technological family and a maximum fan-out is then selected which

determines the specific realization of a digital subsystem. Considerations of required data processing rates also influence the selection of the microcircuit family. Selection of TTL, Schottky-clamped, ECL, p-MOS or n-MOS arrays fixes the trade-off between switching speed and power dissipation. With CMOS or I²L logic arrays, however, there is additional flexibility in adjusting circuit bias conditions with a trade-off in power dissipation. Generally, once the speed requirements can be satisfied the bias conditions are established for minimum power dissipation. Adding radiation effects consideration to the design will generally lead to a trade-off between radiation hardness and power dissipation.

Design parameters of analog microcircuits are generally more extensive than those of digital microcircuits. In many cases, overall circuit parameters such as open-loop gain, input bias current, output drive capability and maximum slew rate are derated just as the parameters of a bipolar transistor. Parameters of analog microcircuits that must be considered most carefully are those that require matched performance of element pairs. In this case bias conditions during application should also be matched as close as possible to help the radiation-induced degradation in each element match closely.

3.1.3.1 Bipolar Digital

- decrease output fan-out
- increase I²L injector bias current

In many cases, the radiation effects at the Probe exposure level will be negligible. The critical design parameter which must be traded off to gain hardness assurance is fan-out or output drive capability. Long-term ionization and displacement damage effects may be significant in I²L arrays. In this case, the injector bias current can be increased to increase circuit

hardness (up to the point where there are no additional increases in switching speed with increasing bias current) at the penalty of increasing power dissipation.

3.1.3.2 MOS

- decrease output drive requirements
- reduce maximum switching speed
- increase CMOS supply voltage

There are very few design parameters available to adjust the electrical performance and radiation susceptibility of modern MOS microcircuits. This is particularly true for p-MOS and n-MOS arrays that operate at fixed supply voltages. Fan-out and drive capability is a critical parameter if switching speed is a critical concern. Ionizing radiation-induced threshold voltage shifts will reduce the output drive capability of p-type enhancement mode transistors and will result in an increased switching time for a given output capacitive load. As a design parameter, the capacitive loading on outputs should be minimized and the switching speed requirements should be relaxed from the normal performance limits of the array.

The radiation susceptibility of MOS microcircuits may be varied somewhat by the electrical bias conditions during exposure. The best case is dynamic switching during exposure and the worst-case is positive gate-substrate static bias. In general, however, hardening must be accomplished by component selection and shielding. Hardened CMOS microcircuits have been developed by a few semiconductor manufacturers through sophisticated processing techniques and tight controls.

3.1.3.3 Bipolar Analog

- derate open loop gain
- derate input offset voltages, currents
- derate output drive capability
- derate maximum slew rate

Design considerations in analog microcircuits are generally a required derating in critical performance parameters. Radiation-induced effects are of the nature to produce substantial degradation of these performance parameters before catastrophic array failure is observed. Parameters involving cascaded transistor gains and matched device performance are the most critical.

Applications of operational amplifiers in Probe electronics may require increased feedback (or lower closed loop gains) to reduce performance sensitivity to the degradation in open loop gain. If the total gain required cannot be realized for the maximum closed loop gains which can be used, additional amplifier stages must be added.

Degradation in the input offset parameters can be accommodated by input circuit design to a point. If the required performance cannot be achieved by circuit adjustment then additional circuitry is required to implement a chopper-stabilized network.

Design considerations on complex analog microcircuits (e.g., A/D and D/A converters) are more in derating overall performance as required for digital microcircuits. Critical active networks such as high-gain, precision-balanced amplifiers, are internal to the array and cannot be derated from the external terminals. Critical parameters to be derated may include linearity, precision, and maximum operating speed.

3.1.3.4 CCD's and Image Sensors

- decrease data storage times
- derate for increased dark current

The basic failure mechanisms due to ionizing radiation effects in CCD's and semiconductor image sensors are essentially the same as those of MOS microcircuits (i.e., trapped charge at the silicon-silicon dioxide interface). Performance parameters, however, are much different and the levels of complexity are at the limits of LSI technology. Critical performance parameters are those directly affected by the threshold voltages of the transfer elements, charge transfer losses, and recombination rates of stored charge. Changes in threshold voltage will tend to cause loss of data during transfer. Supply voltages can generally be adjusted over a limited range for modest gains in array hardness. Increases in threshold voltage will also increase switching times for internal transfer and for output drives. Maximum data rates should be conservative and output capacitive drive requirements should be minimized.

Increases in dark current can be the result of threshold voltage shifts and/or increase in carrier recombination due to displacement damage-induced lifetime degradation. In either case there will be a decrease in transfer efficiency and a decrease in the time that data can be stored in the array. Little can be done about the transfer efficiency as a design consideration but data loss can be accounted for by an increase in processing rate (or a decrease in required storage time).

Conclusions to be drawn concerning the design features and operating conditions of CCD's for total dose radiation environments are as follows:⁵⁰

- 1) A buried channel structure should be used.
- 2) An n-channel structure should be used.
- 3) The design should use a planar channel insulator (no stepped oxide) and only one type of electrode material.

- 4) The design must control the surface potential in the region between electrodes.
- 5) The use of undoped polysilicon for interelectrode isolation should be avoided. Total doses of 1 to 3×10^4 rads(Si) cause channeling in the isolation regions with resulting deterioration in device performance.
- 6) The reverse bias applied to the buried channel must be large enough to keep the channel depleted after irradiation.

Devices incorporating these design characteristics have been operated with acceptable transfer efficiencies after exposure to gamma doses greater than 10^6 rads(Si), compared to typical array failure between 10^4 - 10^5 rads(Si).

3.1.4 Miscellaneous Materials and Devices

3.1.4.1 Optical Materials

Wherever ultra-violet grade fused silica glasses are used (e.g., Suprasil 1, Corning 7940, Suprasil W1) the coloration from the ionization dose will be negligible within the normal optical passband. If other materials are used specific radiation test data should be sought in the literature to establish that the resultant attenuation, $\exp[-\mu x]$, is acceptable.

Antireflection coatings should be on the inside of optical lenses (e.g., not exposed to the low-energy proton fluence) wherever possible. Where it is necessary to expose them directly to the space environment a radiation test with low energy particles to produce the anticipated outer layer dose ($\sim 5 \times 10^8$ rad) should be performed unless data can be found. The existing test data on MgF_2 coatings appears promising, even at this high dose, but the response can be a function of specific impurities.

When optical glasses are viewed by sensors that may respond to low levels of light, the effect of radiation-induced luminescence should be estimated. The first step is to assume a worst case luminescence efficiency, $\epsilon \sim 10^{-2}$. The signal expected from the detector, S_1 is:

$$S = 10^{-5} \frac{\epsilon R \times D \times M}{4\pi r^2}$$

where R is the response of the detector in output units per W/cm^2 of illumination,
 D (rad/sec) is the dose rate at the glass,
 M (gm) is the mass of irradiated glass,
and r (cm) is the distance from the glass to the detector.

If S calculated with $\epsilon \sim 10^{-2}$ is negligible, we expect no luminescence problems. If it is significant, the estimate should be repeated using luminescence data on the specific material. If feasible, a particularly useful hardening technique is to place an optical spectral filter in front of the detector. Since the luminescence is broad band, its noise can be effectively rejected compared to a narrow-band optical signal.

3.1.4.2 Quartz Crystal Oscillators and Filters

If frequency changes as large as 10 ppm are tolerable no special provisions need to be made for quartz crystals. If they are not, but a change of 0.1 ppm is acceptable, swept synthetic quartz should be used. To ensure proper sweeping, a resonator made from a sample of the quartz stone used should be irradiated and tested to check the response. If a precision less than 0.1 ppm is required, a bar should be specially selected and samples irradiated to characterize the response.

3.1.4.3 Cabling

All cabling runs in which a background current of $< 1\text{nA}$ can be significant should be identified. For each of these the radiation incident on the cable should be calculated and the interference current due to electrons stopping in the cable insulator and conductors estimated. This interference current should be added to the "primary photocurrent" generated in the sensor and pre-amp input to evaluate the importance of interference. Minimum photocurrents are observed in solid-dielectric, minimum-geometry cables such as RG162.

If this current is unacceptable it can be decreased by shielding, shortening the cable run, balancing and subtraction, modulation/demodulation, and other appropriate design techniques.

3.1.5 Interference

Interference is not treated statistically in Section 3.2, because it can be eliminated from concern in all but a few cases. In these it must be treated by special analysis and possibly testing.

In electronic circuit components interference can be neglected except in the following cases:

- 1) Where a dark current of $\sim 1\text{nA}$ is significant
- 2) In dynamic MOS memory array (e.g., MOS shift register)
- 3) In CCD arrays
- 4) In low level optical and radiation detectors

3.2 COMPONENT SELECTION AND PROCUREMENT - STATISTICAL APPROACH

3.2.1 Introduction

The selection of components in a system is the most critical part of the design consideration; a reliable system cannot be realized with marginal components. The same generalization exists for radiation hardness assurance. If radiation hard components are used in a system, little redesign or shielding will be necessary. Usually, if there is a redesign, trade-offs must be made and the system ends up only capable of doing a portion of the intended task.

The following guidelines are designed to make the hardened design process as straightforward as possible. The methods recommended are simply an extension of good design techniques for the conditions of limited, expensive component data associated with hardened systems. By necessity of assuring hardness, the steps taken to accept a group of components must have checks on the assurance levels. To be 100% confident that a system will operate in the Probe radiation environment is unrealizable; but it is reasonable to achieve 90% confidence that a design is 99% reliable after encountering a radiation environment.

To determine the radiation reliability of a system, data on the failure of the components must be available. This means that unless someone has done an experiment which irradiated the same device type at or above the radiation levels of concern for the Probe, additional tests will be required. Even if data is available it will only tell the designer that in the past, looking at only one or two points of time, the device type was or was not hard enough to meet the Probe criteria. Although there is an apparently large quantity of radiation test data available, these should be used only as a guide in the initial selection of components and reviewed carefully before application as a criterion. There are various reasons for this point of view:

- 1) The time-frame of use of a given solid-state device is very short, since new and improved devices are being made

available at a rapid rate. The fact that a new device has improved electrical performance characteristics does not imply that its response to the effects of irradiation have also improved. The contrary frequently occurs.

- 2) Manufacturers are continuously working at improving processing techniques even in established, well-known electrical device types. A change in processing can radically alter the radiation effects characteristics of a device, possibly for the worse, even though the nominal electrical characteristics which determine its "2N" classification have not changed.
- 3) Where established devices have undergone no change in manufacturing techniques, there is still the condition, due to poor reproducibility of semiconductor surface conditions and other device characteristics, that devices can vary from batch to batch in radiation-sensitivity. It is also well known that even devices out of the same batch and with the same "date code" can vary.
- 4) The same device type, manufactured by several different companies, can be distinctively different in radiation response. This difference can be put to good advantage if the characteristics of that device type are highly desirable; while test data on the device obtained from the first manufacturer tried might indicate undesirable results, a broader collection of test data covering other manufacturers could show from which manufacturer an acceptable device can be obtained. Thus, in planning a test program, a sampling of products from several manufacturers should be anticipated.
- 5) There is a serious anomaly that is also a continual cause for concern. It arises unheralded, except through test results. It is the anomalous degradation of a single device (unit) that

could be of any type number of any manufacturer. These "maverick" type of degradations occur for no well-understood reason. The behavior of the "maverick" is so widely different from the norm (in the direction of excessive sensitivity to radiation) that the occurrence of such a degradation effect could be catastrophic to a spacecraft subsystem. Statistically, "mavericks" occur sufficiently frequently that the possibility of such an occurrence cannot be overlooked.

- 6) Certain "bulk" materials, such as thermal coating, optical windows, and some organics, where stability of properties is important, must also be tested carefully for damage effects in the properties of interest, for the following reason. The exact chemical mix of a commercial material will often vary from lot to lot and produce results similar to those described in Items 1 through 5 above. Such batch variations can have an important bearing on radiation hardness. Organic paints and glasses are important examples of such materials.

Therefore, data on the radiation hardness of the actual device groups used in the Probe systems is necessary for all critical components. Available data can be used if a large, stable safety margin is established.

Development of a component data base for hardened design is also complicated by the destructive nature of ionization and displacement damage effects. Unlike temperature, shock, acceleration and reliability characterization, test devices are not recommended for system application. Two schemes have been proposed for non-destructive screens: irradiation to a small fraction of the expected radiation level, and post-irradiation anneal to recover the initial electrical performance characteristics. In the first case, the damage is frequently a non-linear function of exposure level and parameter degradation at low exposure levels does not predict the component

hardness to the levels of confidence required for the Probe. This is particularly true for complex microcircuits. Meanwhile, the process of radiation testing actually causes the device to move closer to the radiation failure level and have that much less assurance of withstanding the Probe radiation requirements test.

Irradiation/annealing (IRAN) techniques cannot be used in general, because in many device types the response to a second irradiation is more severe than on the first screening irradiation, and may not even be correlated with the screening response, even if the anneal appears to be complete by electrical measurements. If IRAN is to be used, it must be qualified by an elaborate statistical test program involving re-irradiation and objective correlation analysis.

The only approach which appears reasonable then, is to sample the device group, test the sample, and then if the sample (with its statistical indication of what the rest of the group will do in the same radiation test) passes the specified criteria, accept the total group.

The approach then to obtain assurance in adequate hardness of components used in a Probe system is as follows:

- 1) Collect past data on each part type to determine how soft the devices may be and how much data will need to be collected in new tests.
- 2) Collect new data over several small groups of devices if no past data exist or if the past data gave an indication of wide variability in radiation hardness.
- 3) Procure the total group when enough data is available that demonstrates a method of procurement that will give a high probability of getting an acceptable group of devices.

- 4) Sample the procured group to make sure the group satisfies the radiation criteria.
- 5) If the sample does not pass the criteria after spending the money on procurement, then use every "trick-in-the-Handbook" either through design techniques or as a last resort, shielding to force the groups to pass. Self-shielding by component positioning is the first step, with additional shielding realized by adding materials.
- 6) If none of these techniques work, then selection of another device or devices that will pass the criteria is necessary.

As can be seen above, statistics play a major part in the test results when compared to the radiation criteria. By obtaining enough past data and then applying statistical methods to the data, we can get some assurance that further testing will tell us the same results. Unfortunately, past data on the exact device type that will be used in our system may not be available, either because the device is too new or no one had an interest in testing the device type previously. To find these past data is sometimes very difficult but there are three sources that can provide a good survey of what good data does exist. These are:

- 1) JPL Component Characterization Data.⁸
- 2) Harry Diamond Labs Data Bank - Washington, D.C.¹⁴
- 3) IEEE Transactions on Nuclear Science.

During the MJS program JPL performed numerous device irradiations, primarily with 2.5 MeV electrons and Co⁶⁰. The Harry Diamond Labs maintain a data bank which summarizes radiation response data for various semiconductor devices. Usually the sample size is relatively small. Many experiments that have been performed on device types are summarized in the

IEEE Transactions on Nuclear Science. Between these and the designer's own sources, collection of usable past data can be done with the least amount of pain. For the designer's convenience, we have referenced the location of articles which helped formulate this handbook.

This handbook has not tried to provide a comprehensive list of data on every device type known, since this approach could not hope to cover new device types. It would be wasteful, since most of the devices will not be used in the Probe.

The past data is important since it will possibly save a significant amount of radiation testing on small groups. Radiation testing is expensive and justifies spending some time reviewing past data. The past data will hopefully tell the designer which options are available to him for procuring radiation hardened devices.

A final point about the past data before the actual design guidelines are presented: the data should represent a similar or worst-case condition when related to the Probe worst-case operating condition. Otherwise the data will give a false beginning point in the guideline flow charts and end up costing time and money for an experiment to eventually pass the acceptance criteria. The previous sections of this handbook tell how to determine what parameters are most important and what conditions are worst case.

The flow charts presented in the following subsections are designed for specific component types based on what is known about the critical parameters, the nature of failure, and the stability of the technology. Each block in the flow charts is discussed in the narrative following the charts to provide details of how to do the operation, what an example looks like and where supplemental data can be found in this handbook to help the designer complete the block. After going through the chart for the first few device types, the flow charts will probably be the only parts of the handbook needed by the designer for the remaining device types.

The flow charts were designed to pass proven radiation hardened device types with a minimum cost of hardness assurance. If device types have not been proven hard from past data, then the task of assuring success of the Probe mission becomes more involved, but necessary if each experiment is to do its' job with a high probability of success. The flow charts were constructed to give the designer a way to objectively determine the options he must consider for every device type and application. How the device is used, who makes the device and new types of devices are all variables in determining the radiation hardness that must be considered when the system is built and during the hardness assurance process.

Simultaneous accumulation of displacement effects and long-term ionization effects are taken into account. Also, the displacement effects can be the result of protons or electrons at various energy levels. Since there is an energy level dependence and particle type dependence, we have normalized all displacement data used in the flow charts to neutrons/cm² (1-MeV equivalent). This allows past neutron data to be used for qualifying various component types for displacement effects.

3.2.2 Statistical Considerations

Statistical variations must be recognized and treated in using experimental data in the design process. In effect, each statistical variable must be considered by an increase in the safety margin between the response of the average device and the system requirements. The important variables are of two types:

- 1) the variation between device units for a particular device type (e.g., the population distribution), and
- 2) the uncertainty in our knowledge of the population distribution parameters (e.g., due to limits on size of test sample).

It is obvious that safety margins can be smaller if the population distribution is narrower (e.g., single manufacturer, few proximate date code lots or still better, selected diffusion lots or wafers). The safety margin can also be smaller for larger test samples. Therefore, it is most efficient to purchase each device type for a system at one time and perform a single irradiation sample test to characterize the entire lot.

We will assume that for each device type the radiation response variation between units will produce a log-normal distribution (i.e., a statistically normal distribution against the log of the device parameter) in radiation level at which the device falls outside a specified performance limit; i.e., a log-normal distribution in susceptibility levels. Although this assumption may appear to be bold, it is borne out by some limited data.⁵¹ It should be noted that a log-normal and normal distribution become equivalent for small standard deviations.

The alternate to some assumption on the distribution is to use Bayesian statistics. These would produce unreasonable test requirements (e.g., radiation test many systems worth of parts). Instead, we recommend assuming the log-normal distribution but remain alert for any data that violate this assumption.

Given a log-normal distribution with a mean, M , and a standard deviation, σ (in units of multiples of M), we can consult standard statistical tables to relate the failure budget for each part, p_{fi} , to the safe design point, $M\sigma^{\pm u}$. Table 3.1 presents a summary of such data. For example, if a device has a failure budget of 10^{-6} per unit, its design point should be a factor of $\sigma^{4.8}$ away from the mean failure level, where σ is the true standard deviation of the population.

Note: M and σ are the mean and standard deviation of the true population while M_s and s are the mean and standard deviation of the measured sample.

Unfortunately, the mean, M , and standard deviation of the population are generally known imperfectly, being estimated only by the mean, M_s , and standard deviation, s , of a test sample of size n . Again, assuming the true population is log-normal, the χ^2 and Student's t distribution can be used to estimate the additional margin of safety required between M_s and s . For small p_{fi} , the uncertainty in σ is usually most important. Table 3.2 presents the exponent, w , of the measured s to calculate the desired worst-case σ , at 90% confidence level.

TABLE 3.1: Values of Power of Standard Deviation for Required Probability of Failure

Design Factor		Design Factor	
P_{fi}	(in $\sigma^{\pm u}$)	P_{fi}	(in $\sigma^{\pm u}$)
10^{-9}	~ 5.9	10^{-5}	~ 4.3
10^{-8}	~ 5.5	10^{-4}	~ 3.9
10^{-7}	~ 5.2	10^{-3}	~ 3.3
10^{-6}	~ 4.8	10^{-2}	~ 2.3

Note: Assumes a log-normal distribution. p_{fi} = probability of failure allowed for each unit.

TABLE 3.2: Standard Deviation Factors for 90% Confidence

n	s-factor (w)	n	s-factor (w)
3	4.9	10	1.5
4	2.6	20	1.3
5	2.2	30	1.2

Note: Derived from the relationship $\chi^2 = \frac{n(s)^2}{\sigma^2}$ where χ^2 is the value from statistical tables for $c = 90\%$ confidence, n = number of samples, σ = overall group standard deviation, and s = sample standard deviation, $n-1$ = degrees of freedom.

The correction factor on the mean to obtain a 90% confidence value is $S^w \left(\frac{1.28}{\sqrt{n}} \right)$. Therefore, the mean and standard deviation values obtained from the sample data have now been corrected for the small sample sizes and represent worst case values for the true population mean and standard deviation with a 90% confidence. The final expression for the safe design point required to give the probability of failure is then obtained by using the expression:

$$M_s \pm S^w \left(\mu + \frac{1.28}{\sqrt{n}} \right)$$

where M_s = sample mean value

S = sample standard deviation

w = correction factor on the standard deviation for small sample sizes

n = sample size

3.2.3 Data Review

3.2.3.1 Bipolar Transistors and Similar Discrete Components

This section shows how to qualify bipolar transistors*, diodes, JFETS*, SCRS, optical devices and other similar components which have meaningful performance parameters varying continuously with accumulated radiation. As long as the variation is somewhat regular (i.e., no abrupt change in the parameter for increasing radiation levels), flow chart I can be applied for discrete components. The critical criteria is defined as the design margin (DM) for the required levels of survival probability and confidence.

NOTE: Appendix A discusses what a log-normal distribution is, how the above expressions were derived and provides a few examples of how to use the expressions above.

* Note: Exceptions to the list above can be found in Section 3.2.3.3. Check this list for other exceptions

The data used should represent the variation in the parameter response for a single radiation level at or above the Probe system requirement, (i.e., if the system radiation requirement for long-term ionization is 10^5 rad(Si) then the variation in $\Delta(1/h_{FE})$ over several bipolar transistors of the same type at one radiation level at or above 10^5 rad(Si) is the desired data). The approach in Flow Chart II can also be used for these devices, if desired.

3.2.3.2 Bipolar Integrated Circuits and Complex Devices not Covered in (3.2.3.3) [an abrupt change in parameter with radiation level]

The abrupt change of meaningful parameters with radiation accumulation and/or the complexity of these types of devices make the measurement of parameter variations very difficult. Even if these parameter variations were continuous and regular, it would be hard to relate them to one specific radiation degradation mechanism within the device. The device parameter variation due to radiation may actually be the result of several element parameters interacting non-linearly.

The data on radiation effects is therefore related to how many devices fail a selected parameter criterion versus radiation level. The data is taken over a radiation range that shows a distribution in failure versus increasing radiation levels. It is not necessary to restrict our data to the Probe system design radiation levels since we want only to know where the failure distribution exists and how close it is to our system radiation design level. If the failure distribution is at or below the system design radiation level then there will be a severe problem in assuring the high probability of survival for the system when using this part type. If it falls above the system level, then calculations of DM (Design Margin) on the flow charts will provide the level of hardness assurance.

3.2.3.3 MOS and Bipolar Linear Integrated Circuits

These two device types are exceptions to the complex components considered in Flow Chart II. The variation in radiation hardness of these technologies between manufacturers and over significant time periods has been great. Therefore, to have any chance of procuring a uniform group (in radiation response), a more strict approach to procurement is necessary. The handbook has therefore done the preliminary work for the designer in stating that there is no way the designer can pass the acceptance criteria for these device technologies unless he uses the more strict procurement method, approach "A". (See paragraph 3.2.4.1)

Some past data collection is required but this is designed to aid the designer in determining exactly which techniques appear valid in controlling the radiation hardness during procurement. Procurement will be restricted for these two device technologies to selected manufacturers and only qualified process runs.

Other types of devices which will require some type of process control or traceability are listed below:

- a) Bipolar transistors for hybrid circuits
- b) N-channel JFET's in applications requiring small leakage currents and analog switches containing JFET's and MOS transistors.
- c) Quartz crystal for precision oscillators and filter.

3.2.3.4 Block Descriptions for Flow Charts I, II and III (pp. 133, 134, 135)

Block 1a

The radiation limits to which the component type will be in the system must be defined. The component may not have the same restrictions of radiation levels as the system due to the inherent shielding from other

surrounding subsystems. A calculation of the shielding and the effects on the effective radiation levels at the component location can be calculated using the techniques as were described in Section 1.2.2 of this handbook. A worst-case estimate would be equal to the radiation levels specified for the entire system [e.g., $D = 10^5$ rads(Si), $\phi_{20} = 9 \times 10^{10}$ protons/cm² (20 MeV equivalent) and $\phi_3 = 2.5 \times 10^{12}$ electrons/cm² (3 MeV equivalent)]. If neutron irradiation data are to be used, the proton and electron displacement fluence are converted to a worst case neutron equivalent fluence $\phi_1 \leq 30\phi_{20} + .06 \phi_3$. In some particular cases, where the type of device and injection level can be estimated, smaller values of ϕ_1 can be used for the reduced damage constants as shown in Tables 3.3 through 3.4.

Block 1b

For Flow Chart I the parameter(s) chosen to characterize the device response should have two characteristics:

- 1) Design application is determined by quantitative parameter values.
- 2) The parameter changes are almost linear with radiation exposure near the expected exposure.

For Flow Charts II & III only the first criterion need be met.

The design limits and failure criteria specified must take into account a safety margin for degradation modes other than radiation, (e.g., temperature, end-of-life).

For transistors the most common relevant parameter is $(1/h_{FE})$ at the collector current of interest, or lower. Sometimes $V_{CE_{SAT}}$ is also important. Leakage currents, e.g., I_{CBO} or I_{CEO} , are rarely controlling.

For diodes the change in leakage current are usually small enough to be negligible in almost all applications. In precision temperature-compensated voltage regulator diodes (VRD) the breakdown voltage V_Z may change slightly.

TABLE 3.3: 20 MeV Proton Damage Constants⁴(appendix C)

K_T (cm²/sec)

Resistivity (ohm-cm)	Injection Level	
	10 ⁻³	10 ⁻¹
<u>n-type</u>		
1	2 - 10 x 10 ⁻⁵	1 - 5 x 10 ⁻⁵
10	--	~ 5 x 10 ⁻⁶
100	--	--
<u>p-type</u>		
1	1 - 3 x 10 ⁻⁵	~ 1 x 10 ⁻⁵
10	--	~ 5 x 10 ⁻⁶
100	--	--

TABLE 3.4: 3 MeV Electron Damage Constants⁴(appendix C)

K_T (cm²/sec)

Resistivity (ohm-cm)	Injection Level	
	Low ($\leq 10^{-2}$)	High (>1)
<u>n-type</u>		
1	0.6 - 3 x 10 ⁻⁷	~ 5 x 10 ^{-8*}
10	2 - 10 x 10 ⁻⁸	~ 1 x 10 ^{-8*}
<u>p-type</u>		
1	1 - 4 x 10 ⁻⁸	2 - 8 x 10 ⁻⁹
10	0.5 - 2 x 10 ⁻⁸	1 - 4 x 10 ⁻⁹
100	~ 3 x 10 ⁻⁹	~ 6 x 10 ⁻¹⁰

* Estimated from trends

Blocks 2 and 4

All past data should be considered as old data no matter how recent. This is because the device fabrication procedures can vary significantly, even within one manufacturer's product, and this variation can be directly related to changes in radiation response. Also, bias and temperature can affect the results of a test which means that the data collected may not match the designers system application.

A requirement in this block is therefore imposed, which requires the collection of as much data from several sources as possible. The more data used, the less chance of having to redo the design later.

If very few data exist, which cannot be related directly to the designers application, the design procedure requires going to Block 12 where several options exist. Use of approach "C" is not one of the options in this case.

Assume, from this point on, that some data exist on which an estimate can be made. This will require a minimum of 3 devices tested in a similar or relatable operating mode to the Probe system application.

Data at fluence levels very different from the application can be used as long as the relevant parameter changes are linear with radiation exposure between the radiation limits and test points, or at least the linear assumption produces a case. This restriction usually implies that data can be used in which the parameter changes fall within the acceptable parameter design limits and radiation exposures equal or exceed the radiation design limits. Care must be taken in selecting data that no bias is introduced in the data sample by any selection procedure. It is invalid to reject data only because the changes are large. It is valid to reject all data at high exposures because some of the parameter changes fall outside of the linear assumption.

Transistor pre-selection can be made by considering the relationship between f_T and $\Delta(1/h_{FE})$ discussed in Section 2.1.2. If a choice exists, a transistor with high f_T should be used.

For Flow Charts II and III, the data are usually in the form of failure vs. fluence. Again, all fluences are assumed to be in terms of displacement equivalent fluence. In Flow Chart II, bipolar digital ICs are considered. In general, these are very insensitive to both displacement and long-term ionization effects, and relatively minimal data can serve to qualify these devices for Probe applications.

Flow Chart III requires a restriction to diffusion runs or wafer lots. This is because for MOS integrated circuits (ICs) and Bipolar Linear ICs the variation in long-term ionization effects is so great that these devices must be procured from one manufacturer with diffusion-run and sometimes even wafer traceability.

Displacement effects in MOS can be ignored altogether for Probe applications, since the known threshold for damage is well above the radiation limits.

Linear integrated circuits are extremely sensitive to ionizing radiation effects and somewhat sensitive to displacement effects. The most important parameters to be measured in operational amplifiers and comparators are: input offset voltage, input offset current, input bias current, open loop gain under suitable load conditions and sink current capability. A/D or D/A converters are also very sensitive to total dose effects and the measurement is somewhat complex. Among the more important parameters are output current, gain and offset voltage. Voltage regulators are relatively insensitive to total dose effects. The output voltage and voltage regulation are the relevant parameters.

Therefore for Flow Chart III, data collected and used for the calculations based on past data has two purposes:

- 1) To see if past process control techniques were able to satisfy the component design hardness assurance requirements for this system, and
- 2) what process controls were used so that the same component hardness can be procured for the Probe system components.

The more controls needed, the more expensive the device will be. If no data exists on the controls, then the designer should go to Block 12 and choose one of the options including Option A (now modified).

Block 3

The failure budget of a component in the system is the maximum probability of failure allowed to that component so that the system can perform its function at a given probability of success. For example: If a system had a probability of success assigned to it of 99% and the system contained 1000 transistors, all of one type, then the failure budget for each transistor would be 10^{-5} .

For worst-case evaluations, assume all device units are to have the same maximum probability of failure and that all devices in the system must operate properly for the system to operate satisfactorily. Later on in the Flow Chart, if a device type cannot meet these worst-case requirements, some of the survivability budget can be reassigned to the softer parts and some of the design burden shifted onto inherently harder device types. This will be one of the options considered at Block 12.

Blocks 5 and 7

For each set of data the measured parameters of the population distributions are now determined. In the case of Flow Chart III, these must be evaluated for diffusion-lot or wafer samples. In Flow Charts I and II they

can be aggregated in any assembly that is representative of expected device procurement, including collecting together all data of a particular device type irrespective of manufacturer or date code.

Each data set is then fitted to a log-normal distribution, and the mean, \bar{X} and standard deviation, s , evaluated. Examples of data plots in which the samples are sorted by manufacturer are shown in Figures 3.1 through 3.3. If the data from the two suppliers were assembled into a single population, the method is still applicable, although the value of s would become larger. The particular neutron irradiation data shown in Figures 3.1 - 3.3 would still probably satisfy Probe requirements, since the failure thresholds are high. These illustrate an important option: if the mixed distribution is too wide to be acceptable, the data can be reanalyzed by supplier, or by date code, usually resulting in a more favorable distribution. Of course, if adequate hardness depends on such a selection, the device type must be procured from a single supplier (and possibly date code lot) and sample tested (Method B).

Blocks 6 and 8

We use Table 3.2 to obtain the correction factor, w , on "s" so that the σ values will be obtained with 90% confidence.

Block 9

Based on the survivability budget calculated for the component type in Block 3, Table 3.1 can be used to obtain the power of σ to give the required failure rate.

Blocks 10 and 11

If the measured parameters, \bar{X} and s , are truly representative of the device population, the required value of survivability and confidence can be achieved by using the device at or below the limit:

$$\bar{X}S \pm w \left(\mu + \frac{1.28}{\sqrt{n}} \right)$$

where "+" is used for distributions involving parameter variations at a particular dose or fluence level and "-" is used for distributions involving radiation levels for failure. However, many data are taken on small samples, possibly at one time, and the measured s may be much smaller than the spread in values bridging the tested device to currently manufactured devices. Studies of the distribution of displacement effects⁵² and long-term ionization effects¹² for a few parts extending over a period of years indicate that safe values for displacement is $\sigma \sim 1.5$ and for long-term ionization effects $\sigma \sim 2$. Therefore, we recommend that old data not be extrapolated more favorable than with these values of σ .

Block 12

Taking the values obtained in Blocks 10 and 11 and dividing these numbers into the limits determined in Block 1, will determine which option is available based on past data. If the design margin (DM) value meets the criteria for acceptance of past data then use Flow Chart IV on approach "C".

If the DM values were > 1 for transistors, approach "C" could be used to procure the total group of transistors for the system with a good probability that the components would pass the qualification test (to be discussed later). Even if the test showed a problem, the problem should be small enough so that slight modifications in design or shielding would allow the total group to be accepted.

The design margin (DM) was determined in this Handbook by a statistical approach using calculated values rather than a graphical method on probability graph paper as is sometimes done. Both methods can be used but the calculated value approach requires only a calculator and the mean and standard deviation values of the sample population. Once these tools are acquired, the criteria for qualifying a device type for radiation hardness can be obtained by simply plugging values into a formula and turning the crank. The calculated value approach also allows the designer to determine the simultaneous radiation effects from both displacement and long-term ionization processes. By comparing the calculated values from the sample data to the design limits, the designer can evaluate whether the displacement or long-term ionization effect is the most severe problem and what the relative priority of hardness design has to be assigned to each device type.

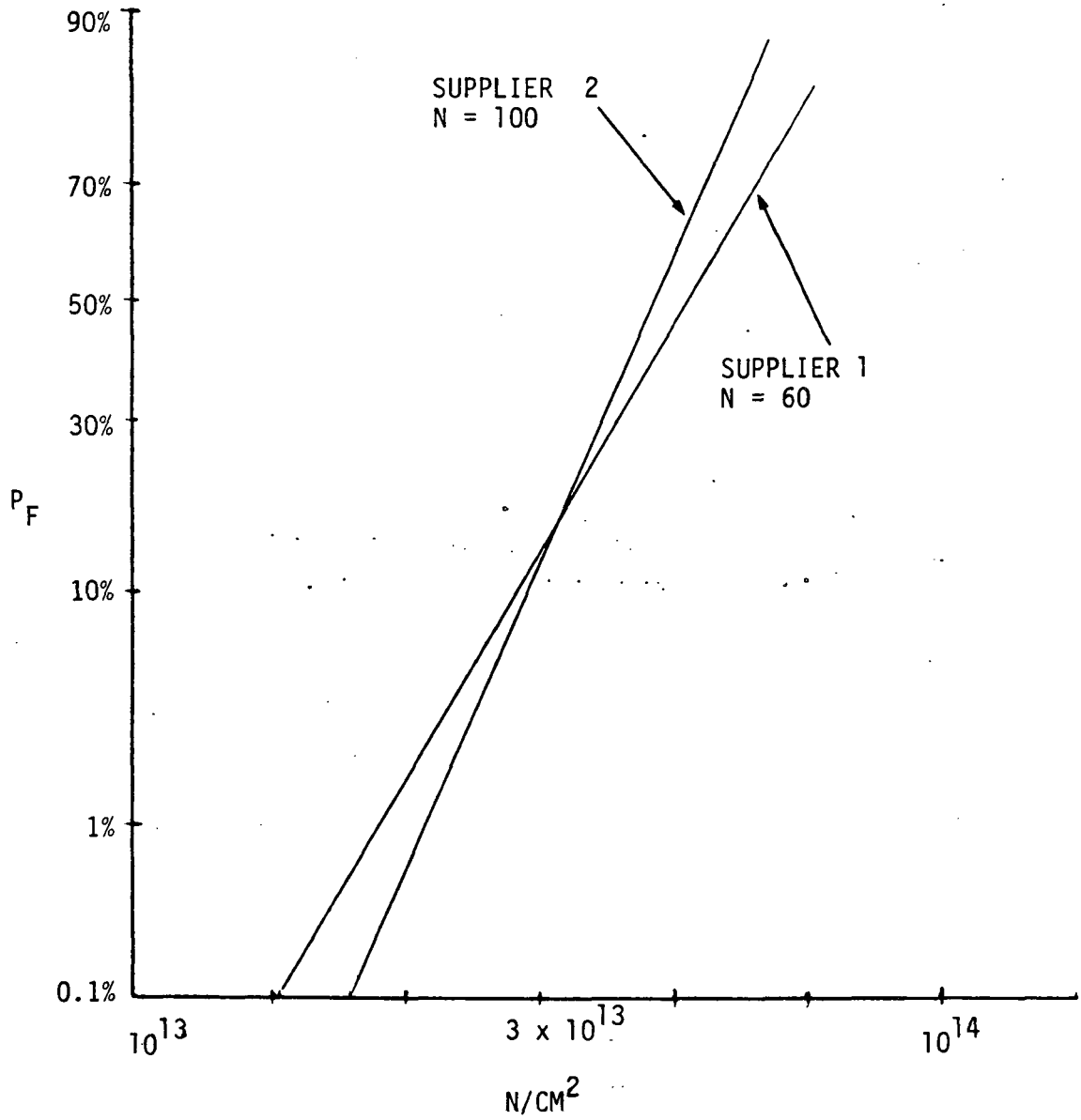


Figure 3.1: Probability of Failure vs Neutron Fluence for Two Suppliers of a DTL flip-flop;⁵² $M = 1.25$.

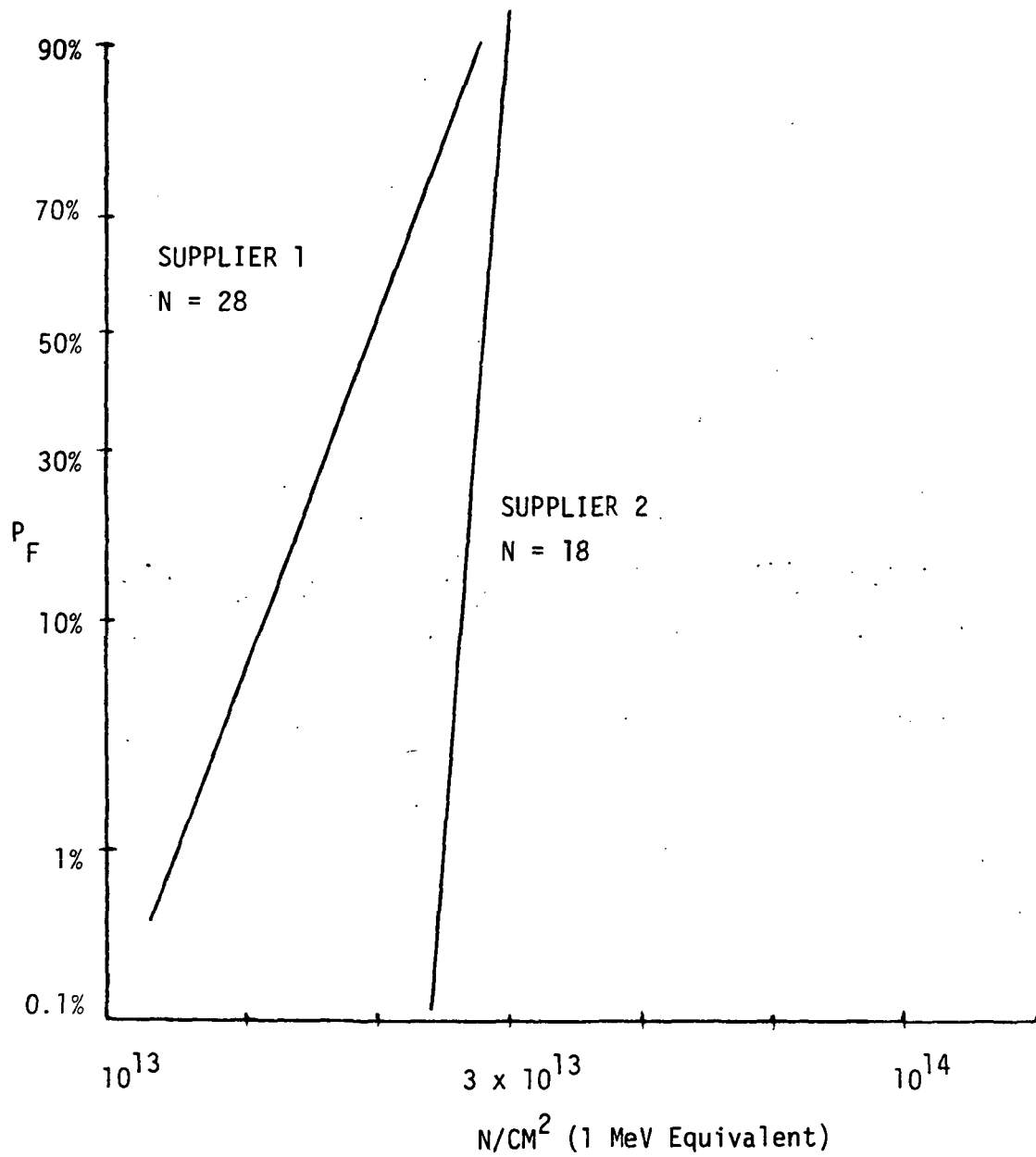


Figure 3.2: Probability of Failure vs Neutron Fluence for Two Suppliers of a General Purpose Amplifier;⁵² M = 1.25.

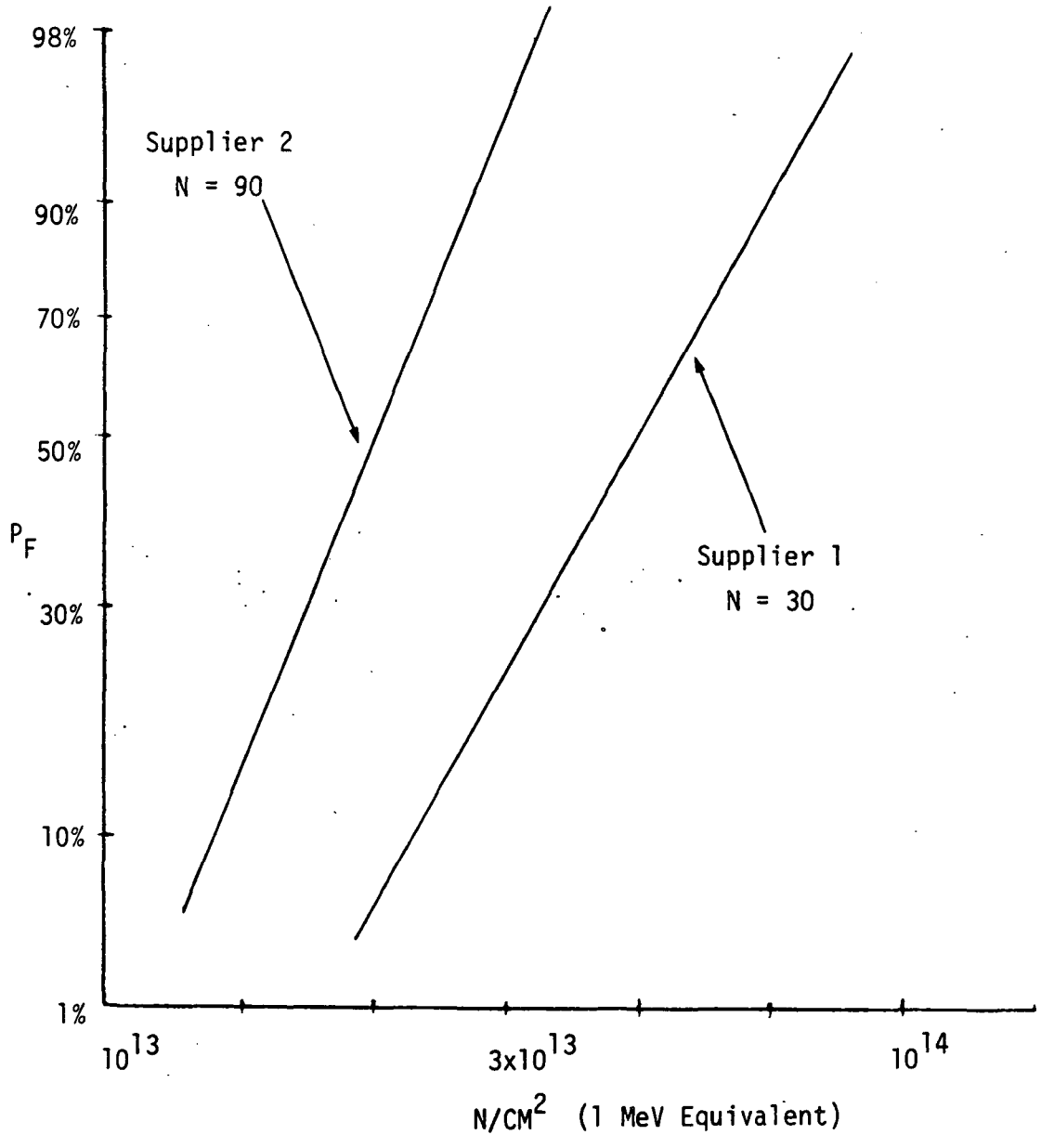


Figure 3.3: Probability of Failure vs Neutron Fluence for Two Suppliers of the 2N5038 Power Transistor; $^{52}M = 1.25$.

Block 14

The first option shown in the Flow Charts is a change in device type. If another device type will do the same function and data can be found which shows that it will provide a $DM > 1$ resulting in a simpler procurement class used, then this may be the most cost effective approach. Most of the work up to using a particular option has been paper calculations with no parts purchased. Once the parts are procured, both component costs and radiation testing time will begin to add costs to the system. Therefore, it is beneficial to evaluate the selection of parts at this point. If another device type is desired, Section 2 should be consulted to determine which types appear less susceptible due to their inherent hardness as a result of construction techniques on electrical properties.

The result of using the option on selecting another part is to restart the Flow Chart with the new selected device type.

Block 15

This option requires an understanding of the limitations and flexibility of the circuit design. If a component type is necessary in the system but degrades under radiation to a point beyond the circuit requirements, a change in circuit design can be attempted.

The result of this option is a change in Block 1b and a recalculation of Block 12. This may provide a fast and effective result especially if DM was initially very close to the acceptance criteria.

Block 16

A change in survivability budget just means that some of the probability for failure required of some very hard components has been shifted to

more soft component. A reliability specialist can make a quick reassessment of this change in budget to determine how much survivability budget can be redistributed.

This option really requires that all parts are initially evaluated by the Flow Charts and then a comparison of the DM values is made. For very large values of DM, the reliability can be tightened-up even further in order to relax some of the reliability restrictions on a few of the very soft and very expensive device types (e.g., MOS microprocessor). As an example, assume the system has a survivability budget of 0.99. Then for 990 transistors all of the same type and 10 microprocessors, the system failure budget for each part was originally 0.01/1000 which for worst-case considerations was 10^{-5} . This required a $\mu = 4.3$ and was a very strict criteria for MOS microprocessors. But if the budget were revised so that the budget for the microprocessor components was only 3×10^{-4} or $\mu = 3.6$, then the new budget for the other 990 devices is $(10^{-2} - 3 \times 10^{-4})/990 = 7 \times 10^{-6}$; resulting in $\mu = 4.4$.

This new power of the standard deviation "s" is only slightly higher than the original 4.3.

The result of redistributing the survivability budget is a recalculation of Blocks 9, 10, 11 and 12 before another decision can be made. More past data do not need to be collected.

Block 17

Shielding can be a very useful technique but there is a limit to how much shielding can be used in a system due to weight and space restrictions; a trade-off is usually required.

Two main types of shielding are available:

- 1) Relocation of the sensitive devices.
- 2) Additional material (e.g., local shielding).

Type 1 shielding imposes no extra weight since it only means placing the more sensitive parts deep within the system to take advantage of the inherent shielding from the rest of the circuitry. It requires additional system layout time and some rough calculations on shielding effectiveness.

Type 2 shielding adds additional protection over and above that already specified for the system. This can be done universally over a large volume or localized over a few sensitive parts.

Either type of shielding results in a difference in the limits determined in Block 1, which requires a re-assessment of the calculations and the data points.

Blocks 13, 18 and 19

These options are related to the restrictions on procurement needed to obtain an acceptable group. Approach "B" is less restrictive than approach "A" and therefore, cost less money. On the other hand, if approach "B" is used when approach "A" should have been used, the designer will eventually end up in approach "A", but only after many tests and much money.

The decision as to which approach is sufficient, is already made for MOS and Bipolar Linear ICs; for these device types, the data shows too wide a variation for any approach other than "A".

Approach "B" is used if there is little or no past data on the device types considered for Flow Charts I and II. Also it is used if the DM is close to acceptance.

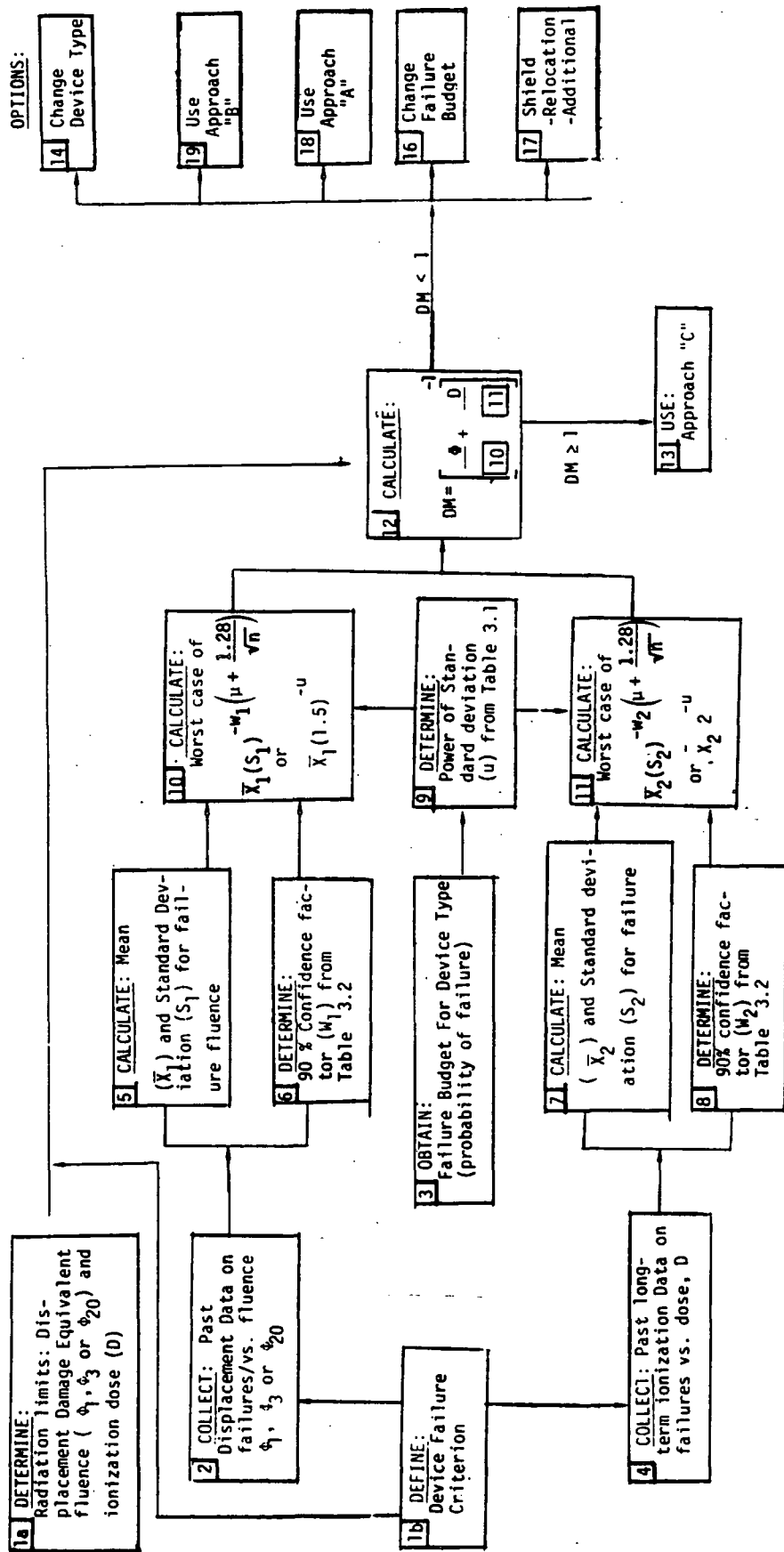


Figure 3.5: FLOW CHART II: Radiation Hardness Assurance Guideline for Bipolar Integrated Circuit (Digital Only) Selection and Device Technologies Not Covered in Flow Charts I and III, Which Show Data Only in Terms of Number of Failures vs. Radiation Level: (each type)

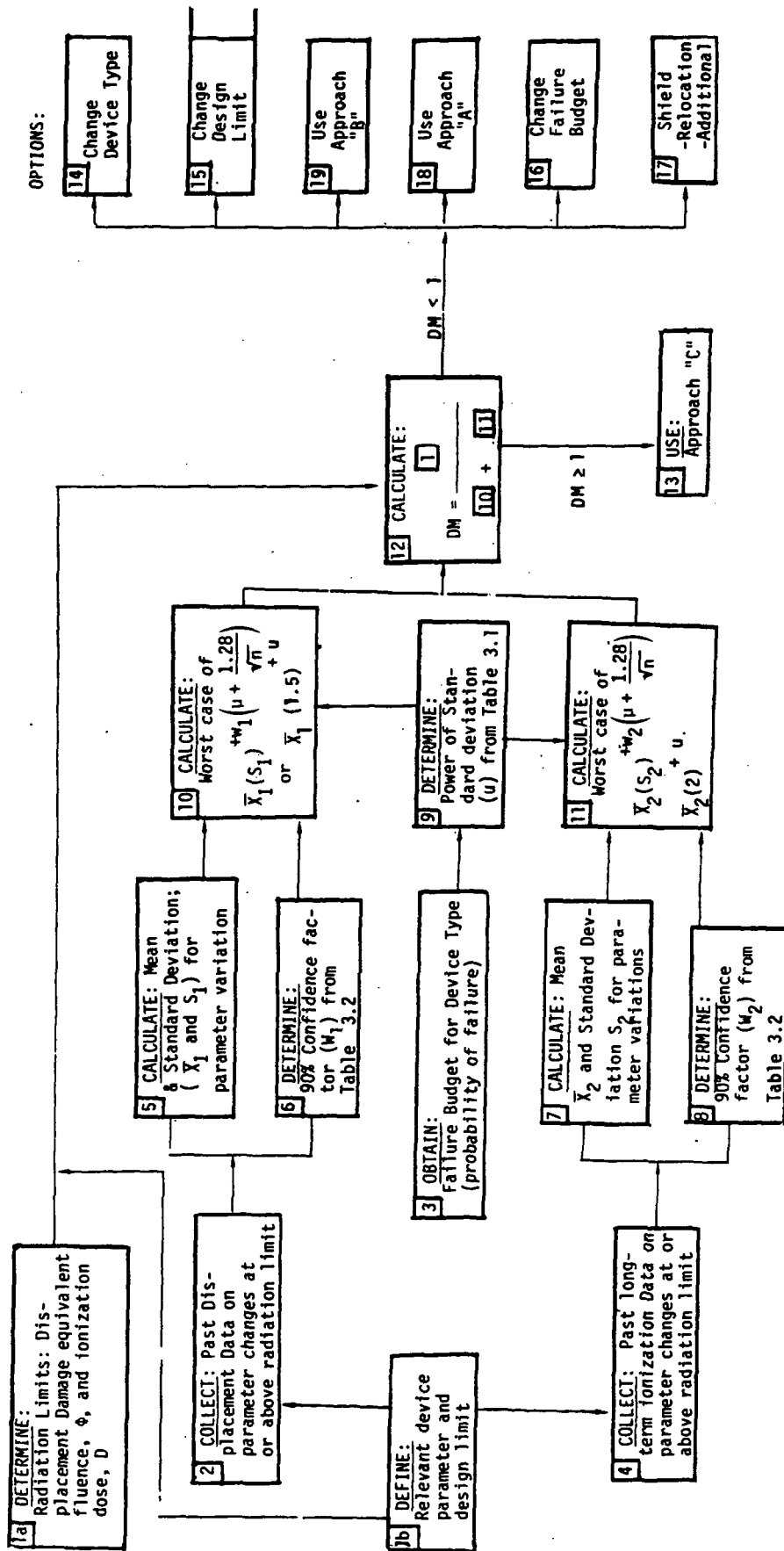


Figure 3.4: FLOW CHART I: Radiation Hardness Assurance Guideline for Bipolar Transistor Component Selection and Other Components which Show Data on Parameter Variations at Some Radiation Level. (See exceptions in narrative.)

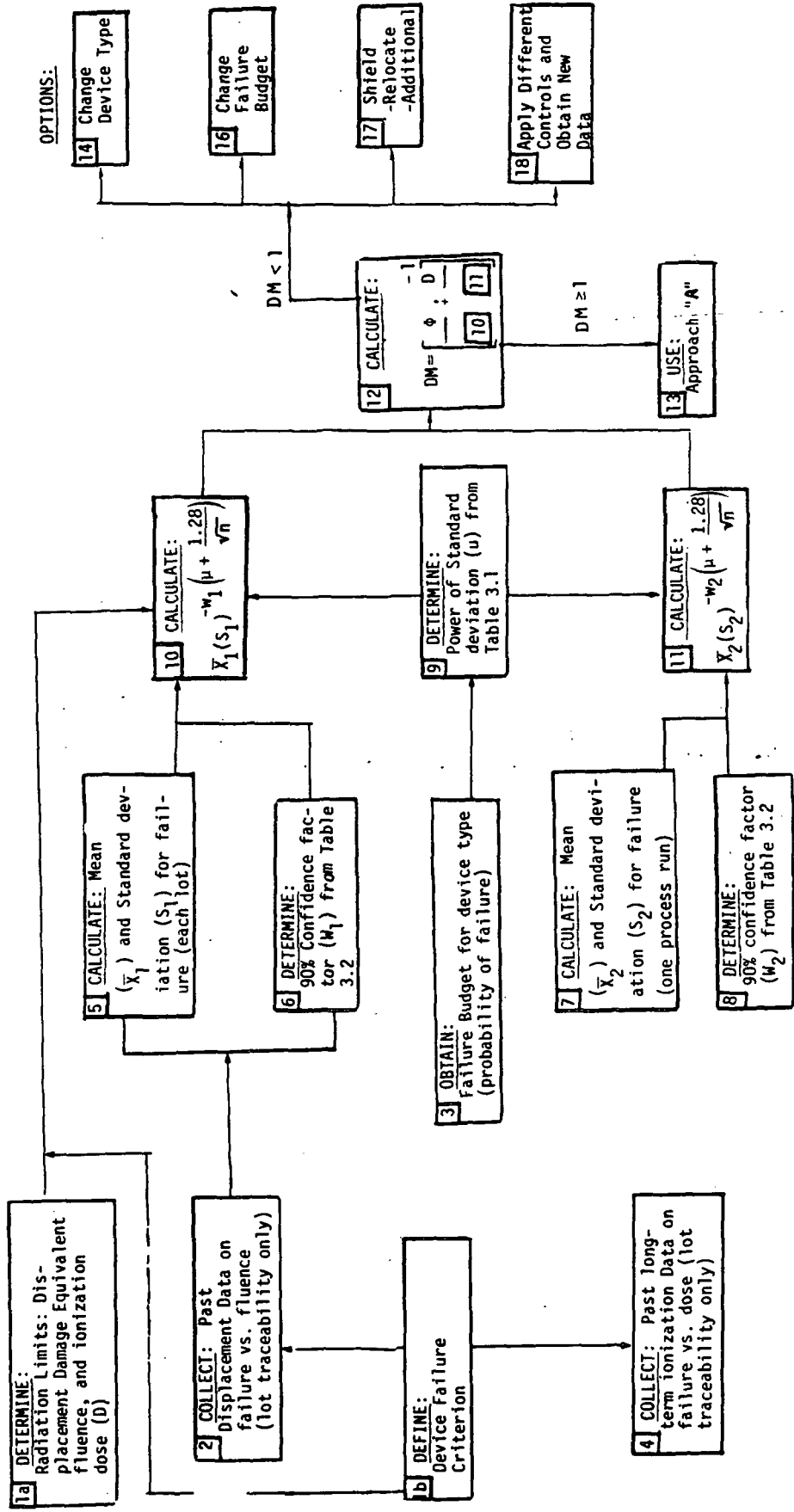


Figure 3.6: Radiation Hardness Assurance Guideline for MOS and Bipolar Linear Integrated Circuit Selection (Each Device Type).

Approach "C" can be used if the old data demonstrate a clear safety margin between parts performance and Probe requirements.

3.2.4 Hardness Assurance Approaches For Procurement

3.2.4.1 Approaches "A", "B" and "C"

Three approaches to device procurement and testing are described in Flow Charts IV, V and VI (Figures 3.7 - 3.9).

Approach "C" is the most straightforward and least costly, while Approach "A" is the most strict and most expensive. If a large amount of past data show a very narrow change in radiation hardness over several years and for several manufacturers, and the hardness level is high enough to give a good probability of successful completion of the experiment or system function, then Approach "C" will probably be the selected approach.

In reality, Approach "B" will probably be the approach used for a majority of the device types, just due to a lack of data.

Approach "A" is already determined to be necessary for MOS and bipolar linear IC's in which long-term ionization effects are known to cause large variation.

Again, each block in the Flow Charts IV, V and VI is described in a narrative section following each Flow Chart.

Figure 3.7: FLOW CHART IV: Approach "C" to Hardness Assurance

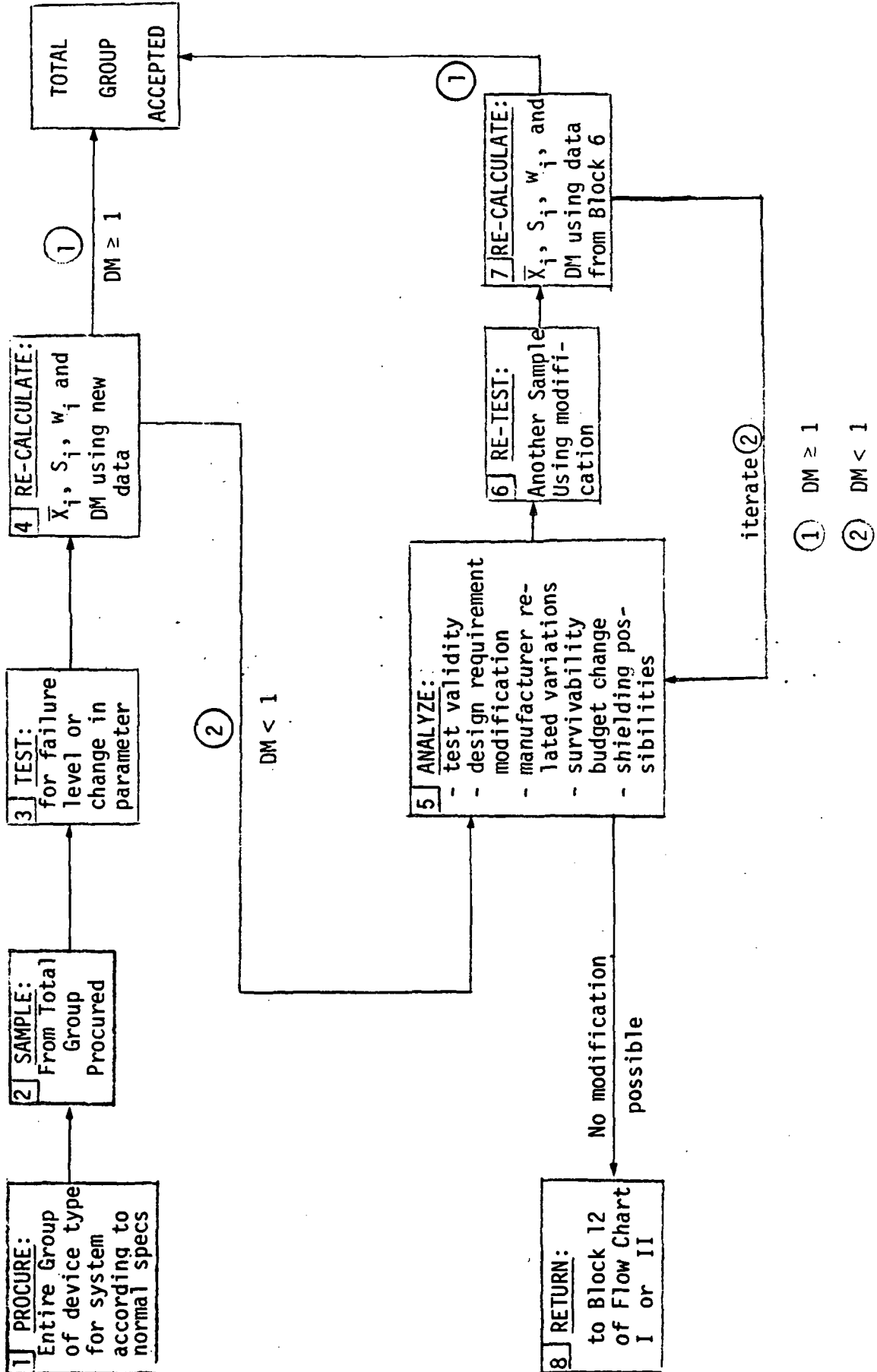


Figure 3.8: FLOW CHART V: Approach "B" for Hardness Assurance

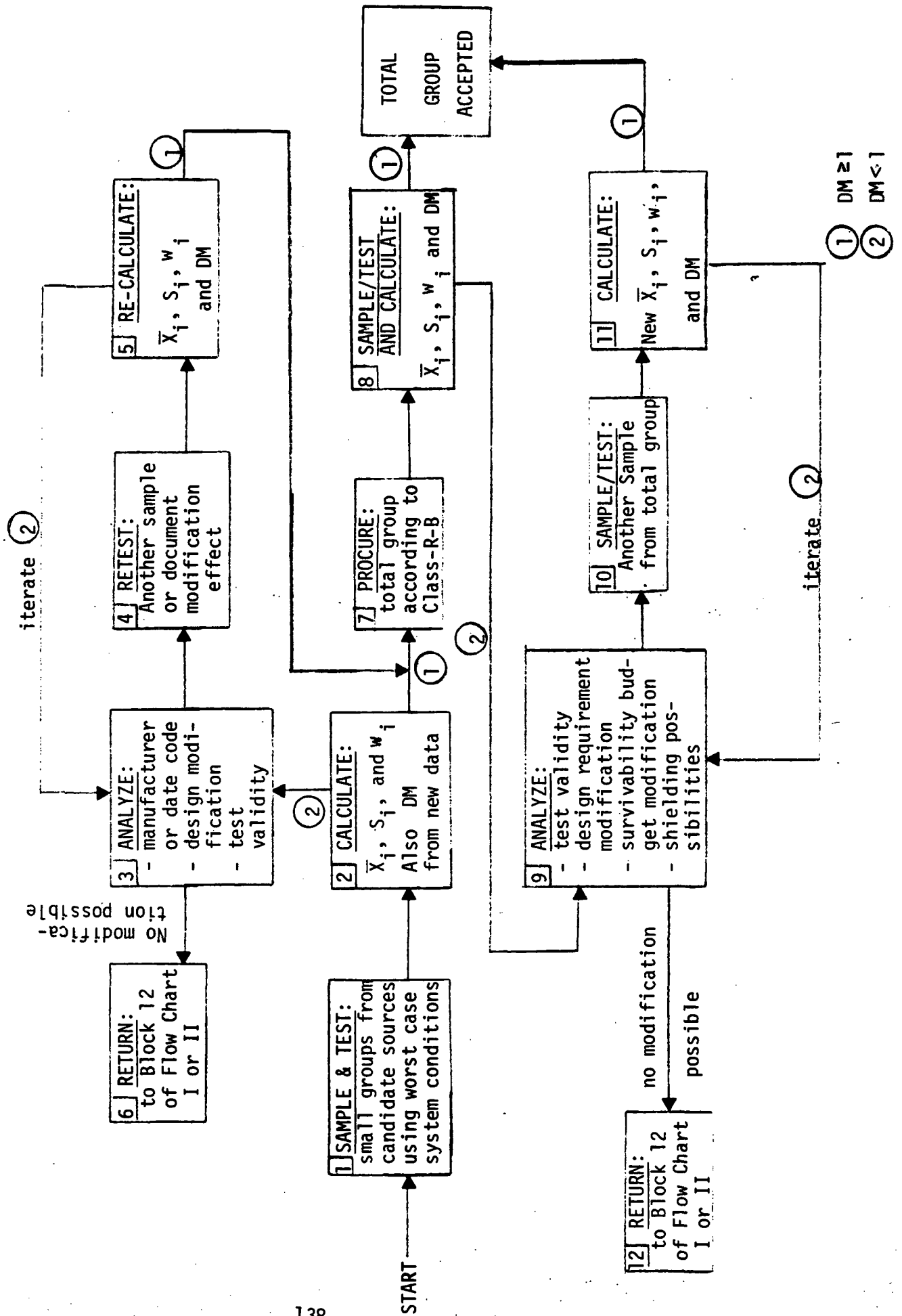
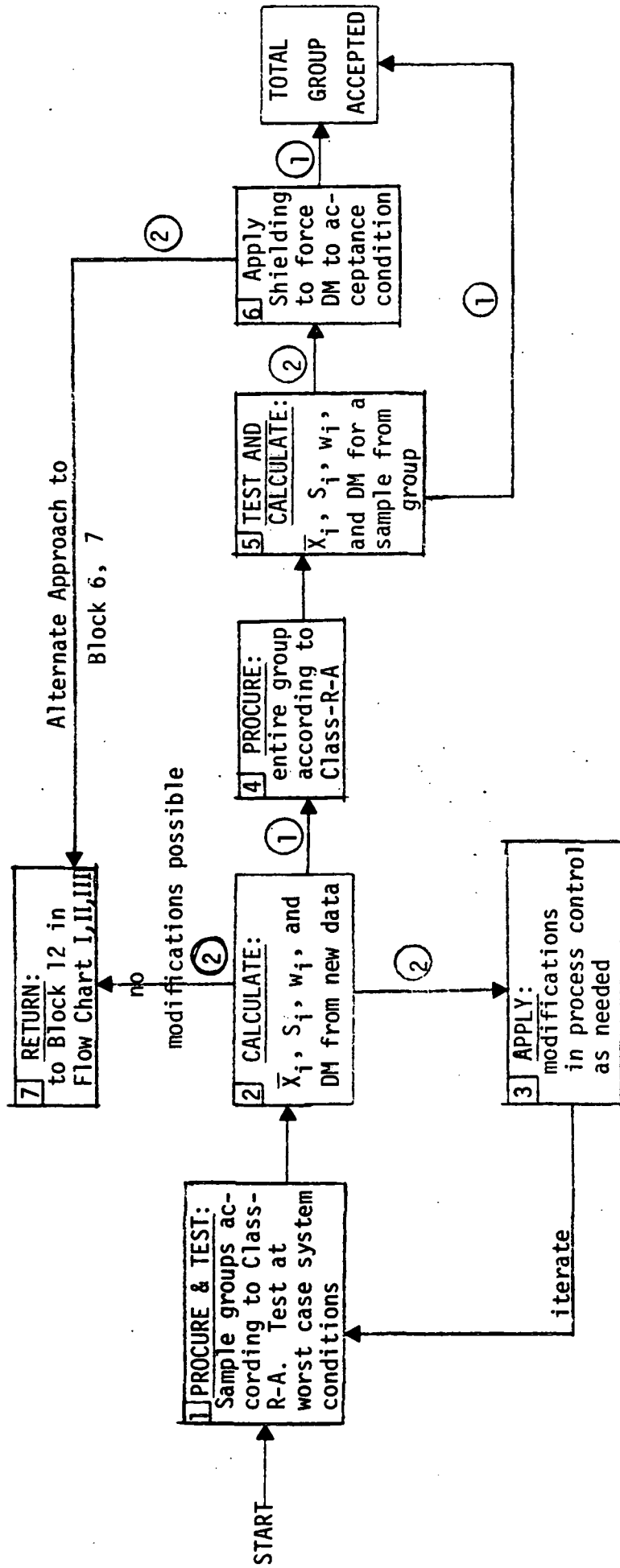


Figure 3.9: FLOW CHART VI: Approach "A" for Hardness Assurance



① DM ≥ 1
 ② DM < 1

FLOW CHART IV - BLOCK DESCRIPTION (C)

Block (C1) The designer is at this block because past data showed that these devices have a good chance of passing the more general procurement test. Therefore, the entire group of devices to be used in the system (plus a few extra for sampling) are procured according to normal spacecraft procurement standards.

Block (C2) Samples of at least 5 devices are required for radiation tests in each of the displacement and ionization environments of concern. The number of devices should be greater than 5 if possible, since another calculation of DM is going to be made and this time the actual "S" value will be used along with the $C = 90\%$ correction factor, w . If the number of devices (n) = 30 or greater, then $w \sim 1$ and the group will be evaluated on its own data, not on data with a large error factor.

Block (C3) The radiation tests will require worst-case system conditions both electrical and temperature.

Block (C4) Recalculate the variables as was done in Flow Charts I, II and III and use the same criteria for acceptance, except that the restriction on $\sigma \geq 1.5$ for displacement and $\sigma \geq 2$ for ionization effects is eliminated. Since this sample was taken from the total group, and acceptable value for DM means that the particular device type is accepted for application in the system with no restrictions.

Block (C5) This block resulted from several possibilities:

- (a) The past data was not sufficient to give a true variability in degradation and now we are seeing the true variability.
- (b) The tests on the sample group from Block (C2) were performed incorrectly.
- (c) There is a strong manufacturer related variability or date code variability that has made s too large.

Since we have already purchased the entire group of devices of this type, it would be fairly expensive to just throw away the parts and try one of the other options on Flow Charts I, II or III without trying to force the group into acceptance by applying tools that are available.

These tools or techniques include:

1. Modify Design Requirements
2. Separate Manufacturers
3. Change the surviveability budget of this device type
4. Apply Shielding Techniques

Techniques 3 and 4 were discussed in Blocks (16) and (17) of the Flow Charts I, II and III. Technique 2 is self-explanatory. By using 2, at least part of the group may be salvaged. Technique 1 relates primarily to discrete parts, in which the design requirements can be relaxed by component biasing or performance derating.

If no modification is possible then, we must return to Flow Chart I or II and select a different option.

Blocks (C6) and (C7) If a modification is possible then depending on the severity of the modification, another test sample may be required to verify the technique. Iteration of Block (C5) may be required to find an acceptable technique.

1. Date Code Lot Sampling

This is usually done where wafer or diffusion-metallization lot control does not exist.

10 samples per lot.

Non-uniformity of measured parameters over lot indicates lack of process control.

2. Production Lot Sampling

A production lot from one manufacturer usually contains more than one date code, and may represent production starts over a two month period.

Block (B4) and (B5) If another sample is needed to verify the new modification, then these blocks are used for all sampling and retesting. Recalculation of the DM value using only the data from Block (B4) is required.

If DM meets the acceptance criteria then an approach similar to Approach "C" in the remaining blocks is used. If DM does not meet the criteria, an iteration of (B3) is used. If no further modification is possible, then we must return to Block (12) of Flow Charts I or II for selection of another option.

FLOW CHART V - BLOCK DESCRIPTIONS (B)

After Blocks (B1) and (B2) are completed successfully, the rest of the flow chart is very similar to flow chart IV - Approach "C" except that a pre-selection process was used prior to the purchase of the total group for the system. This may restrict some of the options available in the analysis section of Approach "C". The blocks discussed here will emphasize only the difference between Approach "B" and Approach "C".

Block (B1) Since past data was not sufficient to make DM pass the acceptance criteria, new data must be obtained. By new data, it is meant that radiation tests (displacement and/or ionization) are performed on small groups of devices (between 5 and 30 in number) from selected candidate manufacturers. Worst case Probe operating conditions should be used in these tests.

Block (B2) Calculate the variables discussed in Flow Charts I, II and III from the new data only, eliminating the previous restrictions on σ . If DM meets the acceptance criteria, use Approach "C" procedure for the rest of the flow chart. If DM fails the criteria, an analysis mode is attempted in Block (B3).

Block (B3) Small modifications may be possible in redefining the new data on sample groups. If for example, a manufacturer selection will make DM acceptable, then this change is documented and becomes an amendment to procurement class R-B for this device type. The following are two examples of limitations on the procurement class.

FLOW CHART VI - BLOCK DESCRIPTION (A)

The necessity of using Approach "A" is usually generated by two important factors: a critical need for this device type and the fact that the device type could not satisfy the DM acceptance criteria by any other means. Localized shielding may still be a possibility but the limits on this approach may force a procurement into Approach "A".

Block (A1) Sample groups should be procured from one or more manufacturers but the devices should be separated into groups by diffusion lot or wafer. Each device, during fabrication should have as many radiation control techniques applied as is necessary to reduce the susceptibility to radiation levels of concern. The complete set of processing techniques necessary for the state-of-the-art in hardened device fabrication are unique for each device type and manufacturer. At this level careful negotiations are required in the trade-off of electrical performance parameters, radiation hardness and device yield (i.e., cost and delivery). General guidelines for device hardening have been developed for displacement damage and long term ionization effects and are familiar to manufacturers such as Fairchild, Harris, Motorola, National, RCA and Texas Instruments.

When using the devices obtained from the diffusion runs, test the samples in displacement and/or ionization environments, as needed, using worst case system conditions.

When procuring devices using some of the above techniques, it would be cost effective to contact several manufacturers to see if a hardened device of this type already exists and obtain the information as to which techniques were used.

Two techniques for sampling components out of a process run to determine if the group will meet the DM acceptance criteria are diffusion lot sampling and wafer lot sampling. The latter is usually used to screen out non-acceptable wafers in a diffusion run. The techniques are summarized below:

1. Wafer Lot Sampling

Most rigorous: guarantees wafer fabrication control, but not assembly mavericks.

Sampling Plan: 5 to 10 samples from different parts of wafer in accordance with standard sampling procedure.

Non-uniformity of measured parameters over wafer indicates lack of process control and rejection of lot.

Execution: Die attach, bond and seal package, test in package. This is the simplest method and works. Other methods involving wafer probing have problems due to the need for irradiation under correct bias conditions, in situ measurements immediately after irradiation and ambient effects during irradiation.

2. Diffusion - Metallization Lot Sampling

Next best sampling method.

It is necessary to obtain the samples from more than one wafer.

5 to 10 samples per lot.

Non-uniformity of measured parameters over lot indicates lack of process control and necessity to go to wafer lot sampling.

Execution: as for wafer lot sampling.

Total dose effects are sometimes affected by die attach, sealing, stabilization bake and burn-in operations. If the devices used for lot sampling did not undergo precisely the same treatment and on the same line as the final procurement lot, additional tests must be carried out on samples drawn from the procurement lot. This can be done at infrequent intervals compared to the original sampling plan. Any variation from the original results must be immediately investigated and may lead to rejection of the procurement lot.

Block (A2) Make the calculations for DM using only new data from one process run at a time. Compare this DM value to the acceptance criteria.

Block (A3) If the DM value did not meet the acceptance criteria, other modification should be attempted and new devices fabricated. This is quite an expensive iteration process and requires the commitment of a manufacturer to use one of his process lines for essentially an R & D effort.

If no modifications are possible, this probably means that the total group will have a radiation susceptibility level too low even for localized shielding. Either return to Block (12) of Flow Charts I, II or III and choose another option or as a last resort, proceed with the purchase of the entire group using every radiation hardening technique possible and then shield that specific part as required.

Block (A4) This procurement used all the techniques for fabrication defined as necessary from Block (A2). If process and wafer traceability are required, then they should be applied to the total group as well.

Some sort of wafer qualification may be useful where five devices are extracted from each wafer (one from each quadrant and one from the center) before the devices in the wafer have been packaged. Package each of the five devices and radiation test. If the response is satisfactory for the system requirements, then accept the wafer for processing through the normal high reliability screen and packaging procedures.

Block (A5) Radiation test the devices from a single process run and recalculate DM. If DM passes, then the total process run is accepted, assuming all other high reliability requirements are satisfied. If it does not pass, then try localized shielding.

Block (A6) Apply localized shielding to force the DM value to pass the acceptance criteria.

3.2.4.2 Radiation Procurement Classes - Definition*

Normal - Class - R - C

Devices are off-the-shelf high-rel parts meeting no special requirements on manufacturer or date code controls for radiation response.

Class-R-B

Devices are off-the-shelf high-rel parts having some restrictions based on results of new data obtained from sample tests (Block (B1) and (B2)). Specific manufacturers, date code uniformity, electrical parameters or special features are examples of types of restrictions which may be imposed as amendments.

* These are our own definitions which should be coordinated with specific NASA procurement direction.

Class-R-A

Devices are special parts procured from one or more manufacturers using diffusion-lot or wafer controls (whichever is needed) and application of known processing techniques to improve the probability for survival of the devices during radiation tests. High-rel requirements must still be satisfied.

3.3 Experimental Characterization

Design of hardened systems is probably limited more often by inadequate, irrelevant and inaccurate experimental data on component radiation effects than any other single step in the design process. The total resources which must be involved in the experimental characterization are: 1) management, 2) technical support in relating test conditions to those in system application, 3) definition of adequate test facilities and sources, 4) accurate and thorough documentation of test data, as well as 5) analysis and review of data for design application. Experimental characterization is expensive, but not as expensive as a vulnerable system.

The component evaluation process outlined in this Handbook is intended to establish the cost-effective data base necessary for high-surviveability system design. In this section considerations in experimental characterization will be presented as critical from the viewpoint of the designer. It is assumed that detailed knowledge of the radiation environments of simulators, measurements of the particle flux and absorbed ionizing radiation dose (i.e., dosimetry), as well as accurate recording of electrical test conditions and performance parameters of the components is familiar to the organization(s) directly involved in the experimental characterization. It is the designer's responsibility, however, to identify the test conditions on the device during radiation exposure, electrical performance parameters measured during and/or after radiation exposure, to interpret the data in the form of critical parameters, to be aware of the

details of the experimental simulation that may affect an accurate representation of the Probe exposure and performance conditions, and to define requirements for additional test data if required.

3.3.1 Electrical Bias Conditions During Radiation Exposure

The electrical bias on all MOS-type microcircuits (p-MOS, n-MOS, CMOS, CCD's, image sensors, etc.) during radiation exposure has a first-order effect on the magnitude of the radiation-induced damage. The worst-case bias conditions in terms of decreasing severity are:

- static d-c bias, all transistors with maximum positive gate-substrate voltage (p-channel and n-channel devices)

- static d-c bias, p-channel transistors with zero gate-substrate voltage and n-channel transistors with maximum positive gate-substrate voltage

- static d-c bias, p-channel transistors with negative gate-substrate bias voltage and n-channel transistors with positive gate-substrate voltage.

- dynamic, clocked operation during exposure at maximum supply voltage

The first test condition is representative of an array in which transmission gates are used which allow positive gate-substrate bias on the p-channel transistor elements. This results in the worst-case threshold voltage shift on the p-channel transistors and generally the worst-case test condition for array vulnerability. The second test condition is the worst-case for an array with no transmission gates. The third test condition is one that would be selected as representative of a typical static bias

throughout the array and represents a severe, but not a worst-case bias condition. The fourth test condition is generally the least-severe bias condition during radiation exposure, and can be used if it accurately simulates Probe operating conditions.

Electrical bias conditions during radiation exposure are also critical on sensitive bipolar devices and microcircuits, particularly high-performance analog microcircuits. For an individual bipolar transistor element, worst-case bias conditions during radiation exposure are d-c bias of the p-n junctions at the minimum forward bias or maximum reverse-bias values to be experienced during circuit operation. These test conditions also hold for the bipolar transistor elements in a microcircuit. In a balanced microcircuit, however, additional consideration must be given to the worst-case bias assymetry on the paired transistors. In this case, the worst-case is generally the d-c bias condition of greatest assymetry. Dynamic, or clocked exposure during radiation exposure is not the worst-case test condition but is a reasonable simulation of actual damage if it is an accurate representation of device operation in the system. It is the purpose of the statistical analysis described in Section 3.2 to establish system surviveability. Hopefully, it is not necessary to compound the worst-case by test conditions that are more severe than the worst experiences in system application.

3.3.2 Electrical Parameter Measurement

Displacement damage resulting from electron, proton, or neutron exposure is essentially stable over the temperature range of interest for the Probe. Because of this, the radiation flux during exposure and the time delay between exposure and electrical performance measurement should always be noted but are generally not critical. That is, the effect depends on the fluence and is stable at system ambient temperatures. Measurements of

electrical performance can be made with the components in situ or removed from the exposure facility to another laboratory.

Unfortunately, however, there is significant annealing of long-term ionizing radiation effects at room temperature and above. This has led to studies to quantitatively determine the influence of dose rate of exposure and the results of delaying device performance measurement following exposure. Fortunately, for much of the Probe electronic components, it is possible to almost directly simulate the exposure and required performance conditions. The ionizing radiation environment of a cobalt-60 source of high-energy electron beam can be defined such that a dose rate of 10 - 20 rads(Si)/s is obtained in the components under test. Accelerating the test by up to a factor of 5 is probably acceptable. Following component exposure, or at a time delay up to that between the end of radiation exposure during the Probe mission and the time required for active performance, the electrical performance parameters can be measured in situ. Lower ionizing radiation dose rates may be used, of course, if the shielded environment of the component is lower than that determined from the worst-case exposure. Under these conditions, we feel that accurate simulation of the electrical bias conditions during exposure is more critical to an accurate assessment of radiation damage than the uncertainties of dose rate during exposure and short (less than 16 hours) delays in the measurement of post-exposure electrical characteristics.

In review, then, displacement damage effects are stable, but long-term ionizing radiation effects show significant (factors of 2 - 4 in effective total dose) annealing effects. The ionizing radiation exposure of the Probe electronics can be simulated with available facilities. The presence of this effect should, however, be kept in mind when reviewing component data obtained for application in non-space radiation environments. It should also be pointed out that those experiments intended to simulate displacement

damage effects also produce an ionizing radiation environment. Devices sensitive to both ionizing and displacement damage effects will reflect the combination of both in the displacement damage experiment and test conditions of the ionizing radiation environment must be imposed to get usable data.

3.3.3 Characterization of Complex Microcircuits

The principal considerations in evaluating radiation-induced permanent damage effects on MSI/LSI arrays are: 1) comprehensive evaluation of pre-/post-electrical performance characterization, 2) selection of electrical bias conditions during irradiation, and 3) determination of the number of samples that must be characterized to insure adequate statistical representation for component system qualification.

Electrical performance characterization of MSI/LSI arrays is a well documented problem even without considering radiation-induced damage effects. The most straightforward method of verifying the overall logic function of the array is simply to compare the outputs of a damaged device to those of a good reference device under the same input signal sequence for all possible input conditions. The array interface, typically outputs, must also be characterized in terms of the terminal current-voltage characteristic to assure performance for specified external loads. In some cases it is more convenient to simulate the reference "good" device logically with a minicomputer programmed to direct the input sequence and compare the output results. If the array is very complex and a large number of samples must be tested the total number of input combinations can be reduced to the set just sufficient to detect the failure of any logic cells. Generation of test sequences can also be used to isolate the radiation-induced failure analysis and possible hardening. Application of the test sequences to a given array can be implemented analytically with logic simulation computer programs that consider the array as a network of idealized logic functions.⁵³

Pre-/post-evaluation of array performance must also include the system-defined temperature range. Bipolar transistor gain degradation becomes most critical when the gain is low at low temperatures. Junction leakage currents, increased by displacement damage or surface effects, on the other hand, become most critical at high temperatures. Variation in the damage failure level due to both transistor gain degradation and junction leakage currents over a wide range of case temperature was observed in the neutron/electron-induced degradation of the SMS 8228 4,096-bit Schottky-clamped TTL Read-Only-Memory. In this case, the room temperature evaluation was the best-case compared to either low-or-high-temperature operation.³⁴

Damage assessment of MSI/LSI arrays is sufficient to assure adequate performance of internal logic cells, but not the safety margin to the threshold of failure. The safety margin of the internal cells must be determined experimentally. Damage effects at the interface cells, however, can be measured quantitatively and a safety margin estimated, given load requirements, by extrapolating slightly to higher exposure levels.

SECTION 4

4.0 SUMMARY

The design handbook as presented has been intended as one of many means to the hardened systems of the Probe. Principal emphasis has been placed on methods rather than available data because the data base must be as current as the evolving design. It is hoped that application of this handbook will produce greater insight into the development of hardened space systems and handbooks which can reflect more cost-effective methods.

REFERENCES

1. Baze, M.P., et. al., "Preliminary Jupiter Probe Radiation Hardness Assessment", NASA-CR-137837.
2. "Mission Description Document for Jupiter Orbiter Probe 1981/1982 Mission", JPL #660-21, August 1976.
3. "Jupiter Charged-Particle Environment for Jupiter Orbiter Probe 1981/1982 Mission", JPL #660-24, August 1976.
4. Gindorf, T. E., et. al., "MJS77 Radiation Control Requirements Document", PD 618-229, April 18, 1975.
5. van Lint, Victor A. J., et. al., "Correlation of Displacement Effects Produced by Electrons, Protons, and Neutrons in Silicon", IEEE Trans. on Nuclear Science, Vol. NS-22, No. 6, p.2667, December 1975.
6. Nelson, D. L., and R. J. Sweet, "Mechanisms of Ionizing Radiation Surface Effects on Transistors", IEEE Trans. on Nuclear Science, Vol. NS-13, No. 6, p. 197, December 1966.
7. Horne, W. E., and R. R. Brown, "Correlation of Electron-Induced changes in Transistor Gain with Components of Recombination Current", IEEE Trans. on Nucl. Science, Vol. NS-13, No. 6, p. 181, December 1966.
8. Stanley, A. G., et. al., "Radiation Design Criteria Handbook", JPL TM-33-763, 1976.
9. Prince, J. L., and R. A. Stehlin, "Effects of CO^{60} Gamma Radiation on Noise Parameters of Bipolar Transistors", IEEE Trans. on Nucl. Science, Vol. NS-18, No. 6, p. 404, December 1971.
10. Coppage, F. N., and E. D. Graham Jr., "Device Degradations from the Effects of Nuclear Radiation on Passivation Materials", IEEE Trans. on Nuclear Science, Vol. NS-19, No. 6, p. 320, December 1972.
11. Measel, P. R., and R. R. Brown, "Low Dose Ionization-Induced Failures in Active Bipolar Transistors", IEEE Trans. on Nucl. Science, Vol. NS-15, No. 6, p. 224, December 1968.

12. Stanley, A. G., and K. E. Martin, "Statistical Analysis of Long-Term Ionization Effects on Bipolar Transistors", JPL Report 365-J-46-76 (Preliminary); November 23, 1976.
13. Brown, R. P., and W. E. Home, "Space Radiation Equivalence for Effects on Transistors", NASA CR-814; 1966.
14. "Radiation Effects on Semiconductor Devices - Summary of Data", HDL-DS-74-1, p. 192; Harry Diamond Labs, June 1974.
15. Messenger, G. C., "Hardness Assurance Considerations for the Neutron Environment", IEEE Transactions on Nuclear Science, Vol. NS-22, No. 6, p. 2308; December 1975.
16. Donovan, R. P., et. al., "Radiation Vulnerability of Contemporary Solid-State Devices", Digest of Papers for Government Microelectronics Applications Conference (GOMAC)- 1974, Boulder, Colorado, p. 144.
17. George, W. L., "Optimization of the Neutron Radiation Tolerance of Junction Field Effect Transistors", IEEE Trans. on Nucl. Sci., Vol. NS-16, No. 6, p. 81; December 1969.
18. Shedd, W., B. Buchanan, and R. Dolan, "Radiation Effects on Junction Field Effect Transistors", IEEE Trans. on Nucl. Sci., Vol. NS-16, No. 6, p. 87; December 1969.
19. Zuleeg, R., "Neutron Radiation Hardened GaAs Junction Field-Effect Transistors Operating in the Hot Electron Range", Digest of Papers for Government Microelectronic Applications Conference - 1972, San Diego, CA, p. 107.
20. Stanley, A. G., and W. E. Price, "Irradiate-Anneal Screening of Total Dose Effects in Semiconductor Devices", IEEE Trans. on Nucl. Sci., Vol. NS-23, No. 6, p. 2035; December 1976.
21. Parker, Richard H., "Effects on Proton Irradiation on Several Spacecraft Science Components", IEEE Trans. on Nucl. Sci., Vol. NS-19, No. 6, p. 156; December 1972.
22. Molnar, B., "Fast Neutron Irradiation Damage on Room Temperature PbS Detectors", IEEE Trans. on Nucl. Sci., Vol. NS-21, No. 6, p. 103; December 1974.
23. Shepherd, F. D. Jr., "Radiation Effects on Spectral Response of HgCdTe", IEEE Trans. on Nucl. Sci., Vol. NS-21, p. 34; December 1974.

24. Mallon, C. E., et. al., "Effects of Electron Radiation on the Electrical and Optical Properties of HgCdTe", IEEE Trans. on Nucl. Sci., Vol. NS-20, No. 6, p. 214; December 1973.
25. Mallon, C. E., et. al., "Radiation Effects in $\text{Hg}_{1-x}\text{Cd}_x\text{Te}$ ", IEEE Trans. on Nucl. Sci., Vol. NS-22, No. 6, p. 2283; December 1975.
26. Pickel, J. C., and M. D. Petroff, "Nuclear Radiation Induced Noise in Infrared Detectors", IEEE Trans. on Nucl. Sci., Vol. NS-22, No. 6, p. 2456; December 1975.
27. Wilsey, N. D., et. al., "A Comparison of Fast Neutron Irradiation Effects in Photoconductive and Photovoltaic InSb Infrared Detectors", IEEE Trans. on Nucl. Sci., Vol. NS-22, No. 6, p. 2448; December 1975.
28. Brucker, G. J., and A. D. Cope, "Radiation Sensitivity of Silicon Imaging Sensors on Missions to the Outer Planets", IEEE Trans. on Nucl. Sci., Vol. NS-19, No. 6, p. 147; December 1972.
29. TREE Handbook, Battelle Memorial Institute, Ed. 2, Rev. 2; September 1969.
30. Hum, R. H., and A. L. Barry, "Radiation Damage Constants of Light-Emitting Diodes by a Los-Current Evaluation Method", IEEE Trans. on Nucl. Sci., Vol. NS-22, No. 6, p. 2482, December 1975.
31. Soda, K. J., et. al., "The Effects of Gamma Irradiation on Optical Isolators", IEEE Trans. on Nucl. Sci., Vol. NS-22, No. 6, p. 2475; December 1975.
32. Barnes, C. E., "Neutron Damage in GaAs Laser Diodes: At and above Laser Threshold", IEEE Trans. on Nucl. Sci., Vol. NS-19, No. 6, p. 382, December 1972.
33. Carter, J. R., Jr., and H. Y. Tada, "Solar Cell Radiation Handbook", JPL 21945-6001-RU-00, (Re-order # 73-88); June 28, 1973.
34. Raymond, James P., "MSI/LSI Radiation Response, Characterization and Testing", IEEE Trans. on Nucl. Sci., Vol. NS-21, p. 308, December 1974.
35. Messenger, G. C., "Radiation Effects on Microcircuits", IEEE Trans. on Nucl. Sci., Vol. NS-13, No. 6, p. 141-159; December 1966.
36. Burghard, R. A., and C. W. Gwyn, "Radiation Failure Modes in CMOS Integrated Circuits", IEEE Trans. on Nucl. Sci., Vol. NS-20, No. 6, p. 300-306, December 1973.

37. Measel, P. R., et. al., "Development of a Hard Microcontroller", IEEE Trans. on Nucl. Sci., Vol. NS-23, No. 6, p. 1738; December 1976.
38. Daniel, M. E., and F. N. Coppage, "Radiation Hardness of a High Speed ECL Microcircuit", IEEE Trans. on Nucl. Sci., Vol. NS-22, No. 6, p. 2595; December 1975.
39. Long, D. M., and C. J. Repper, "Radiation Effects Modeling and Experimental Data on I²L Devices", IEEE Trans. on Nucl. Sci., Vol. NS-23, No. 6, p. 1697; December 1976.
40. Pease, R. L., "Radiation Damage to Integrated Injection Logic Cells", IEEE Trans. on Nucl. Sci., Vol. NS-22, No. 6, p. 2600; December 1975.
41. Myers, D. K., "Radiation Effects on Commercial 4-kilobit NMOS Memories", IEEE Trans. on Nucl. Sci., Vol. NS-23, No. 6, p. 1732; December 1976.
42. King, E. E., and G. P. Nelson, "Radiation Testing of an 8-bit CMOS Microprocessor", IEEE Trans. on Nucl. Sci., Vol. NS-22, No. 5, p. 2120; October 1975.
43. NSWC/WOL/TR-76-90.
44. Hartsell, Glenn A., "Radiation Hardness of Surface and Buried Channel CCD's", Proceedings of the International Conference on Applications of CCD's, p. 375; October 29-31 1975.
45. Killiany, J. M., et. al., "Effects of Ionizing Radiation on Charge-Coupled Device Structures", IEEE Trans. on Nucl. Sci., Vol. NS-21, No. 6, p. 193; December 1974.
46. Raymond, J. P., et. al., "LSI Vulnerability Study" (Final Report), DNA Report 2965F, October 1972.
47. Mattern, P. L., et. al., "The Effects of Radiation on the Absorption and Luminescence of Fiber Optic Waveguides and Materials", IEEE Trans. on Nucl. Sci., Vol. NS-21, p. 81; December 1974.
48. Flanagan, T. M., "Hardness Assurance in Quartz Crystal Resonators", IEEE Trans. on Nucl. Sci., Vol. NS-21, p. 390, December 1974.
49. Neamen, D., W. Shedd, and B. Buchanan, "Effects of Ionizing Radiation on Dielectrically Isolated Junction Field Effect Transistors", IEEE Trans. on Nucl. Sci., Vol. NS-19, No. 6, p. 400; December 1972.

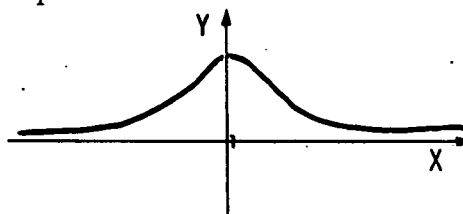
50. Killiany, J. M., et. al., "Effects of Ionizing Radiation on a 256-Stage Linear CCD Imager", IEEE Trans. on Nucl. Sci., NS-22, No. 6, p. 2634; December 1975.
51. Holmes, R. R., D. K. Wilson and R. R. Blair, "Neutron Damage Failure Rates for Large Populations", IEEE Trans. on Nucl. Sci., Vol. NS-19, No. 6, p. 414-417; December 1972.
52. Messenger, G. C., "Hardness Assurance Considerations for the Neutron Environment", IEEE Trans. on Nucl. Sci., Vol. NS-22, No. 6, p. 2308; December 1975.
53. Pocock, D. N., and M. G. Krebs, "Terminal Modeling and Photo-compensation of Complex Microcircuits", IEEE Trans. on Nucl. Sci., Vol. NS-19, No. 6, p. 86-93; December 1972.

APPENDIX A STATISTICAL ANALYSIS

When analyzing a population for an effect such as radiation, sampling is usually used; especially in radiation when the system components cannot be subjected to the radiation tests. Then by applying statistical correction factors to the sample data, a confidence level can be put on the estimate of the total population and its response under the same conditions.

For effects which are dependent on parameters that are additive in nature, the population can usually be expressed in the form of a normal distribution given in the form,

$$y = \frac{1}{\sqrt{2\pi}} e^{-\frac{1}{2} x^2}$$



For radiation effects, the parameters which describe the effects appear to form a product rather than a sum. This was seen for both displacement and long-term ionization effects on $\Delta 1/h_{FE}$ in transistors. For displacement,

$$\Delta \frac{1}{h_{FE}} = \frac{0.2 K\Phi}{f_T}$$

where K was the radiation damage factor,

f_T was the gain-bandwidth product,

and Φ was the fluence.

Both K and f_T have independent distributions and form a product (quotient) of parameters describing the displacement radiation effect. Therefore, a normal distribution of the effect of radiation would not be expected. If a logarithm is taken of the expression of displacement damage on $\Delta 1/h_{FE}$, the expression becomes;

$$\log (\Delta 1/h_{FE}) = \text{constant} + \log \phi + \log K - \log f_T$$

which is now a sum of parameters again. A normal distribution of this expression may then be expected for the population. This relationship is called a log-normal distribution (i.e., a normal distribution of the logarithm of the experimental values). While the number of multiplicative factors contributing to $\Delta (1/h_{FE})$ is not large enough to involve the central limit theorem rigorously; experience has shown that the log-normal distribution is a reasonable approximation to the measured distributions. For example, ionization effects on $\Delta 1/h_{FE}$ in 2N2222 transistors showed a log-normal distribution.¹² Since both types of radiation effects are considered in this handbook, log-normal distributions will be assumed for all semiconductor devices.

The use of the log-normal distribution approach is actually no harder to use than the normal distribution if a small hand scientific calculator is available. By changing all sample values of radiation effects into logarithms before calculating the mean and standard deviation, simple normal distribution approaches can be applied. These approaches include calculating the error bars and appropriate reliability levels on the distribution. Once these calculations are performed, a simple anti-logarithm conversion puts the final values back into measured-parameter space, so the designer can compare the values to his design limits.

From this point on, the approach to calculating the error bars and appropriate reliability levels will be derived, a final expression

will be shown for the number which is compared to the design limit and an example will be presented showing how to use the final expression.

The final expression to be used in comparing with the design limit is;

$$\bar{X} S^{\pm w} \left(\mu + \frac{1.28}{\sqrt{n}} \right)$$

where \bar{X} = mean

S = standard deviation

w = 90% confidence correction factor

μ = multiple of the standard deviation to obtain the desired failure budget

n = sample size

The mean can be calculated on the geometric mean of the measured parameters or as the mean of the logarithms. The standard deviation must use logarithms in its calculation and then convert back to obtain S. Table 3.2 provides the value of w and μ is obtained from Table 3.1. If sample data is found where a normal mean, \bar{X}_n , and a normal standard deviation, S_n , are given, S can be derived by letting

$$S \approx 1 + \frac{S_n}{\bar{X}_n} \quad \text{if} \quad \frac{S_n}{\bar{X}_n} \ll 1$$

(as an example, if $\bar{X}_n = 0.0046$ for $\Delta (1/h_{FE})$ after a fluence of 10^{13} n/cm² and $S_n = 0.0013$ then

$$S \approx 1 + \frac{S_n}{\bar{X}_n} = 1 + \frac{0.0013}{0.0046} = 1 + 0.28 = 1.28$$

To obtain the expression for the design margin value, standard probability and confidence approximations were used (in the logarithm case). First assume that all data has been converted to logarithms, Y_i . Then the problem of estimating errors and probabilities is just that of a normal distribution. For a normal distribution, the standard deviation describes the spread of the data such that 84% of all data points can be found above the 1 standard deviation (σ_y) distance from the mean (\bar{Y}). Above $2 \sigma_y$ from \bar{Y} , 97.7% of the data points can be found and so on as far out as is necessary to satisfy the failure budget for the device being considered. For example if the failure budget of a component is 0.0001 or 10^{-4} , then by Table 3.1, at $\approx 3.9 \sigma_y$ from \bar{Y} , 99.99% of the components will be found above this point. Therefore, to satisfy the failure budget, the design limit must be compared to a point $\mu \sigma$ from the mean \bar{Y} (i.e., $\bar{Y} \pm \mu \sigma_y$) where μ is obtained from Table 3.1.

The standard deviation described above is the actual total population standard deviation; this value is usually not known exactly, but is inferred from a sample standard deviation (S_y). This sample standard deviation has some error associated with it since it is a sample and not the value obtained from the entire population. Therefore a correction factor must be applied to S_y to give a 90% confidence that the total population σ_y is represented.⁵⁴ This correction factor is obtained from Table 3.2 which uses a χ^2 distribution approach where

$$\chi^2 = \frac{n(S_y)^2}{\sigma_y^2}$$

and χ^2 values are obtained from tables found in several mathematical handbooks. Let "w" equal the correction factor on S_y such that $\sigma_y < w S_y$ for 90% confidence. Then the failure budget is satisfied at $\bar{Y} \pm \mu w S_y$.

The only uncertainty still remaining is in the value of the mean. If we desire the same 90% confidence in the mean value, then by using the fact that the mean has an error of $\frac{\sigma_y}{\sqrt{n}}$ for any normal population and at $1.28 \sigma_y$ from the mean, 90% of the values fall above this point, then the worst case error on the mean would be at

$$\bar{Y} \pm \frac{1.28 \sigma_y}{\sqrt{n}}$$

and the failure budget requirements are satisfied at,

$$\bar{Y} \pm \left(\frac{1.28 \sigma_y}{\sqrt{n}} + \mu w S_y \right) =$$

$$\bar{Y} \pm \left(\frac{1.28 S_y}{\sqrt{n}} + \mu w S_y \right) \quad \text{or}$$

$$\bar{Y} \pm w \left(\mu + \frac{1.28}{\sqrt{n}} \right) S_y$$

All that is left now is to convert back to measured parameters out of the logarithm values. This is done by letting $\bar{Y} = \log \bar{X}$ and $S_y = \log S$. Then the expression becomes,

$$\log \bar{X} \pm w \left(\mu + \frac{1.28}{\sqrt{n}} \right) \log S$$

or,

$$\boxed{\bar{X} S^{\pm w \left(\mu + \frac{1.28}{\sqrt{n}} \right)}}$$

APPENDIX B
EXAMPLE OF RADIATION HARDNESS ASSURANCE GUIDELINE ASSESSMENTS

From the Harry Diamond Laboratory data bank, 2N2222 transistors from Fairchild were tested for displacement effects. If $I_C = 1$ mA and $V_{CE} = 5$ volts for the design (or a lower I_C or higher V_{CE}), displacement damage effects at 1×10^{13} n/cm² fluence showed a mean $\Delta (1/h_{FE})$ of 0.0042 with a normal standard deviation of $S_n = 0.0027$. This test was on 12 devices in November of 1971. Therefore $S = 1 + \frac{0.0027}{0.0042} = 1.64$. Since this is one manufacturer at one period of time, the larger of 1.5 or 1.64 for S must be used.

$$\begin{aligned} \text{Displacement} &\implies \bar{X}_1 = 0.0042 \\ &S_1 = 1.64 \\ &n_1 = 12 \end{aligned}$$

For long-term ionization, data on tests¹² of 2N2222 transistors from Texas Instruments using 52 devices with manufacturing date codes from 1973 - 1975 showed a $\Delta (1/h_{FE})$ of 0.0134 and a standard deviation in the log-normal sense of $S = 1.8$ for radiation levels of 150 krads and $I_C = 60$ μ A, $V_{CE} = 40$ volts.

NOTE: All the bias conditions in the long-term ionization example are worst case to the displacement damage example so the long-term ionization data will produce at least a worst case value of the design margin.

Since $S = 1.8$ for the long-term ionization case, $S = 2$ is used due again to past data showing manufacturer variations and date code effects

on radiation levels which would influence the distribution.

$$\begin{aligned} \text{Long-term ionization} &\implies \bar{X}_2 = 0.0134 \\ S_2 &= 2 \\ n_2 &= 52 \end{aligned}$$

Blocks **10** and **11** in the flow charts use the above values and calculate the design margin (DM) in Block **12**. Block **10** shows that the displacement effect on the design margin (DM) has a magnitude of

$$\begin{aligned} \bar{X}_1 S_1^{+w_1} \left(\mu + \frac{1.28}{\sqrt{n_1}} \right) &= (0.0042) (1.64)^+ 1.5 \left(3.9 + \frac{1.28}{\sqrt{12}} \right) \\ &= \underline{0.0998} \quad \text{for } P_{if} = 10^{-4} \end{aligned}$$

and Block **11** shows that the long-term ionization effect on DM has a magnitude of

$$\begin{aligned} \bar{X}_2 S_2^{+w_2} \left(\mu + \frac{1.28}{\sqrt{n_2}} \right) &= (0.0134) (2)^+ 1 \left(3.9 + \frac{1.28}{\sqrt{52}} \right) \\ &= \underline{0.226} \end{aligned}$$

If this type of transistor had a minimum initial gain of 50 at $I_C = 1$ mA and $V_{CE} = 5$ volts and the design limit was set at a minimum gain of 10 then

$$\Delta \left(\frac{1}{h_{FE}} \right)_L = \frac{1}{10} - \frac{1}{50} = 0.08$$

By comparing the design limit of 0.08 for $\Delta 1/h_{FE}$ with the two values obtained above (for displacement and ionization effects), it is observed that each effect will cause DM to be < 1 but that the long-term ionization effect is more than twice as much as the displacement effect.

From this example, several conclusions can be drawn about the use of 2N2222 transistors in the system.

1. Procurement of 2N2222 transistors using class R-C is not possible.
2. Both displacement effects and long-term ionization effects will be a problem but the long-term ionization effects are more severe.
3. Limiting the procurement to one manufacturer will not on its own necessarily provide a viable approach to obtaining a tighter distribution in radiation hardness.

The above example uses a parameter distribution at a particular radiation level. For this type of calculation the positive power on the standard deviation "S" should be used.

If, as in the case of some digital device parameters, a variation in parameter cannot be obtained, then another approach can be used. This approach considers the distribution of failures (of a parameter) versus radiation level. Data in this form can also be obtained from the Harry Diamond Lab data bank. A mean and standard deviation of failures in terms of radiation levels will then be used in the same log-normal formulas derived above with the final comparison in Block 12 made with the fluence and dose radiation limits set for the component. For this kind of approach, a negative power on the standard deviation must be used. If, in this kind of approach, 100% failures are found between two test points with no indication of the distribution, use $S = 1.5$ for displacement and $S = 2$ for long-term ionization.